13th Oxford School on Neutron Scattering

St. Anne's College, University of Oxford
2 - 13 September 2013

Chemical Applications of Neutron Scattering

Part 2

Mainly Inelastic Scattering:
Spectroscopy and Dynamics

Alberto Albinati

University of Milan, Department of Chemistry

Chemical Applications of Neutron Scattering

Part 2: Inelastic Scattering

- INS Spectroscopy: Transition Metals Hydrides
- Rotational Tunnelling and the Nature of the M-H_2 Bond
- Combined use of Diffraction, Spectroscopy and ab-initio calculations
- Hydrogen Storage

Incoherent Scattering Cross Sections

$$\sigma_{incoh} = 4\pi\left(\left\langle b^2\right\rangle - \left\langle b\right\rangle^2\right)$$

- Incoherent Scattering arises from the random distribution of different isotopes with different scattering lengths.

- Incoherent Scattering depends on the correlation between the positions of the same nucleus at different times.

NO INTERFERENCE EFFECTS ≡ SPECTROSCOPY

INS spectrum from a hypothetical molecular crystal

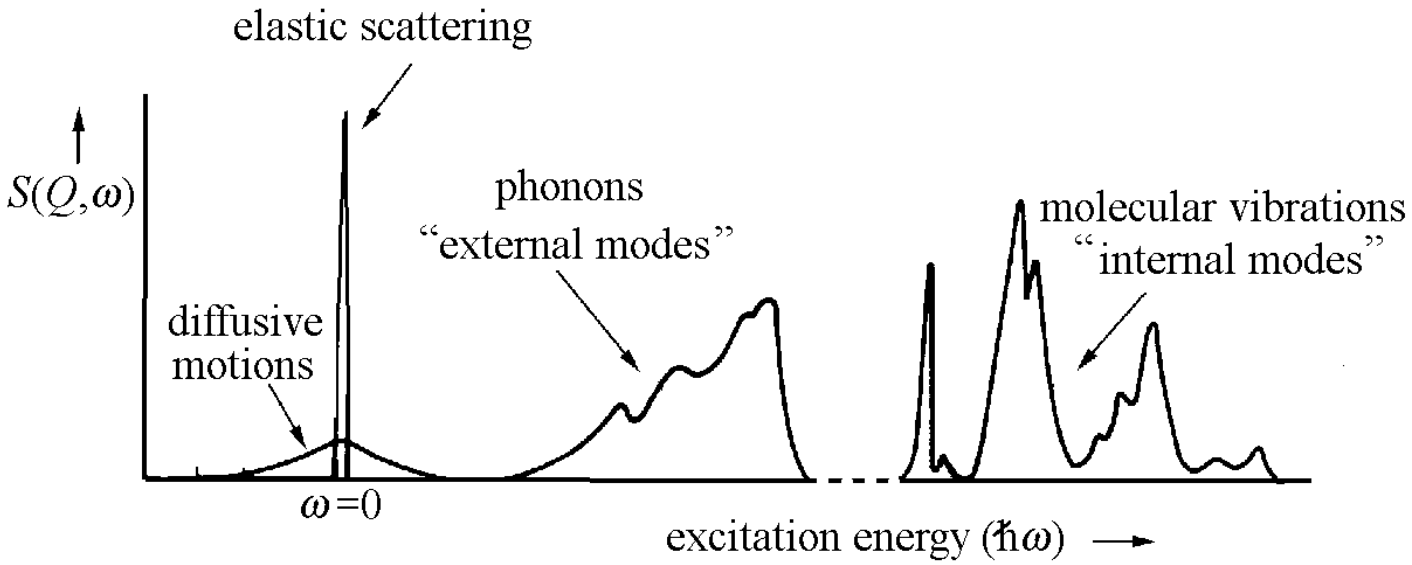

Inelastic and Quasielastic Neutron Spectroscopy

$$\Delta E\,\tau \approx \hbar/2\pi$$

Time Scale τ	Resolution ΔE	Spectroscopic Technique
10^{-11} sec	10 - 100 meV	Direct Geometry TOF
10^{-9} sec	0.3 - 20 meV	Backscattering Crystal Analyzer
10^{-7} sec	5 neV - 1 meV	Spin Echo

$$Q = \frac{4\pi}{\lambda}\sin\vartheta$$

Momentum Transfer Q(Å^{-1})	Distance (Å)	Regime
0.05	100	Continous or Macrospic Diffusion
5	1	Atomic or Microscopic Diffusion

INELASTIC INCOHERENT NEUTRON SCATTERING:

- **The energy of the thermal neutrons is comparable to that of the lattice and molecular vibrations.**
- **The incoherent part of the scattering cross-section (σ_{inc}) arises from the random distribution of different isotopes with different scattering lengths.**
- **The incoherent part of the scattering cross-section describes the single particles dynamics:** ***Vibrational and rotational spectroscopy.***
- **The intensity scattered by each mode depends on the** ***value of the incoherent scattering cross-section (σ_{inc}) and the atomic displacements*****.**
- **The incoherent cross section for Hydrogen is very large:** ***modes involving H atoms will dominate the INS Spectrum***

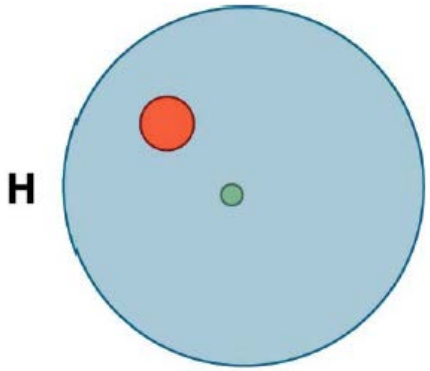

σ_{inc} **(H) = 80.27 (barn)**

σ_{inc} **(D) = 2.05 (barn)**

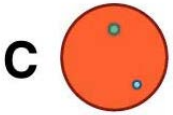

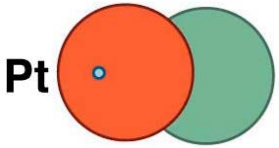

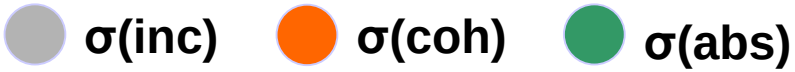

Inelastic neutron scattering measures atomic motion

$$\left(\frac{d^2\sigma}{d\omega dE}\right)_{coh} = b_{coh}^2 \frac{k'}{k} N S(\mathbf{Q},\omega)$$

$$\left(\frac{d^2\sigma}{d\omega dE}\right)_{incoh} = b_{incoh}^2 \frac{k'}{k} N S_i(\mathbf{Q},\omega)$$

$$S(\mathbf{Q},\omega) = \frac{1}{2\pi\hbar}\iint G(\mathbf{r},t) e^{i(\mathbf{Q}\cdot\mathbf{r}-\omega t)} d\mathbf{r}dt$$

$$S_i(\mathbf{Q},\omega) = \frac{1}{2\pi\hbar}\iint G_s(\mathbf{r},t) e^{i(\mathbf{Q}\cdot\mathbf{r}-\omega t)} d\mathbf{r}dt$$

Inelastic coherent scattering measures correlated motions of atoms

Inelastic incoherent scattering measures *self-correlations*
e.g. vibrations, diffusion

Correlation Functions

$$S_{coh}(Q, \omega) \Leftrightarrow F.T. \Rightarrow G(r, t)$$

$$S_{inc}(Q, \omega) \Leftrightarrow F.T. \Rightarrow G_s(r, t)$$

- $G(r, t)$ ≡ Probability of finding an atom at r and at time t when there is an atom at r = 0 at t = 0.

- $G_s(r, t)$ ≡ Probability of finding an atom at r and at time t if the *same atom* was at r = 0 at t = 0.

INCOHERENT INELASTIC NEUTRON SCATTERING

$$\frac{\mathrm{d}^2\sigma}{\mathrm{d}\Omega \mathrm{d}E_f} = \frac{1}{4\pi}\frac{k_f}{k_i}\left[\sigma_{coh} S_{coh}\left(\mathbf{Q},\omega\right) + \sigma_{inc} S_{inc}\left(\mathbf{Q},\omega\right)\right]$$

$$\frac{\mathrm{d}^2\sigma_{inc}}{\mathrm{d}\Omega \mathrm{d}E} = \sum_{\mathbf{q},j}\frac{k'}{k}\delta\left(\hbar\omega \mp \hbar\omega_j\left(\mathbf{q}\right)\right)\frac{\hbar\left(\overline{n}+\frac{1}{2}\pm\frac{1}{2}\right)}{2\omega_j\left(\mathbf{q}\right)}\,\mathrm{x}\sum_r \frac{\left(b_{inc}\right)^2_r}{m_r}\left|\mathbf{Q}.\mathbf{u}_r^j\left(\mathbf{q}\right)\right|^2 \exp\left(-Q^2\left\langle u^2\right\rangle\right)$$

for a powder sample we can average

$$\frac{\mathrm{d}^2\sigma_{inc}}{\mathrm{d}\Omega \mathrm{d}E} = \frac{k'}{k} b_{inc}^2 \frac{Q^2\left\langle u^2\right\rangle}{2m}\left(\overline{n}+\frac{1}{2}\pm\frac{1}{2}\right)\exp\left(-2W\right) N \frac{Z\left(\omega\right)}{\omega}$$

at very low T for hydrogenous materials

$$\frac{\mathrm{d}^2\sigma_{inc}}{\mathrm{d}\Omega \mathrm{d}E} = \frac{k'}{k} b_{inc}^2 S_{inc}\left(\mathbf{Q},\omega\right) \qquad S_{inc}\left(\mathbf{Q},\omega\right) = Q^2\left\langle u^2\right\rangle \exp\left(-2W\right)$$

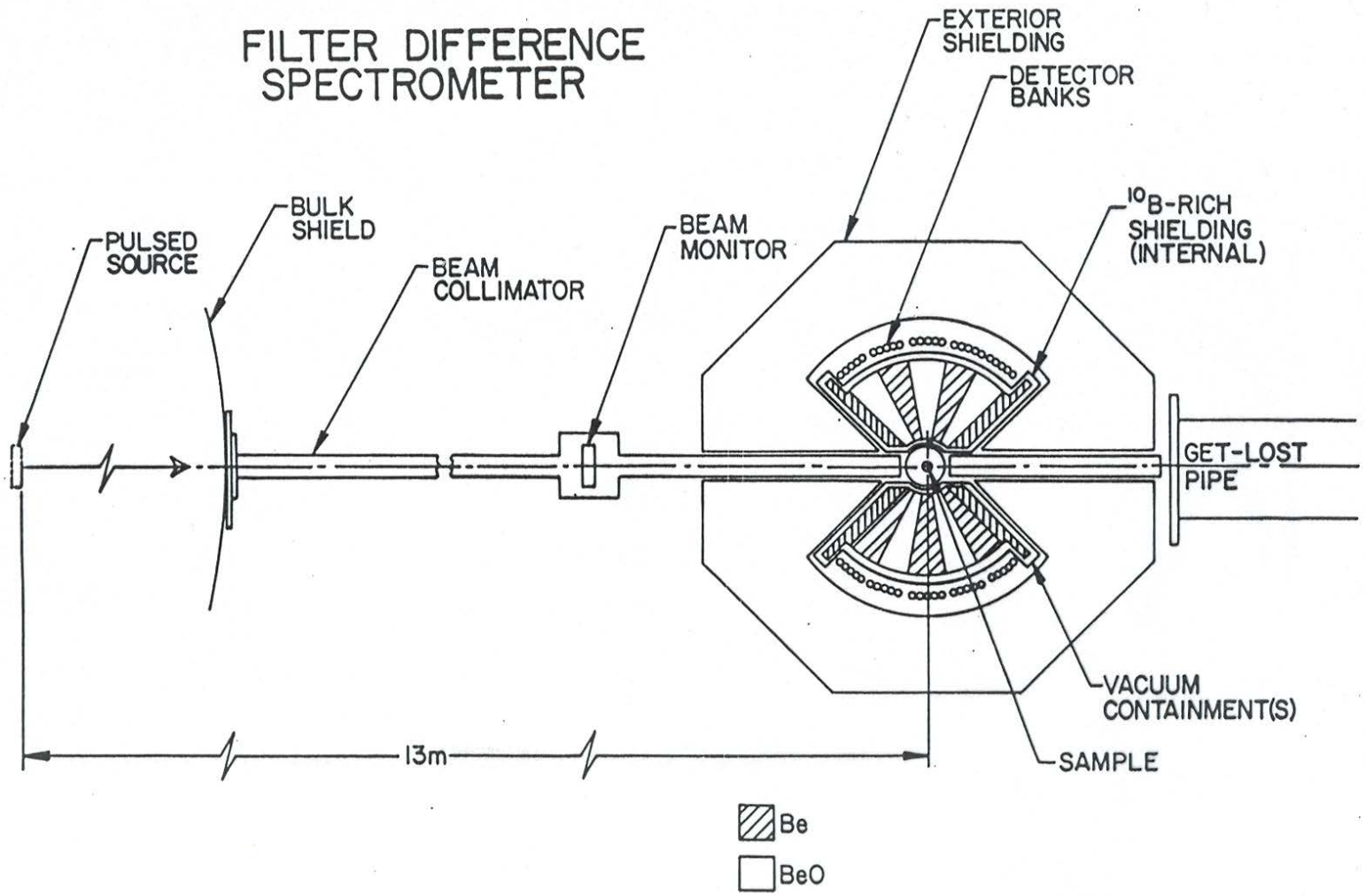
FILTER DIFFERENCE SPECTROMETER
EXTERIOR SHIELDING
DETECTOR BANKS
^{10}B-RICH SHIELDING (INTERNAL)
BULK SHIELD
PULSED SOURCE
BEAM COLLIMATOR
BEAM MONITOR
GET-LOST PIPE
VACUUM CONTAINMENT(S)
SAMPLE
13m
Be
BeO

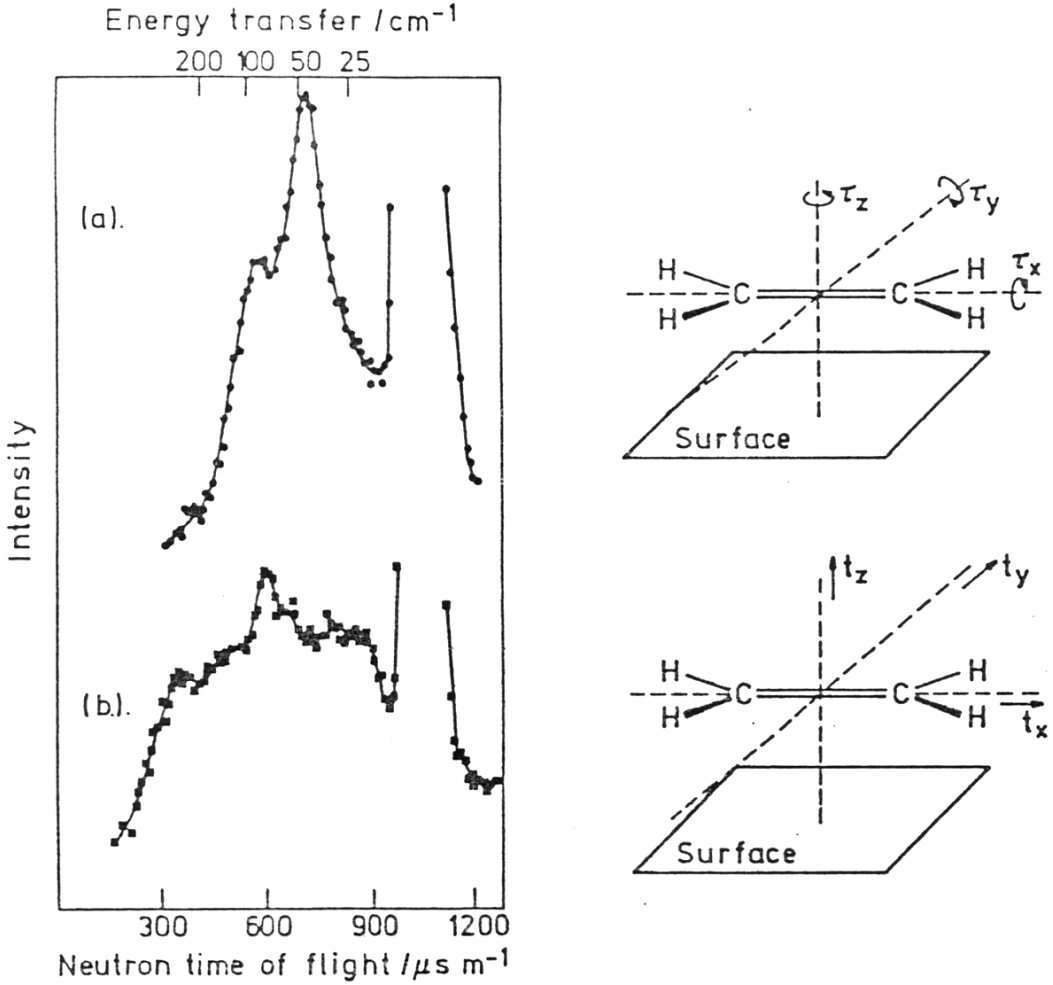

The inelastic neutron scattering from (*a*) ethylene adsorbed on an Ag-13X zeolite catalyst and (*b*) the catalyst alone. The spectra were taken on the Harwell DIDO 6H double rotor spectrometer by Howard et al

The INS Difference-Spectrum of $\{[P_2N_2Zr]_2\ (\mu\text{-}H)(\mu\text{-}N_2H)\}$

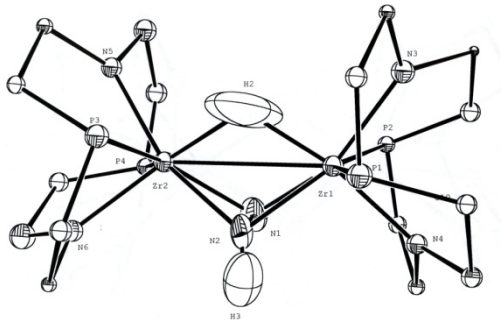

$$\left\langle u_1^2 \right\rangle = \frac{h}{8\pi^2 \mu \nu} \coth\left(\frac{h\nu}{2kT}\right)$$

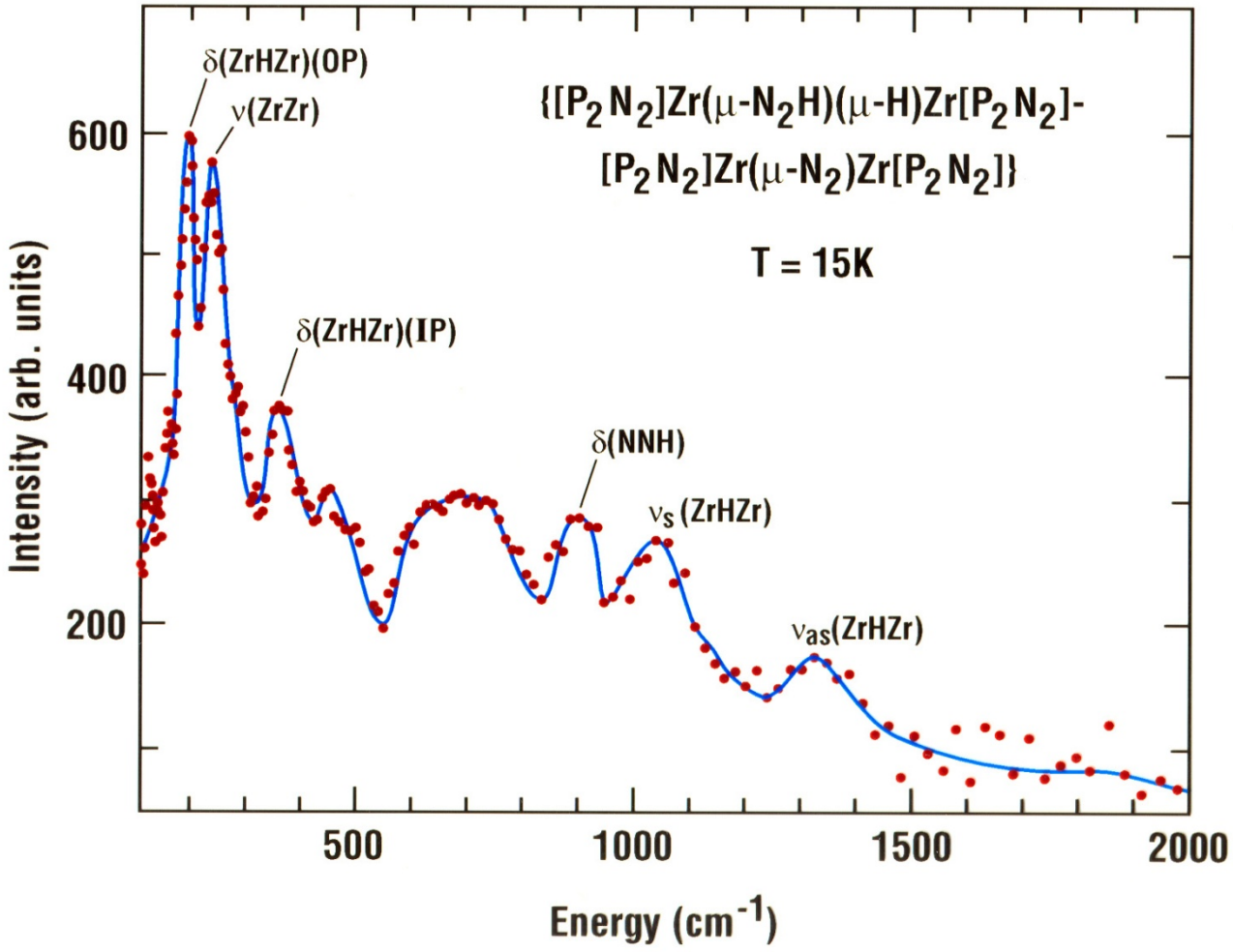

The Structure of $[Co(CO)_{15}H]^-$

$$[Co_6(CO)_{15}]^{2-} + H^+ \longrightarrow [HCo_6(CO)_{15}]^-$$

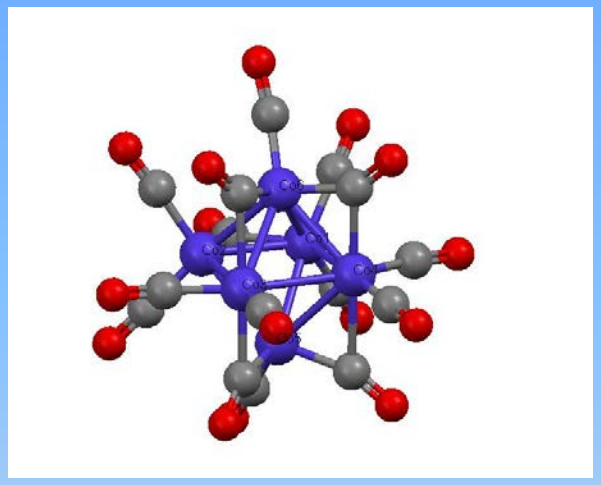

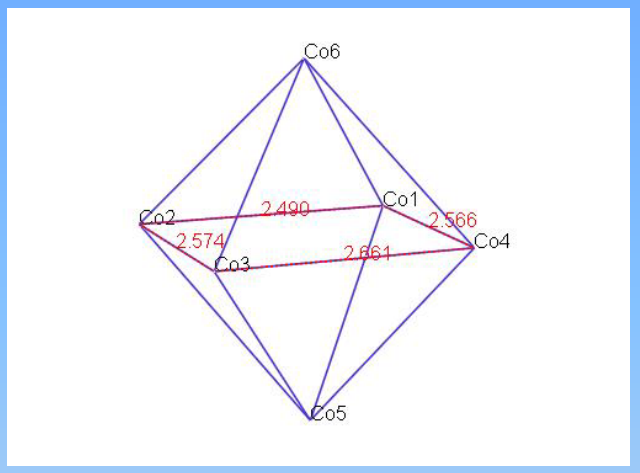

NMR (solution) δ ~ +3

Hydride δ ~ -5 -40

Formyl δ ~ +5 +10

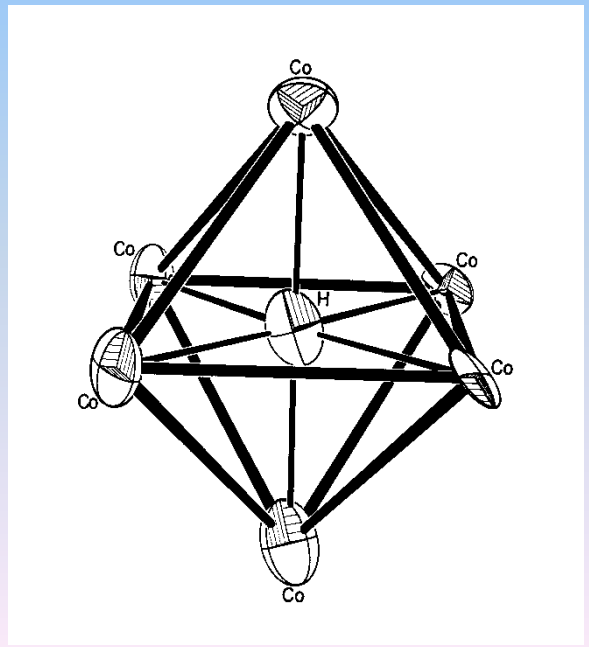

D. Hart & al.*JACS* **1981**, *103* 1458

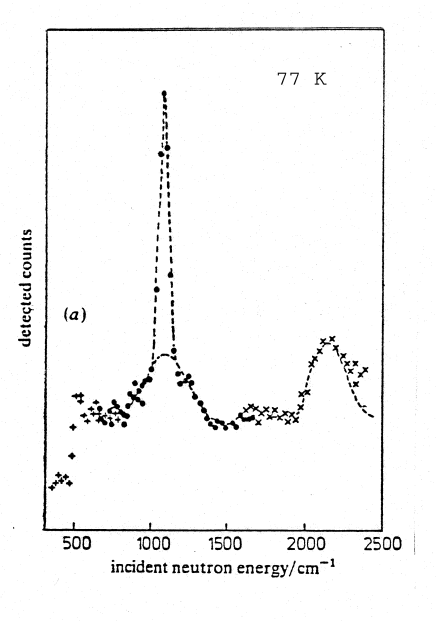

$Cs[Co_6(CO)_{15}H]$

IN1 - ILL (30g)

***J. Howard* (1983)**

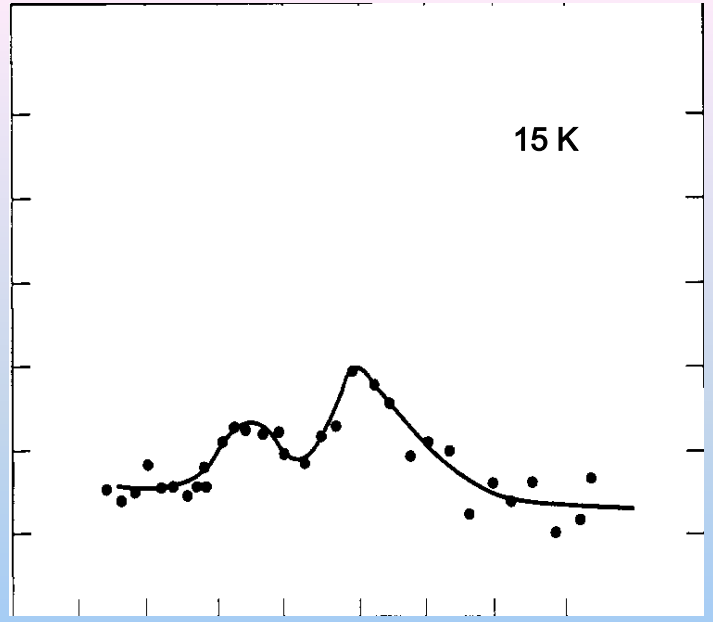

$K[Co_6(CO)_{15}H]$

Be Filter - LANSCE (1987)

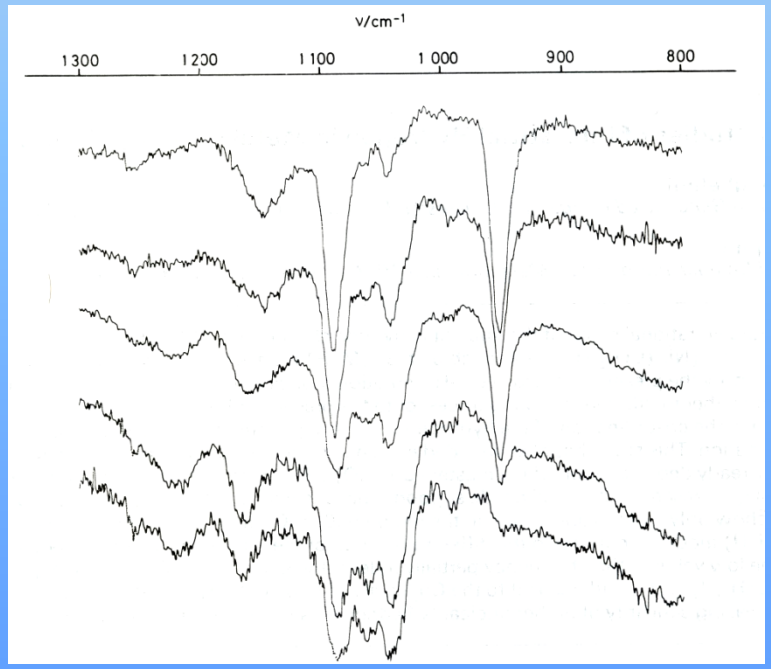

I.R.

$K[Co_6(CO)_{15}H]$ (CsI)

***Longoni & Stanghellini* (1987)**

TFXA

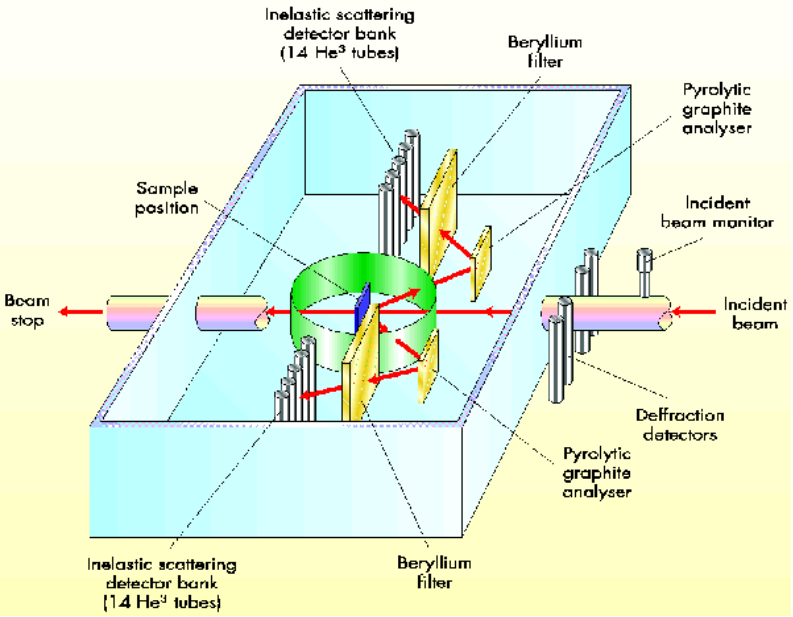
Inelastic scattering detector bank (14 He³ tubes)
Beryllium filter
Pyrolytic graphite analyser
Sample position
Incident beam monitor
Beam stop
Incident beam
Deffraction detectors
Pyrolytic graphite analyser
Inelastic scattering detector bank (14 He³ tubes)
Beryllium filter

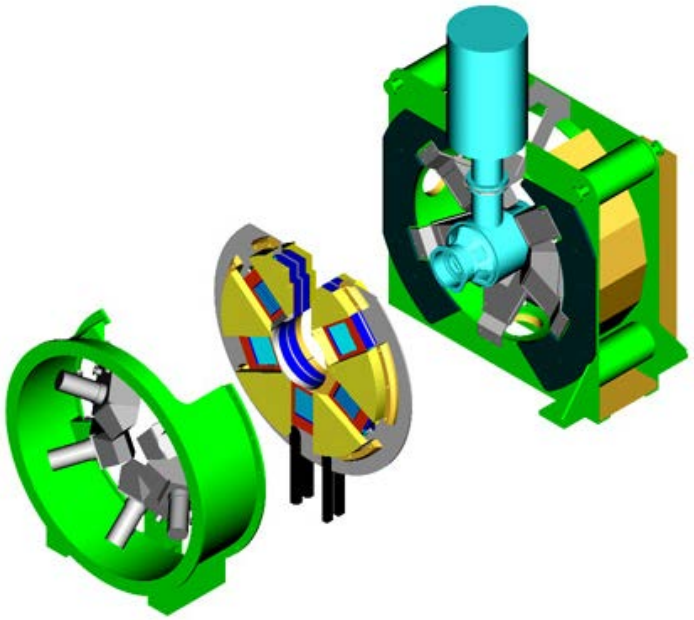

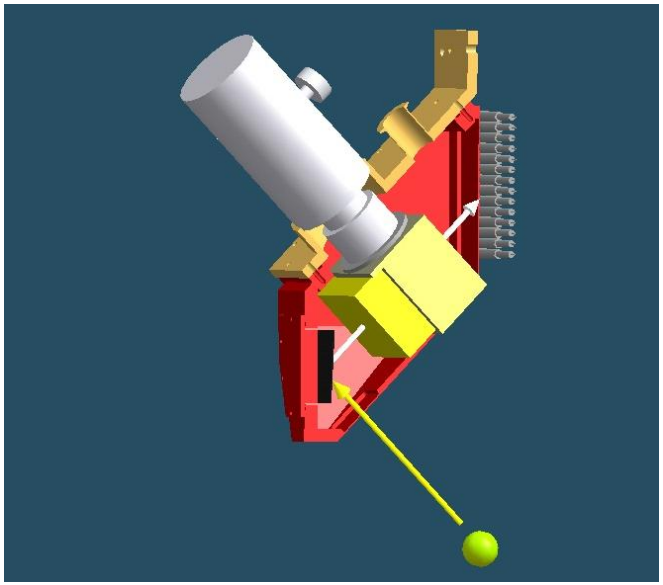

TOSCA

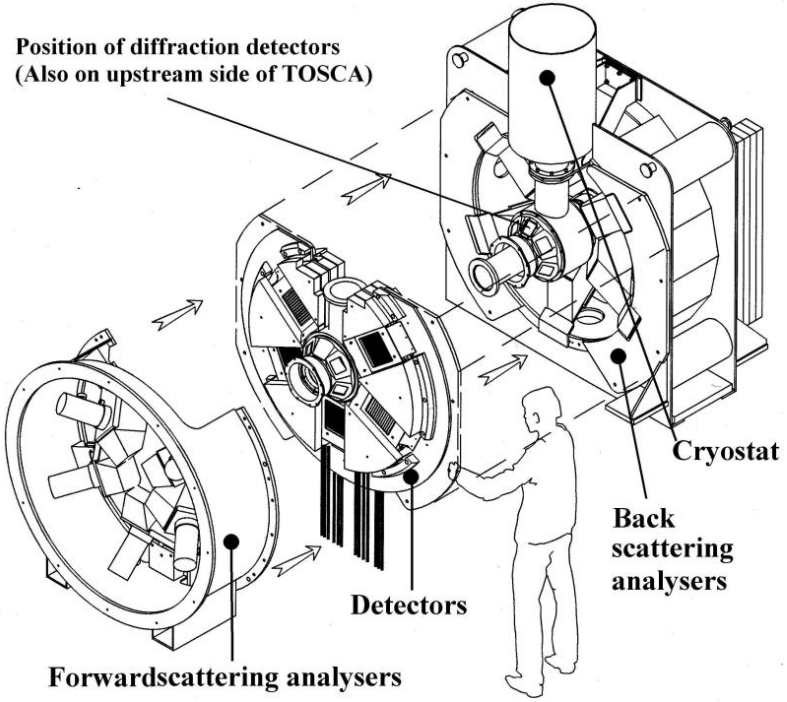
Position of diffraction detectors
(Also on upstream side of TOSCA)
Cryostat
Back scattering analysers
Detectors
Forwardscattering analysers

TOSCA at ISIS

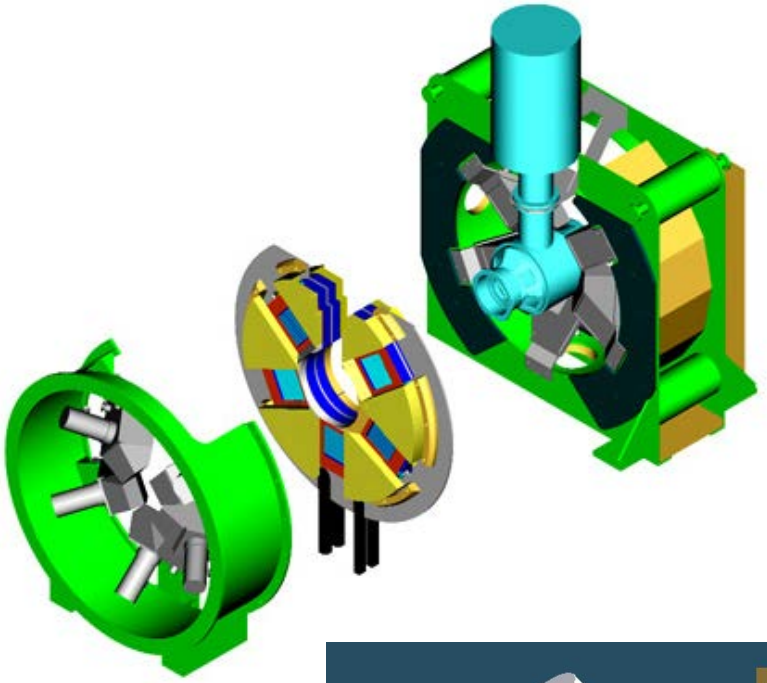

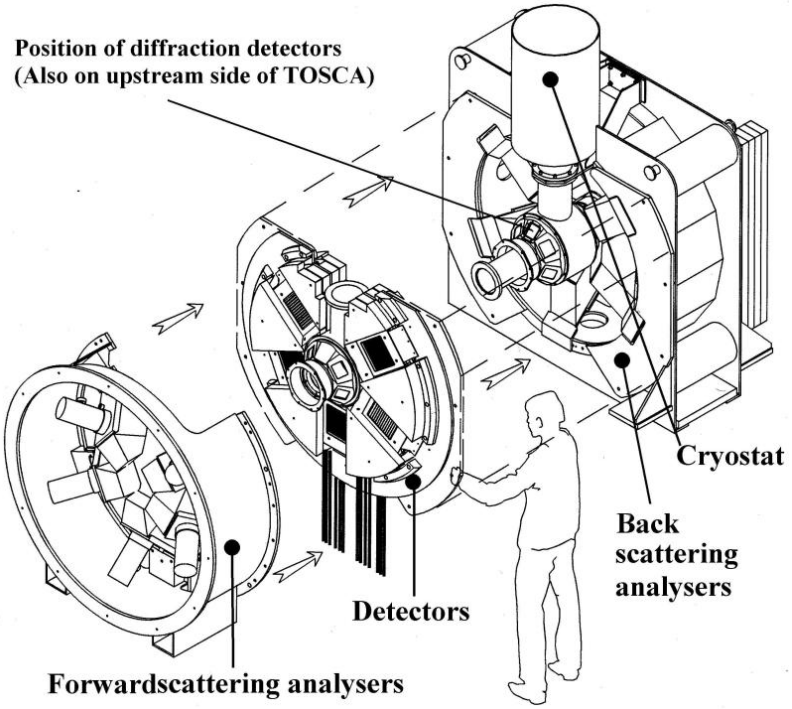

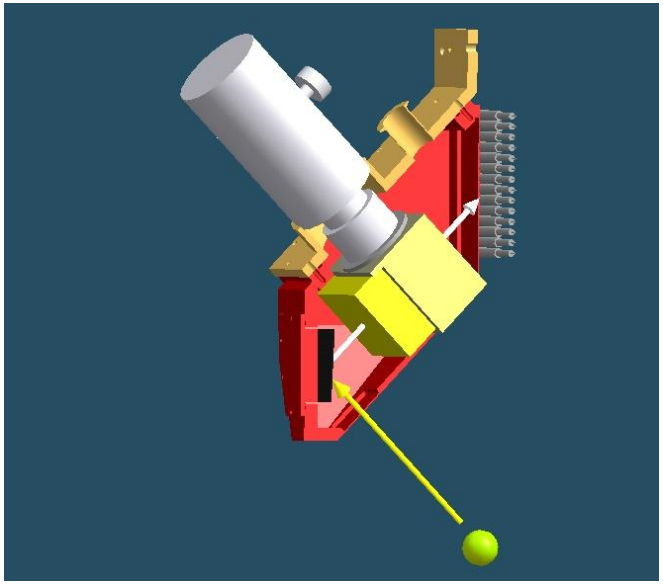

INS & I.R. Spectra of $X[Co_6(CO)_{15}H]$

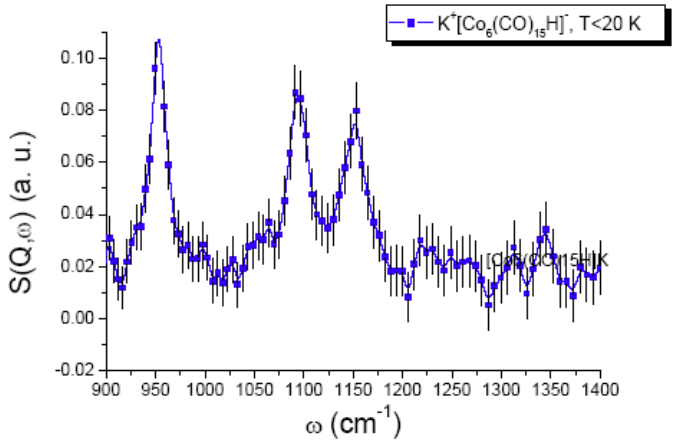

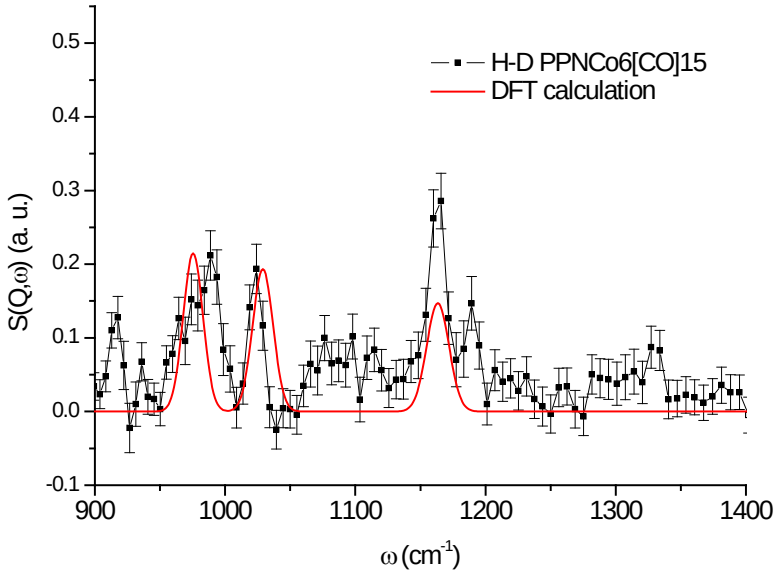

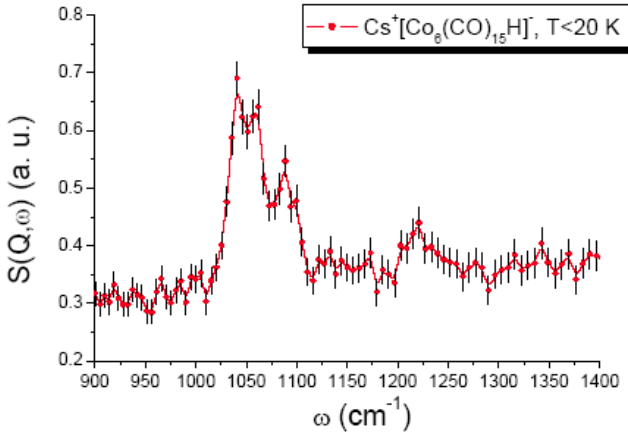

T = 20K

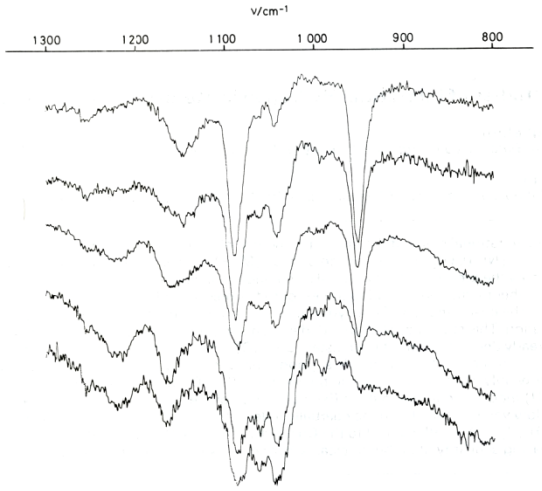

$K[Co_6(CO)_{15}H]$ in CsI

INS & I.R. Spectra of $X[Co_6(CO)_{15}H]$

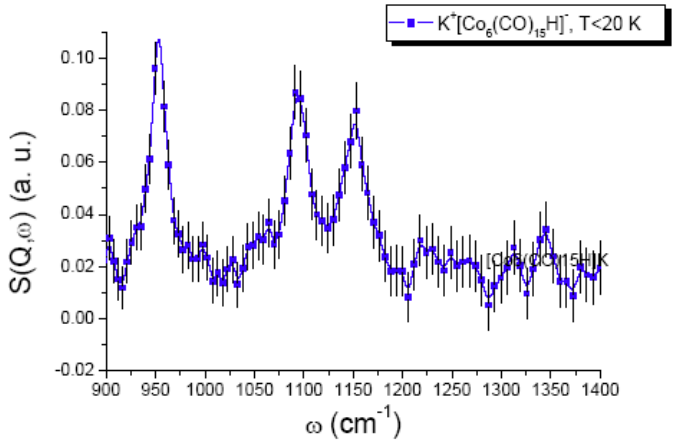

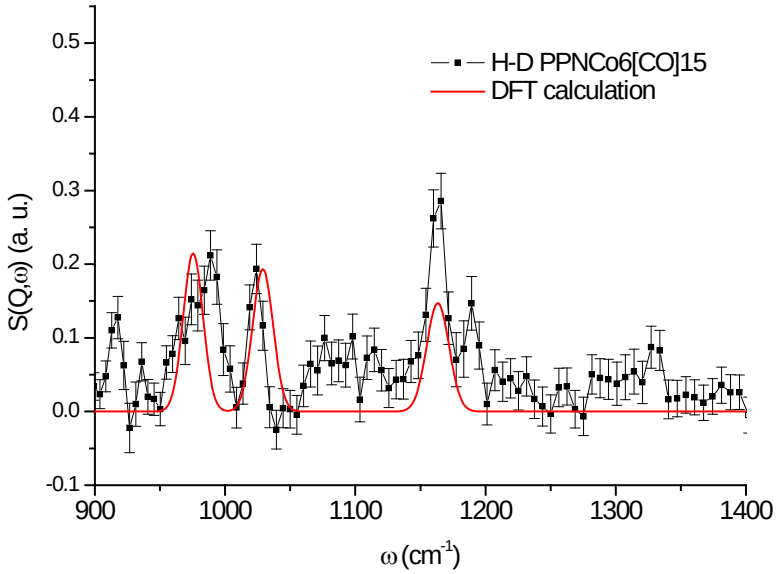

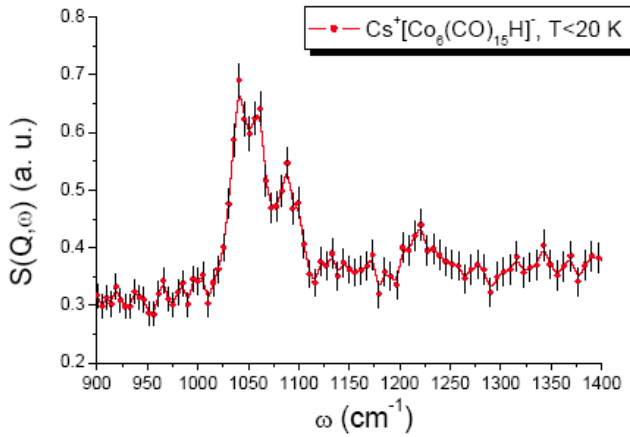

T = 20K

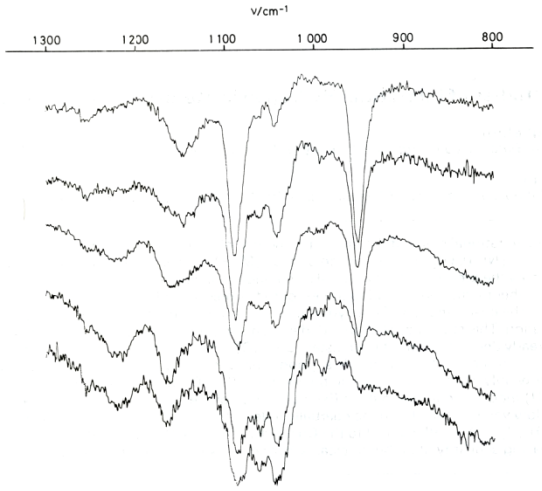

$K[Co_6(CO)_{15}H]$ in CsI

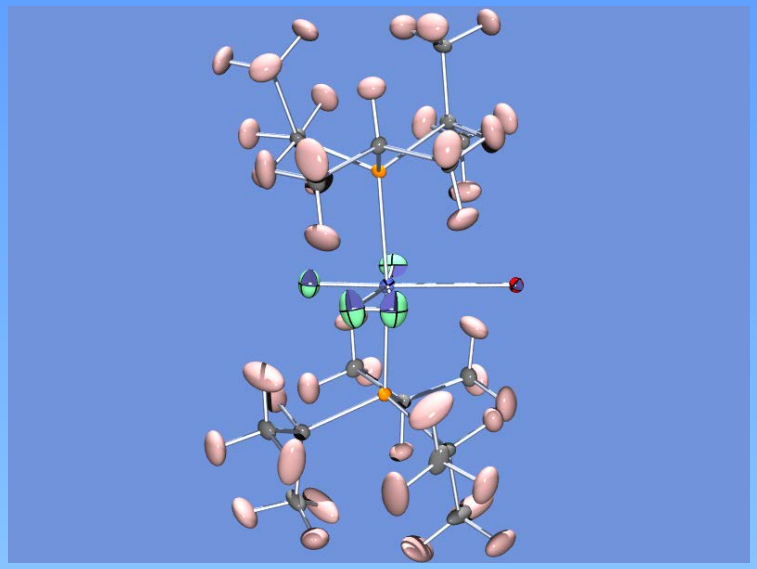

H-H Distances (Å) vs. J^{HD} (Hz)

	$d_{(H-H)}$	J^{HD}
$W(CO)_3(P^iPr_3)_2(H_2)$	0.82 (1)	34.0
$[Fe(dppe)_2(H)(H_2)]^+$	0.82 (2)	30.5
$[Ru(dppe)_2(H)(H_2)]^+$	0.82 (3)	32.0
$[Os(dppe)_2(H)(H_2)]^+$	0.79 (2)	25.5

INS Spectra of M-(H_2) Complexes

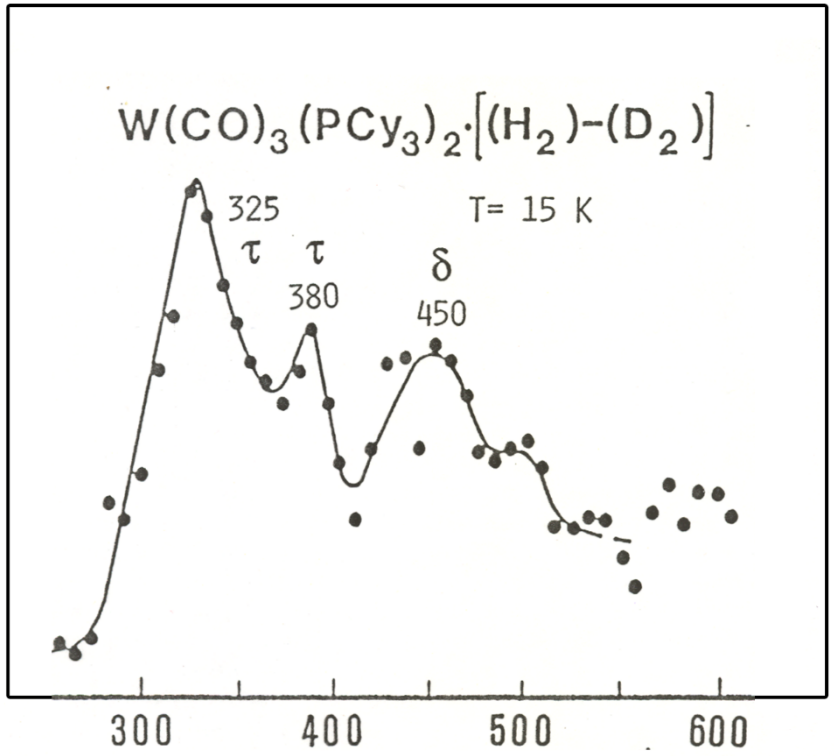

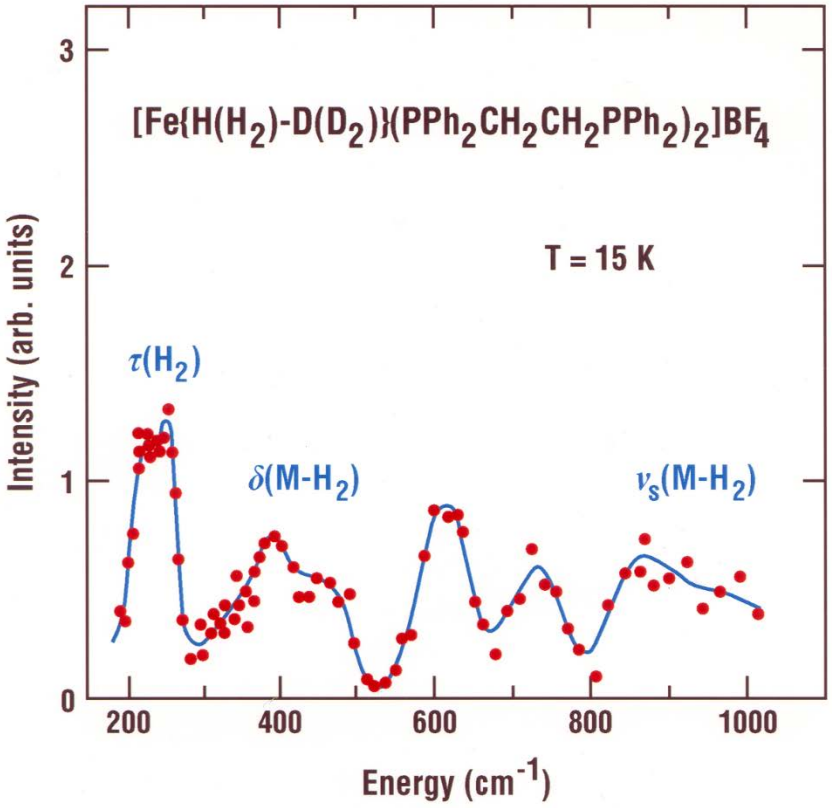

M-(η^2-H_2) Bonding

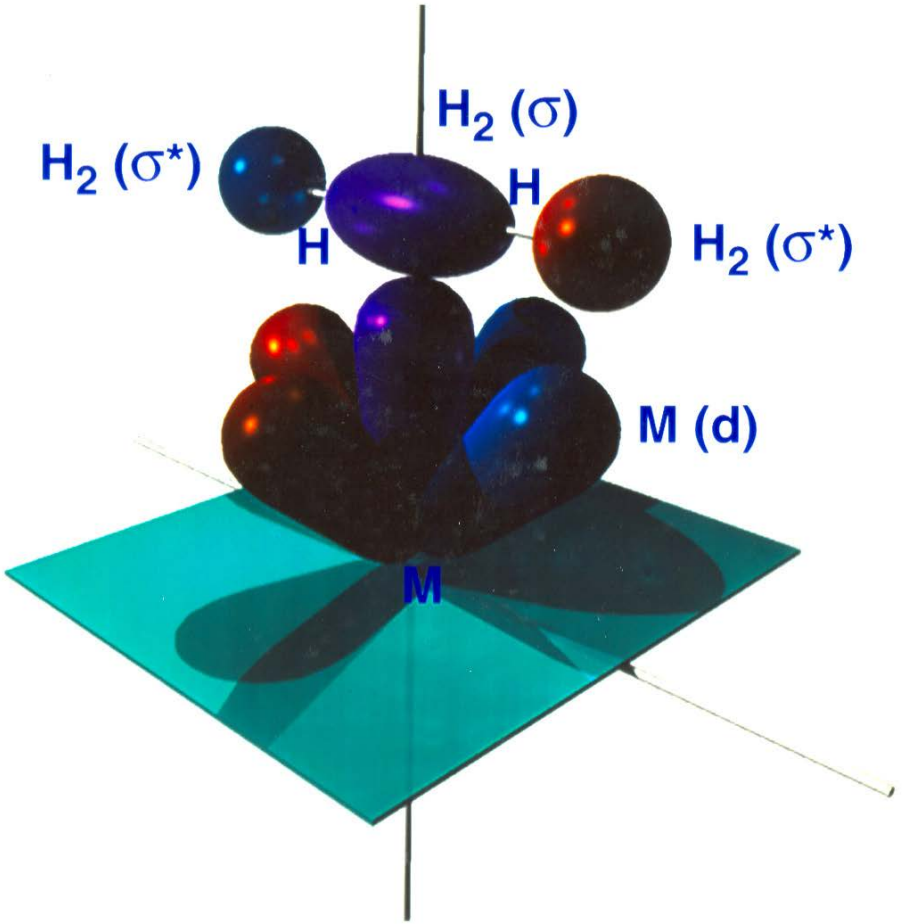

Non-classical Hydrides and Rotational Tunnelling Spectroscopy

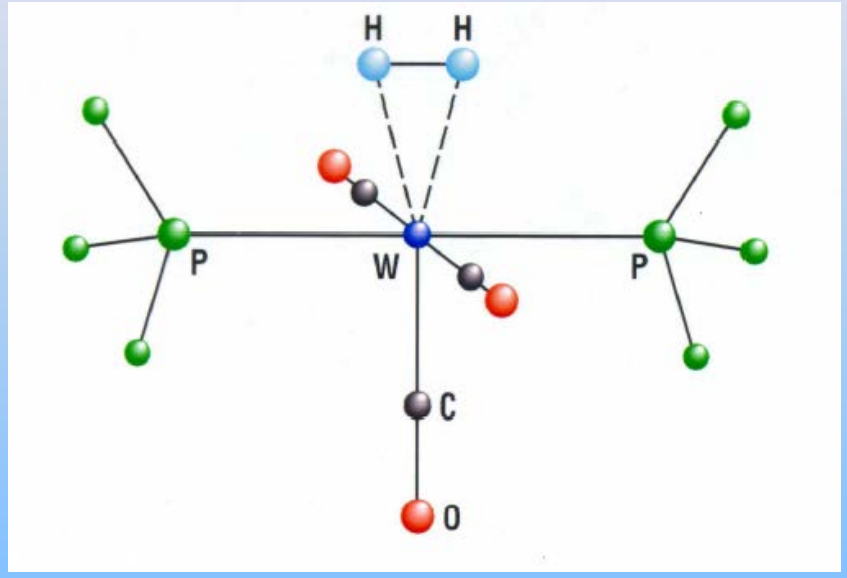

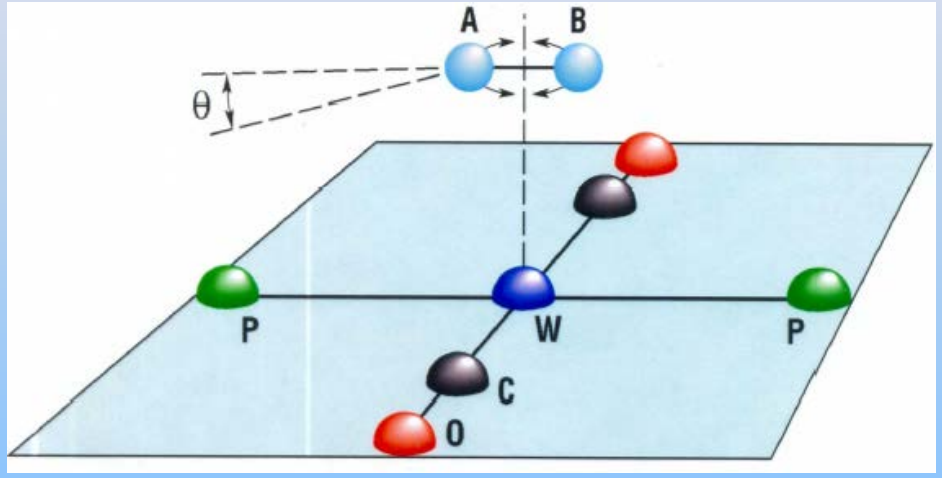

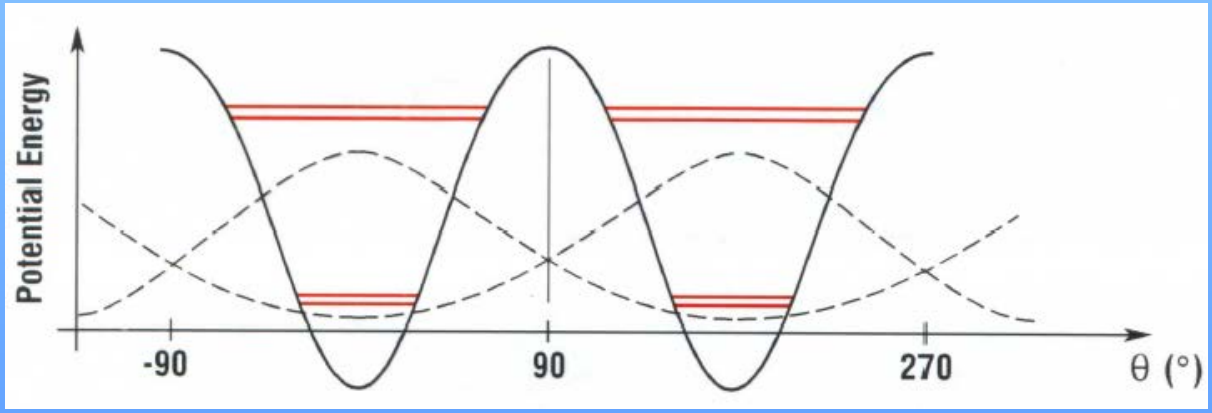

Rotational Tunnelling: Single Particle Rotation

For a single particle model (i.e.: V(ω) describes the system):

$$\mathrm{H}\Phi_i = \varepsilon_i \Phi_i$$

where

$$\mathrm{H} = B\nabla^2 + V(\varphi)$$

$$V(\varphi) = \sum_j \frac{Vnj}{2}\left(1 - \cos njn\varphi\right)$$

n=2 twofold potential
n=3 threefold potential

$$B = \hbar^2 / (2I)$$

The level splitting is proportional to *V*(*φ*) and B

B: H_2 (7.3 meV) > NH_4^+, NH_3 (0.782 meV) > CH_4, $-CH_3$ (0.655 meV)

Single Particle Rotation: Twofold potential

For a 1D rotor in a twofold-potential:

$$V(\varphi) = \tfrac{1}{2} V_2 \cos 2\varphi$$

$$\left(-B \frac{\partial^2}{\partial \varphi^2} + \tfrac{1}{2} V_2 \cos 2\varphi \right) \Psi = E\Psi$$

Eigenvalues (in units of B) are determined by the ratio V(f)/B

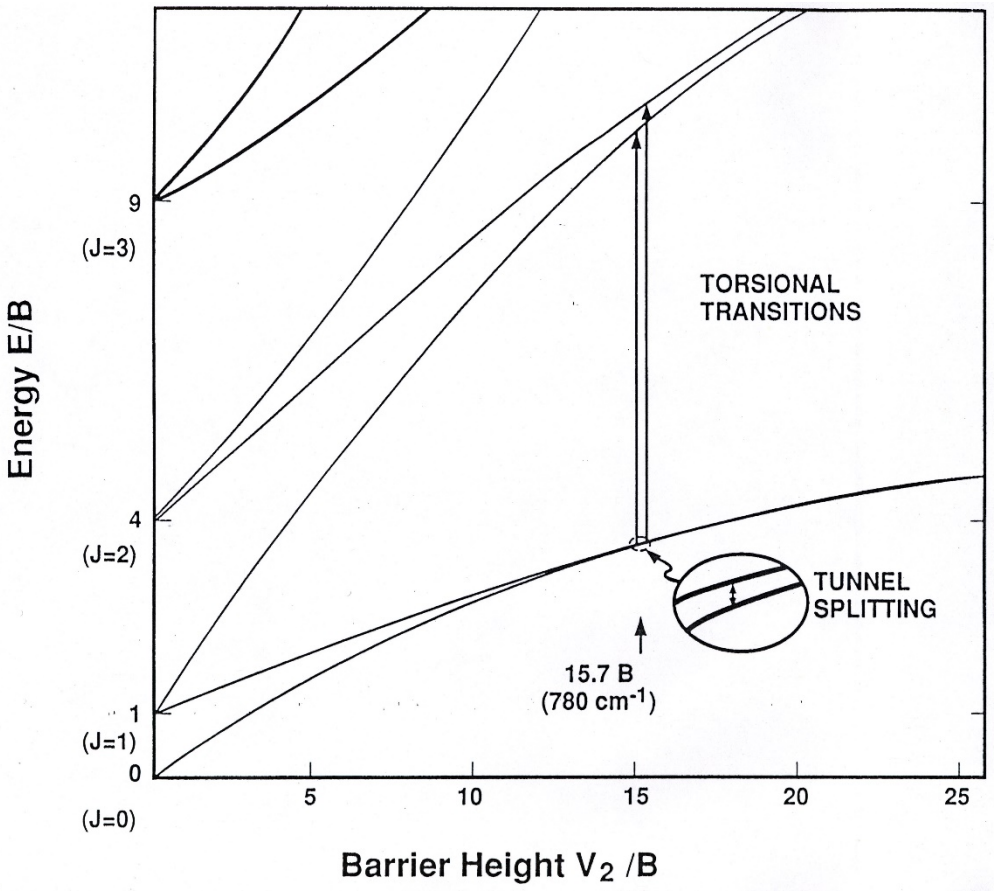

W. Press Single Particle Rotations in Crystals (Springer)

Prager, Heidemann Chem. Rev. ***97***, 2933 (1997)

The new IN5 Spectrometer

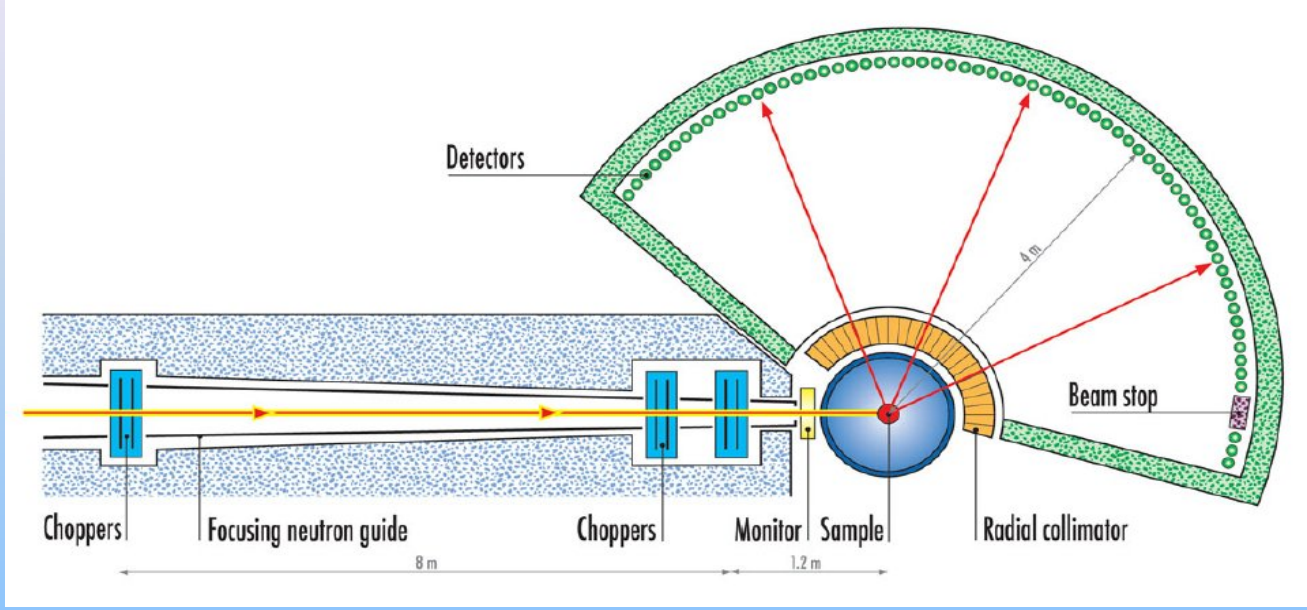

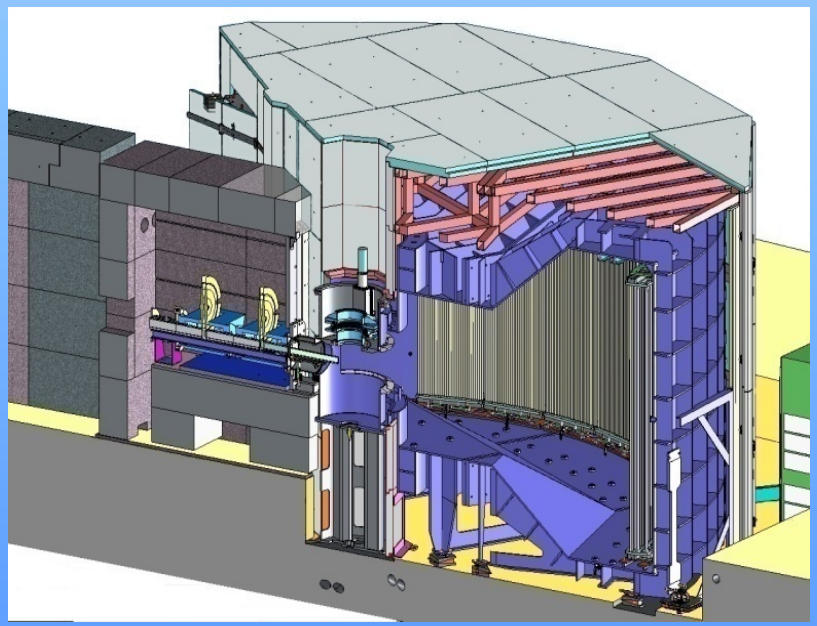

Detectors

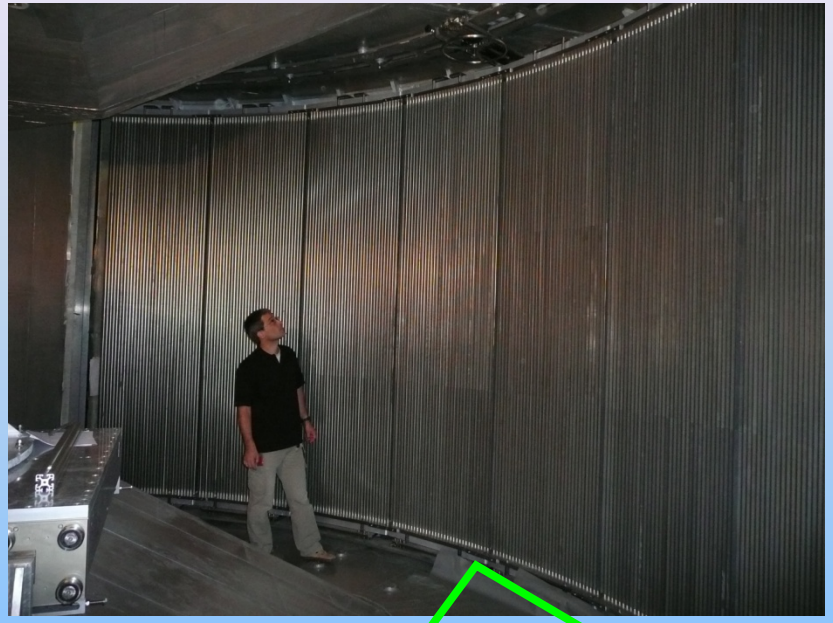

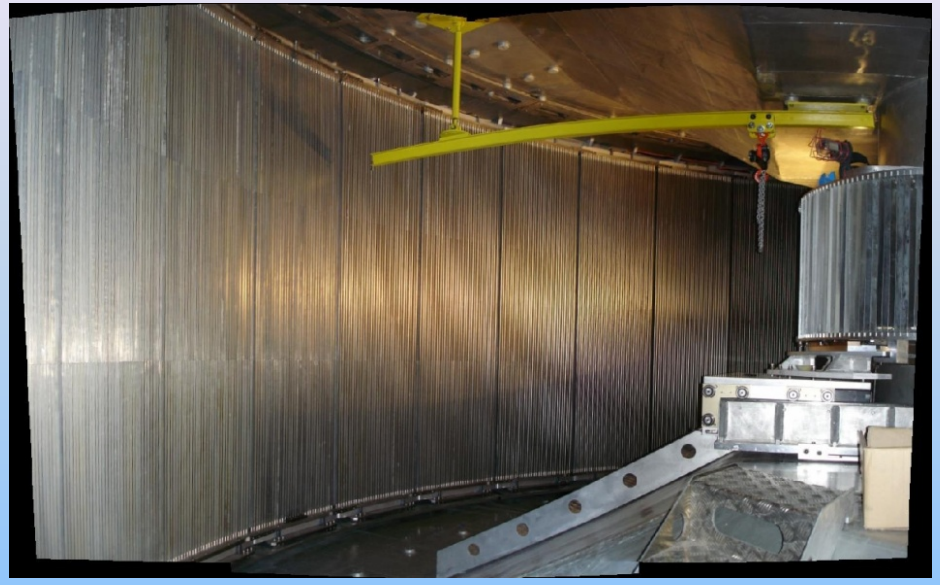

Effective Height 3.0 m

~3000 L ^{3}He + 570 L CF_4

4.75 bar ^{3}He + 1.25 bar CF_4

147.5° Hor - ± 20.55° vert

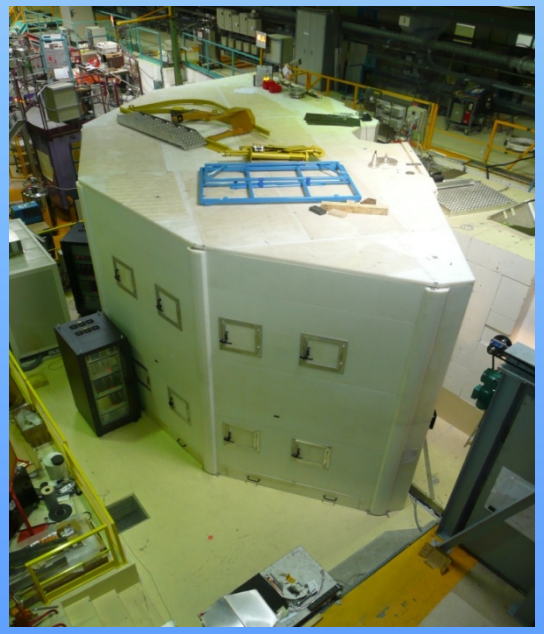

Rotational Tunnelling in $[Fe(H)_2(H_2)L_3]$ and $[Ru(H_2)(H)(dppe)_2]^+$

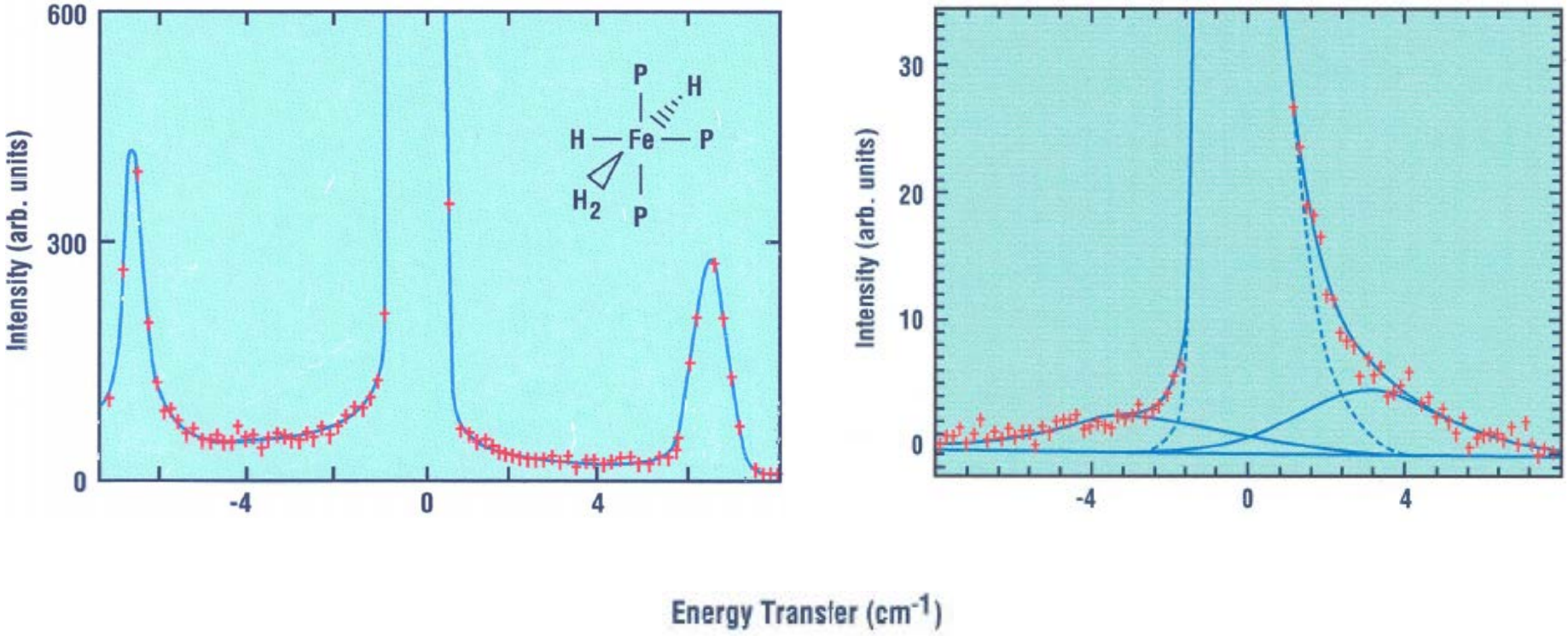

Rotational Tunnelling in $Ru(H_2)_2(H)_2(Pcyp_3)_2$

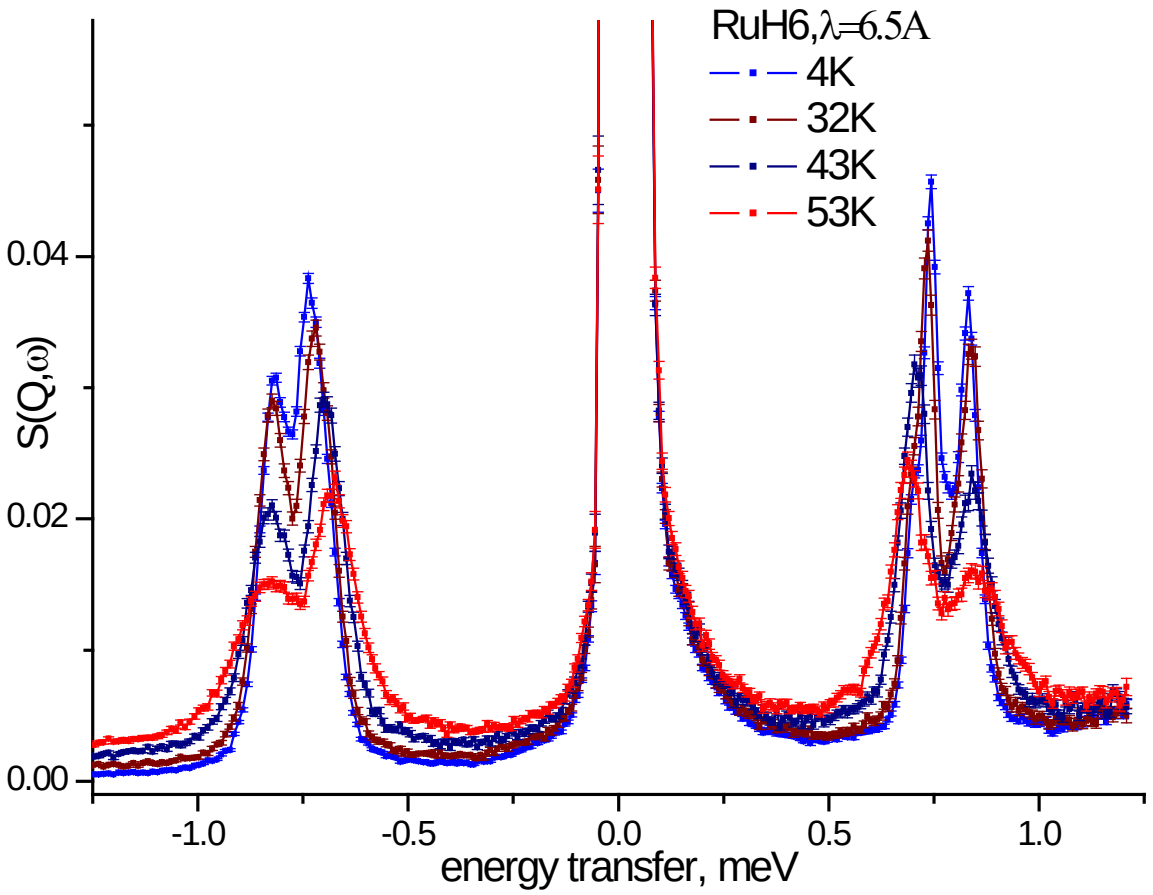

Rotational Tunnelling in $Ru(H)_2(H_2)_2L_2$

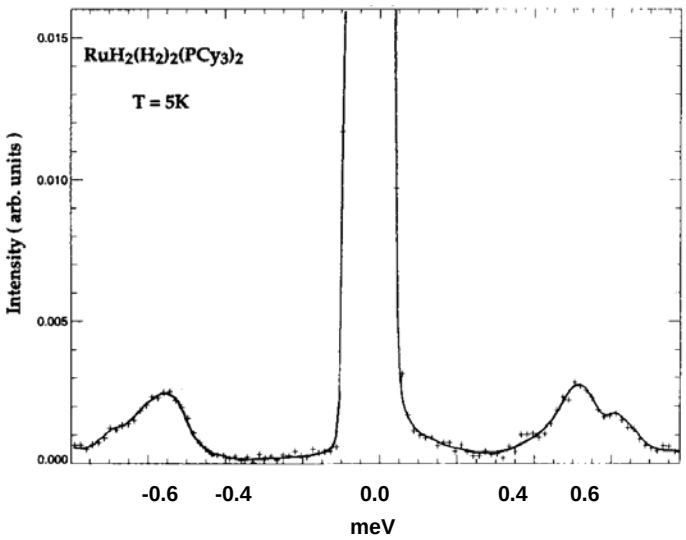

$L = P(cy)_3$

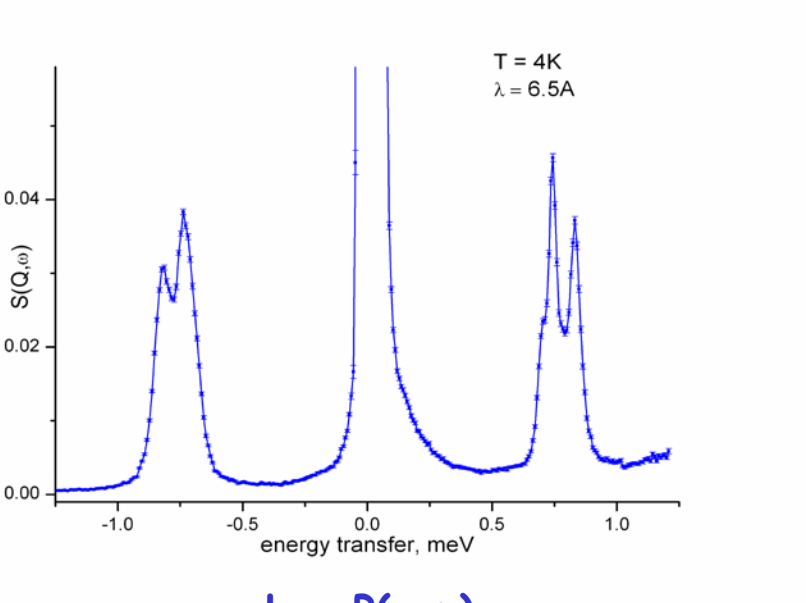

$L = P(cyp)_3$

V_φ = 0.99, 1.09 kcal/mol

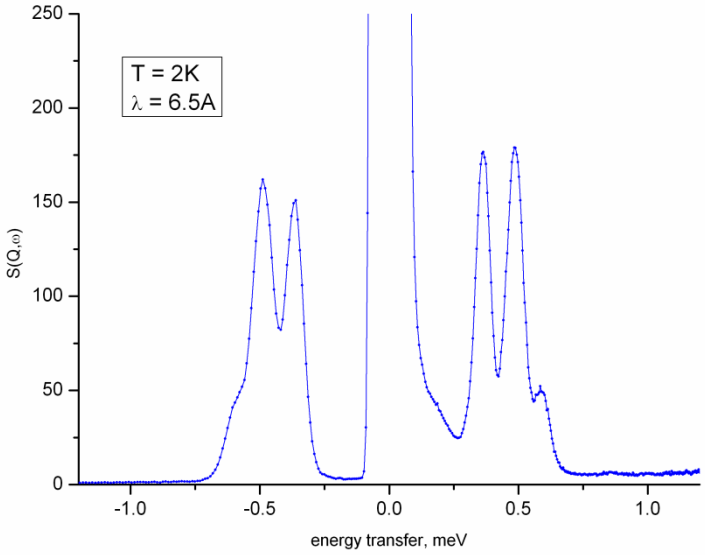

$L = P(cy)_2(^tBut)$

VIBRATIONAL FREQUENCIES and TUNNEL SPLITTINGS for M-H_2 COMPLEXES

Compound	ν(H-H) [cm^{-1}] (IR)	τ(H-H) [cm^{-1}]	ω_t [cm^{-1}]	V_t [kcal/mol]
$W(CO)_3(P\,^iPr_3)_2(H)_2$	2695	370 - 340	0.73	2.4
$W(CO)_3(PCy_3)_2(H)_2$	2690	380 - 325	0.89	2.2
$[Fe(PP_3)(H)(H_2)]^+$		276 - 259	1.15	1.9
$[Ru(PP_3)(H)(H_2)]^+$		225 – 184	2.58	1.6
$IrBr(P\,^iPr_3)_2(H)_2(H_2)$			18.9	0.53
$IrI(P\,^iPr_3)_2(H)_2(H_2)$			9.8	0.98

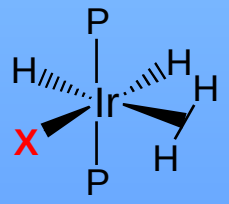

A Schematic Diagram of the Energy Levels of a Methyl Rotor In a Three-Fold Potential

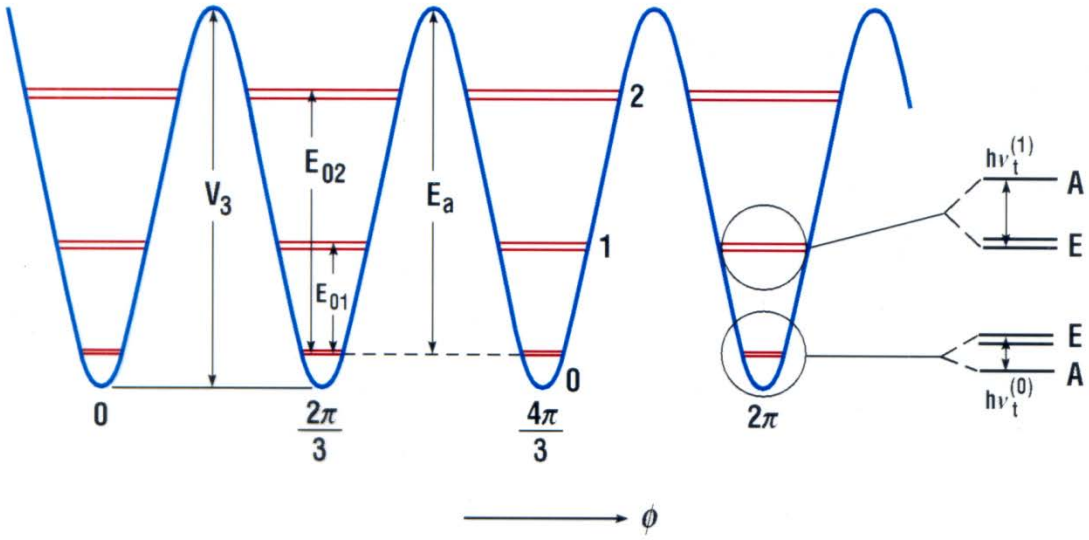

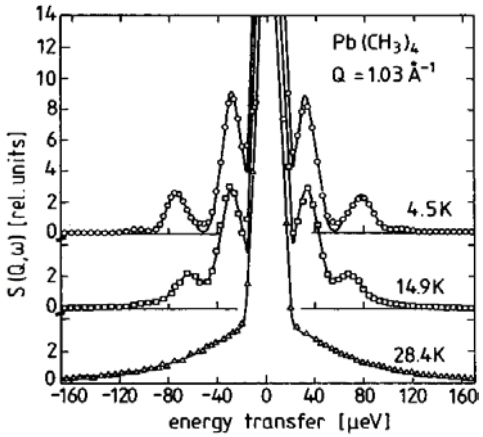

$[(CH_3)_4Pb]$
Prager, Heidemann Chem Rev (1997)

$(^{i}Pr_3P)_2IrI(H)_2(H)_2$

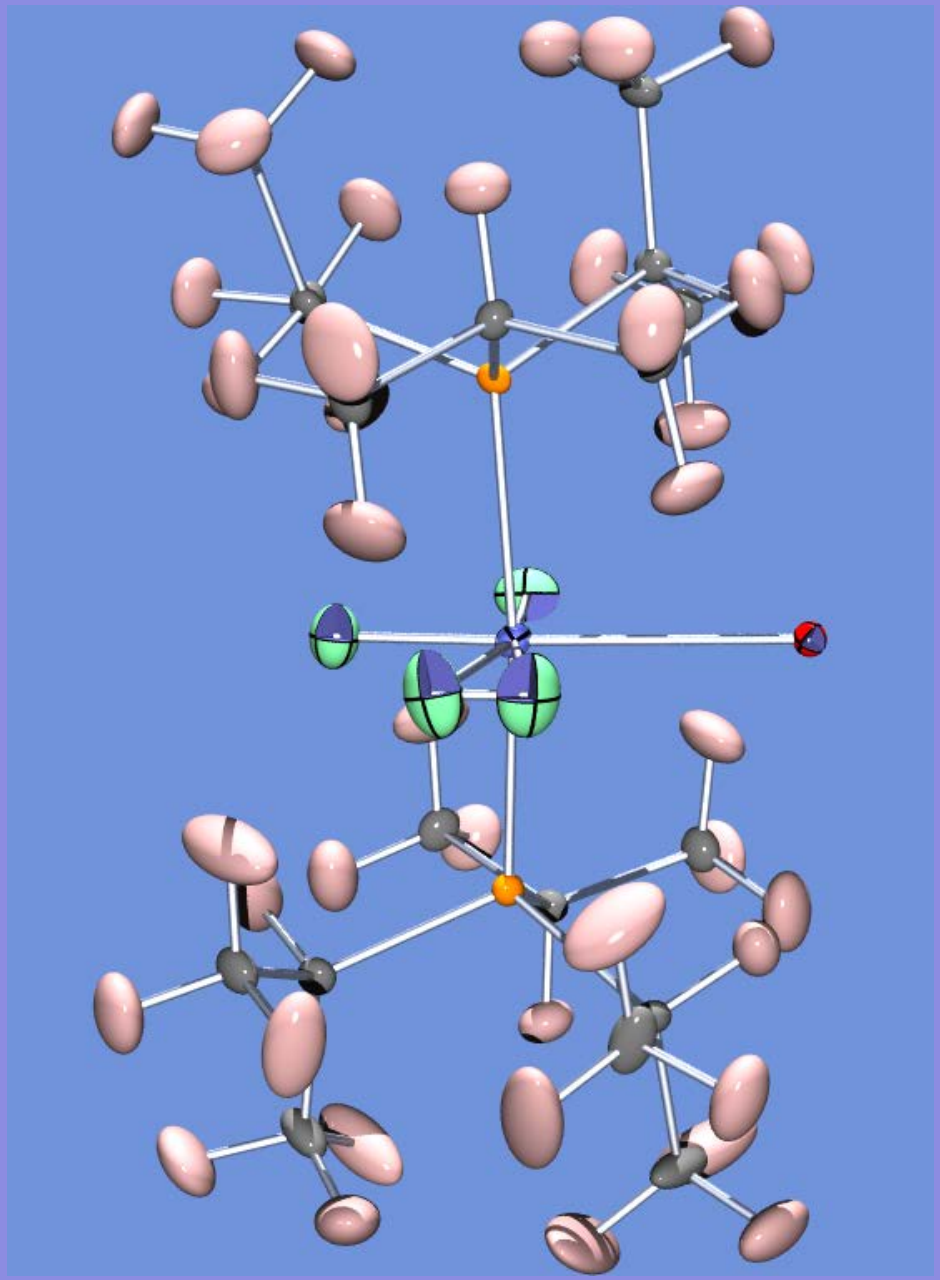

Dihydrogen-Hydride Exchange in $(^{i}Pr_3P)_2IrX(H)_2(H)_2$

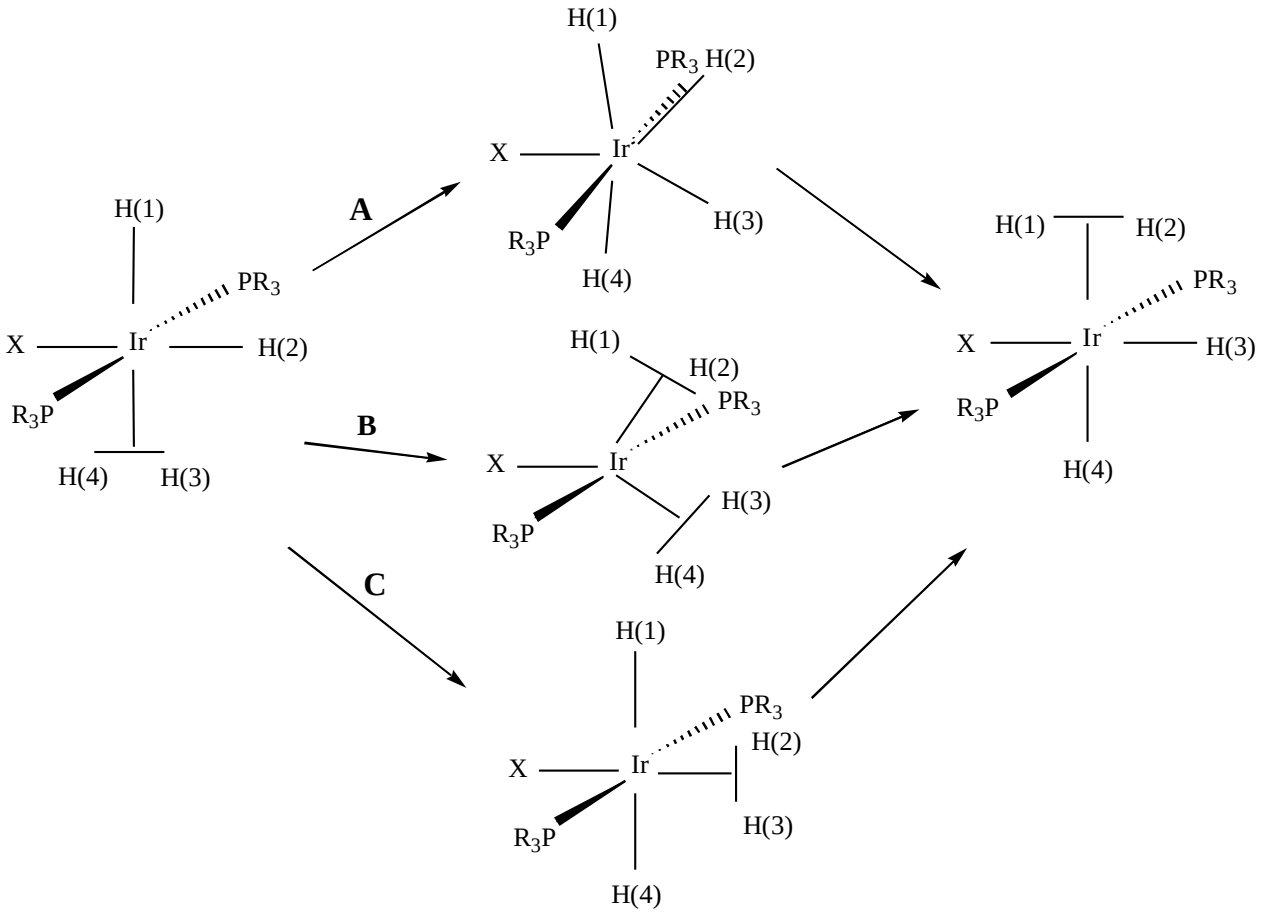

$(^{i}Pr_3P)_2IrX(H)_2(H)_2$

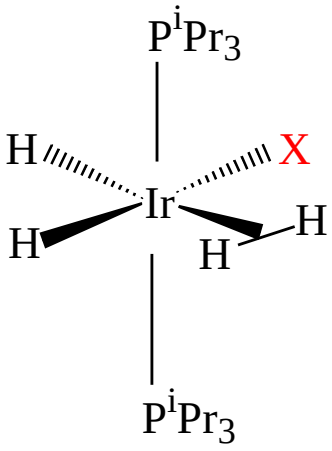

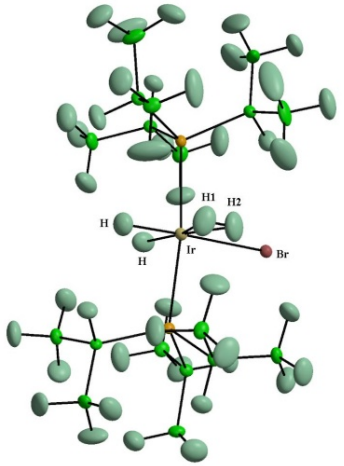

X	**Cl**	**Br**	**I**
Rotat. tunnelling freq. (ω, cm^{-1})	20	19	6
Rotat. barrier V^2_{exp} (kcal/mole)	0.51(3)	0.48(3)	1.00(4)
Rotat. barrier V_{calc} (**PMe_3 / PH_3** kcal/mole)	0.37 (2.04)	0.42 (2.11)	0.66 (2.32)
H-H (exp)	*0.78* (INS)	0.819(8)	0.856(9)
H-H (calc)	0.853	0.857	0.862

$(^iPr_3P)_2IrX(H)_2(H)_2$: Observed and Calculated Exchange Energies (QENS & B3LYP)

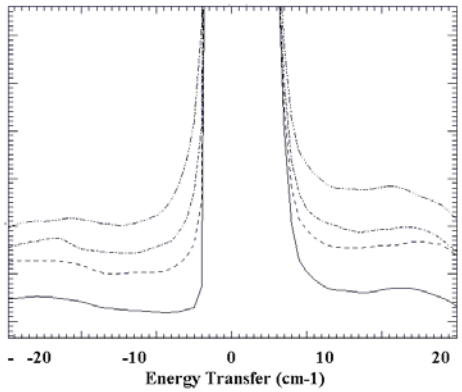

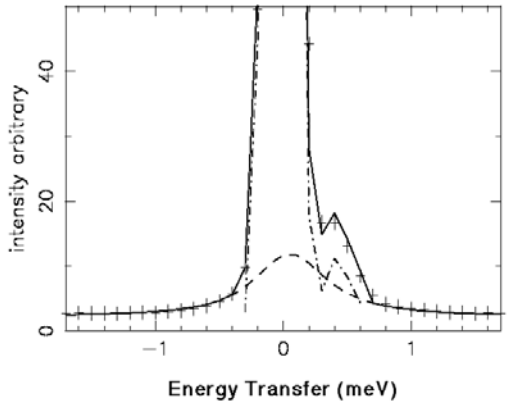

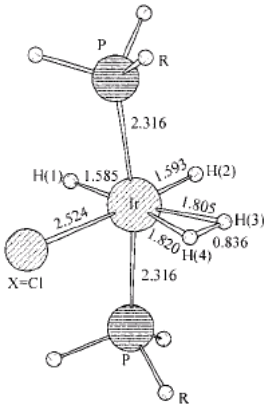

Reactant

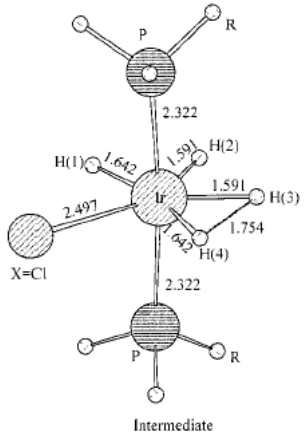

Intermediate

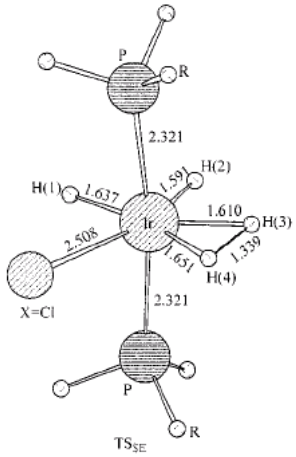

TS_{SE}

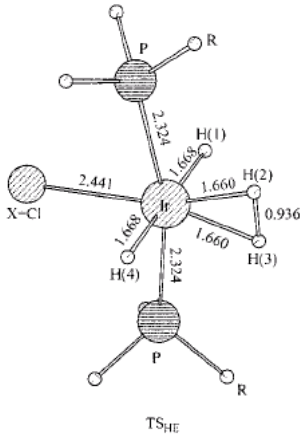

TS_{HE}

Data @ 100, 175, 210, 250 K
ΔE_a = 1.5(2) Kcal/mol

B3LYP/BS4 (reactant, intermediate, TS's)
ΔE_{TS} = 1.87 kcal/mol

Dihydrogen-Hydride Exchange in $(^{i}Pr_3P)_2IrX(H)_2(H)_2$

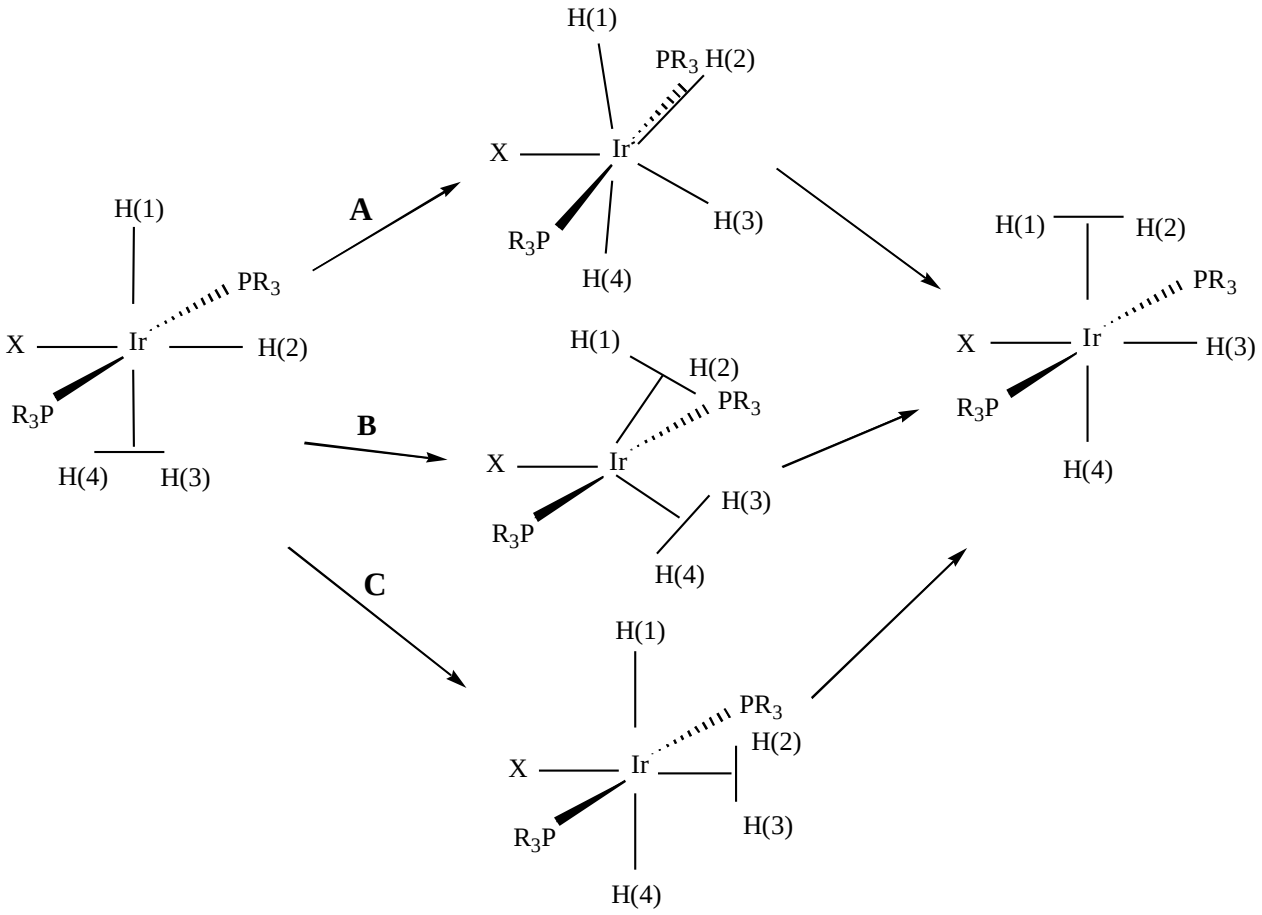

Rotational Tunnelling in $Ru(H_2)_2(H)_2(Pcyp_3)_2$

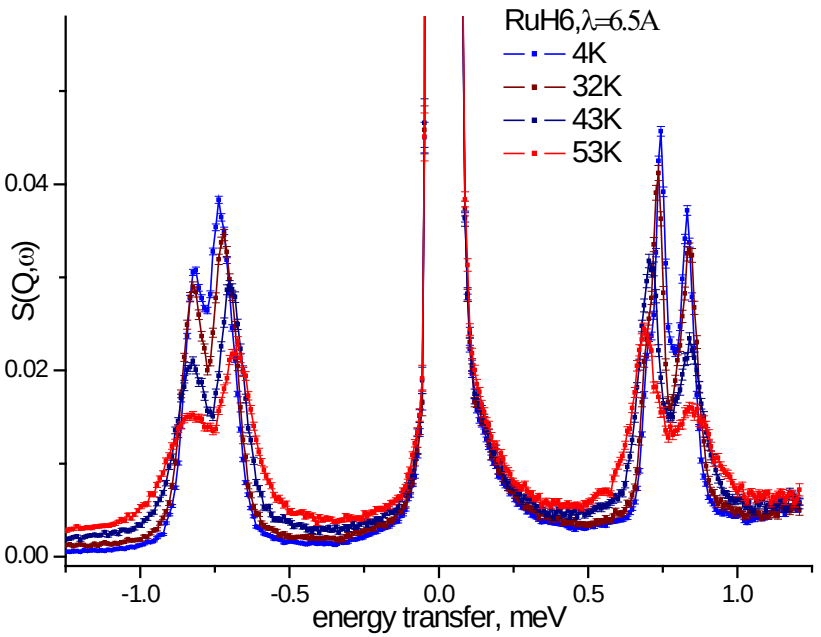

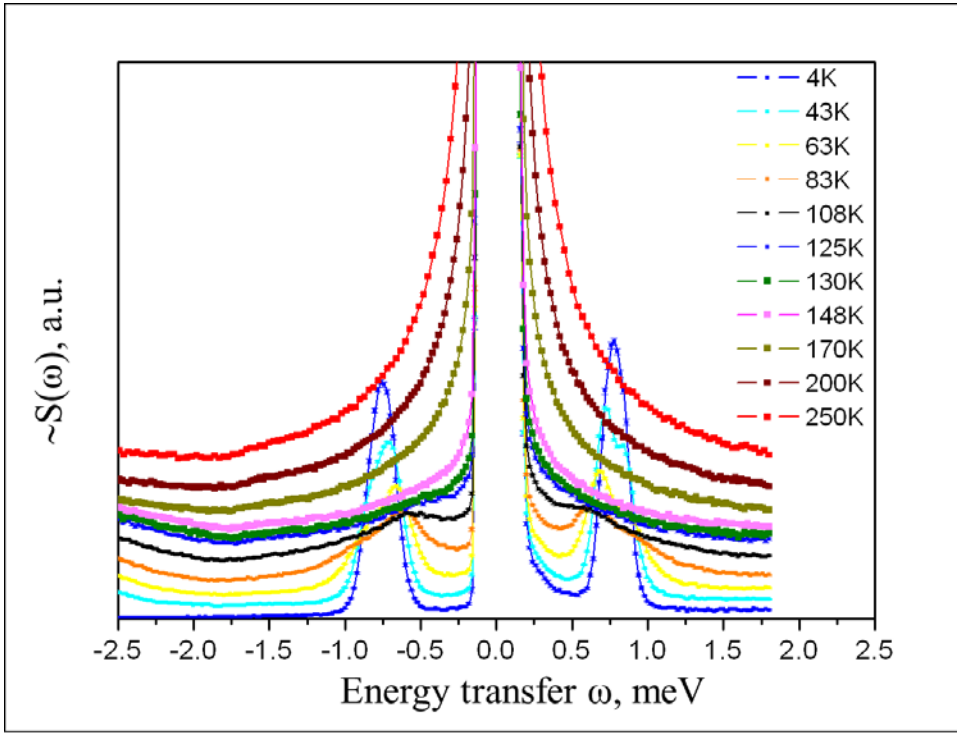

ω = 0.73 0.83 meV

V = 0.99 1.09 kcal/mol

$$\Gamma(T) = \Gamma_0 e^{-\left(\frac{E^*(T)}{kT}\right)}$$

E* = 1.6 kcal/mol

H/H_2 exchange

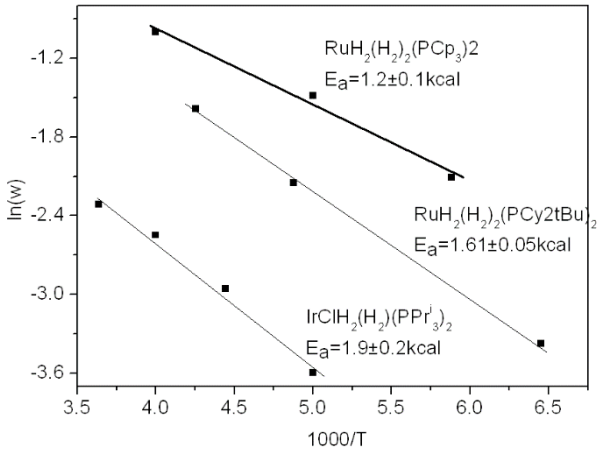

H/H_2 Exchange Mechanism

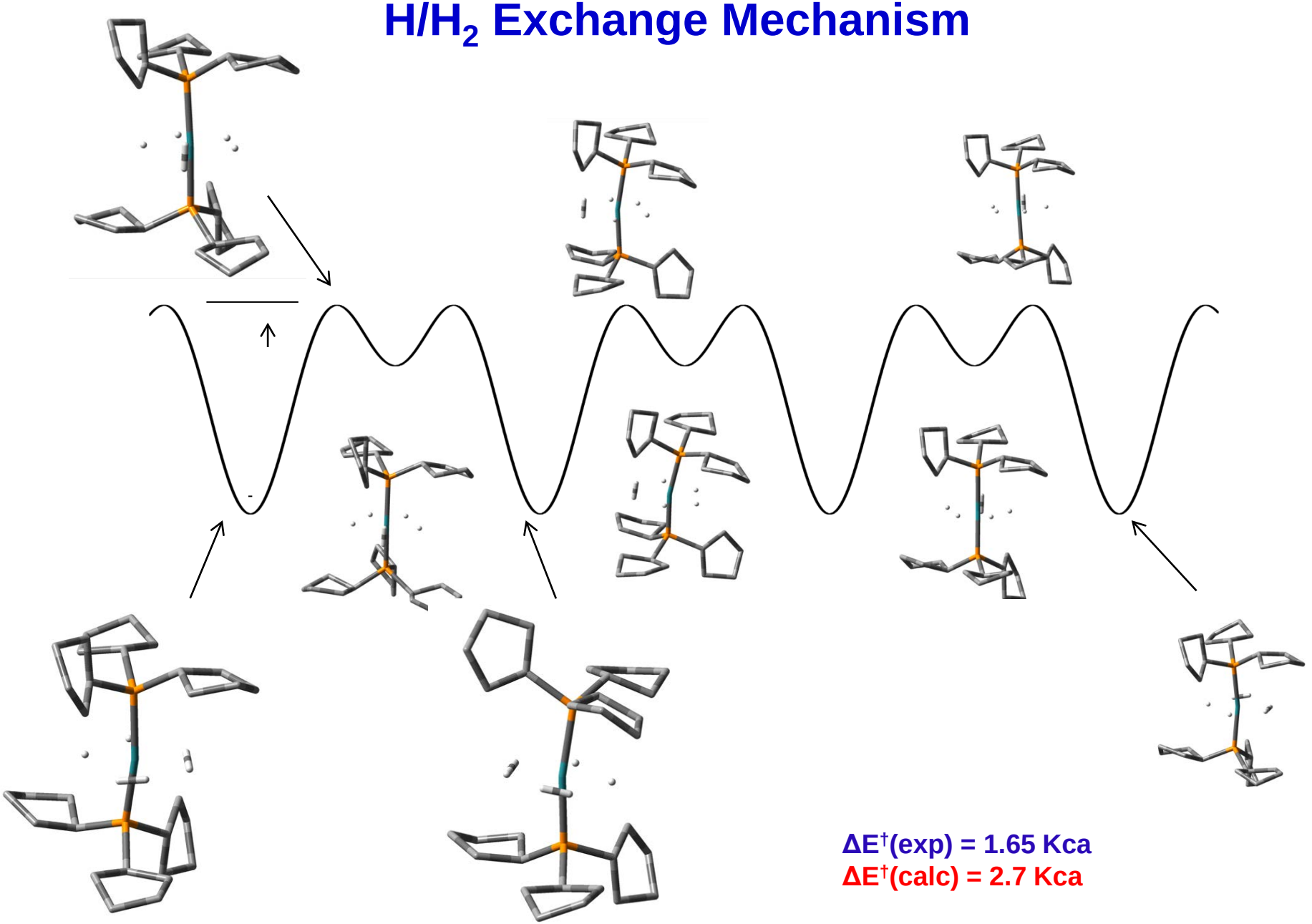

$\Delta E^{\dagger}$(exp) = 1.65 Kca

$\Delta E^{\dagger}$(calc) = 2.7 Kca

Rotational Tunnelling and QENS for Tp*Rh(H_2)H_2

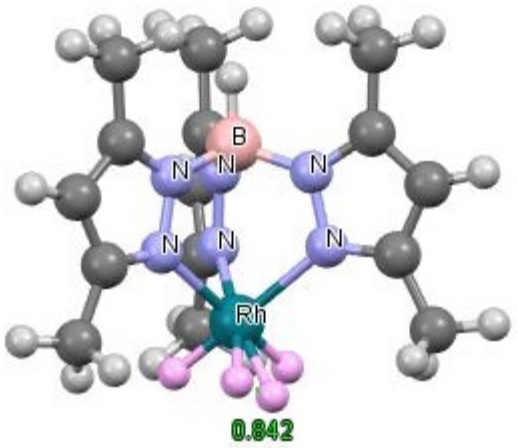

ω = 0.8 meV

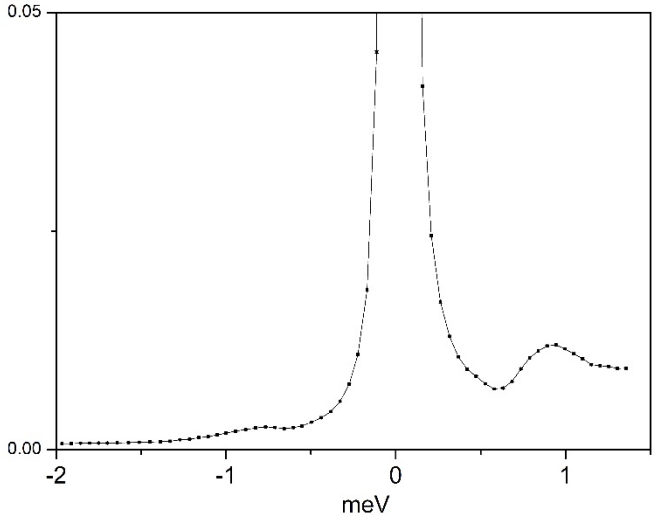

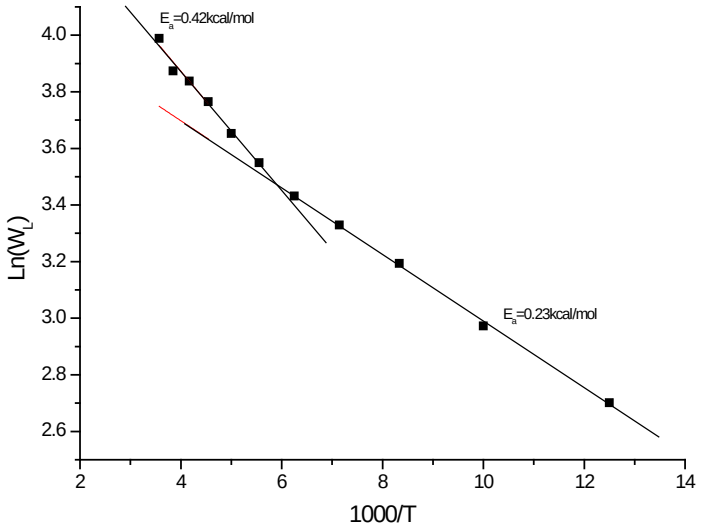

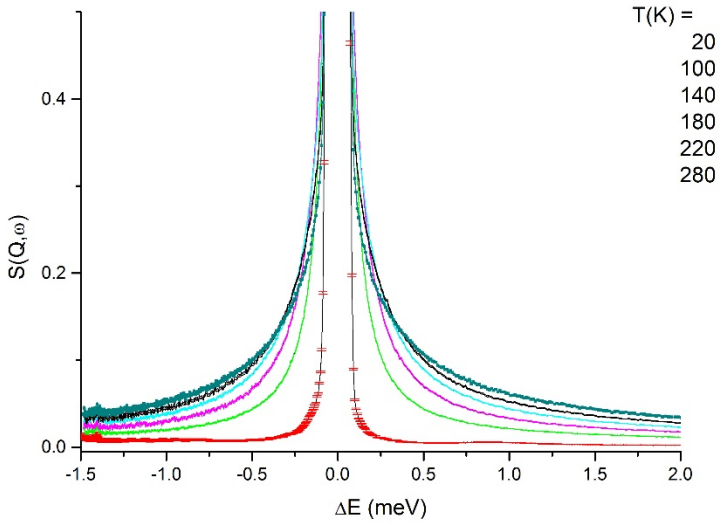

$Tp^*Rh(H_2)H_2$: Exchange Path

$E^* = 3.9$ kcal mol^{-1}

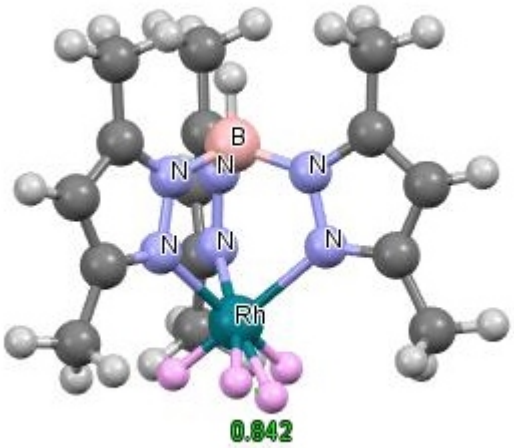

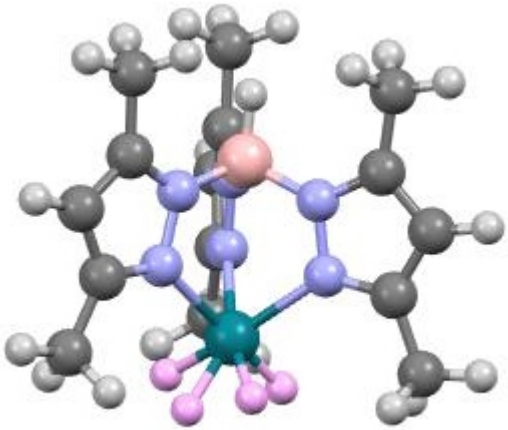

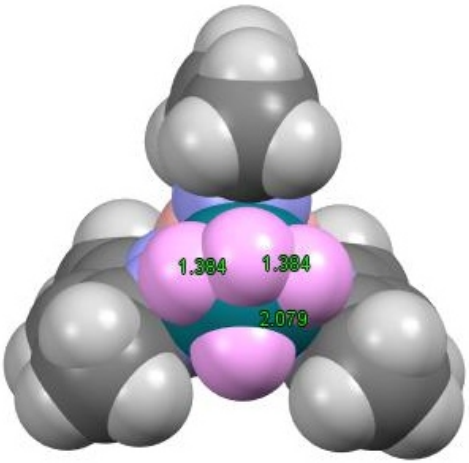

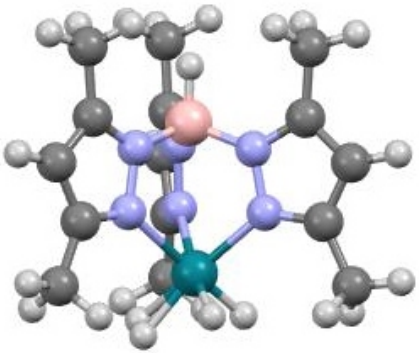

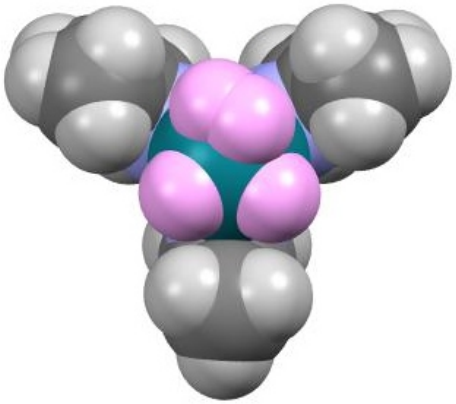

Classical vs. non-classical: $[PP_3Co(H)_2]^+$ and $[PP_3Co(H_2)]^+$

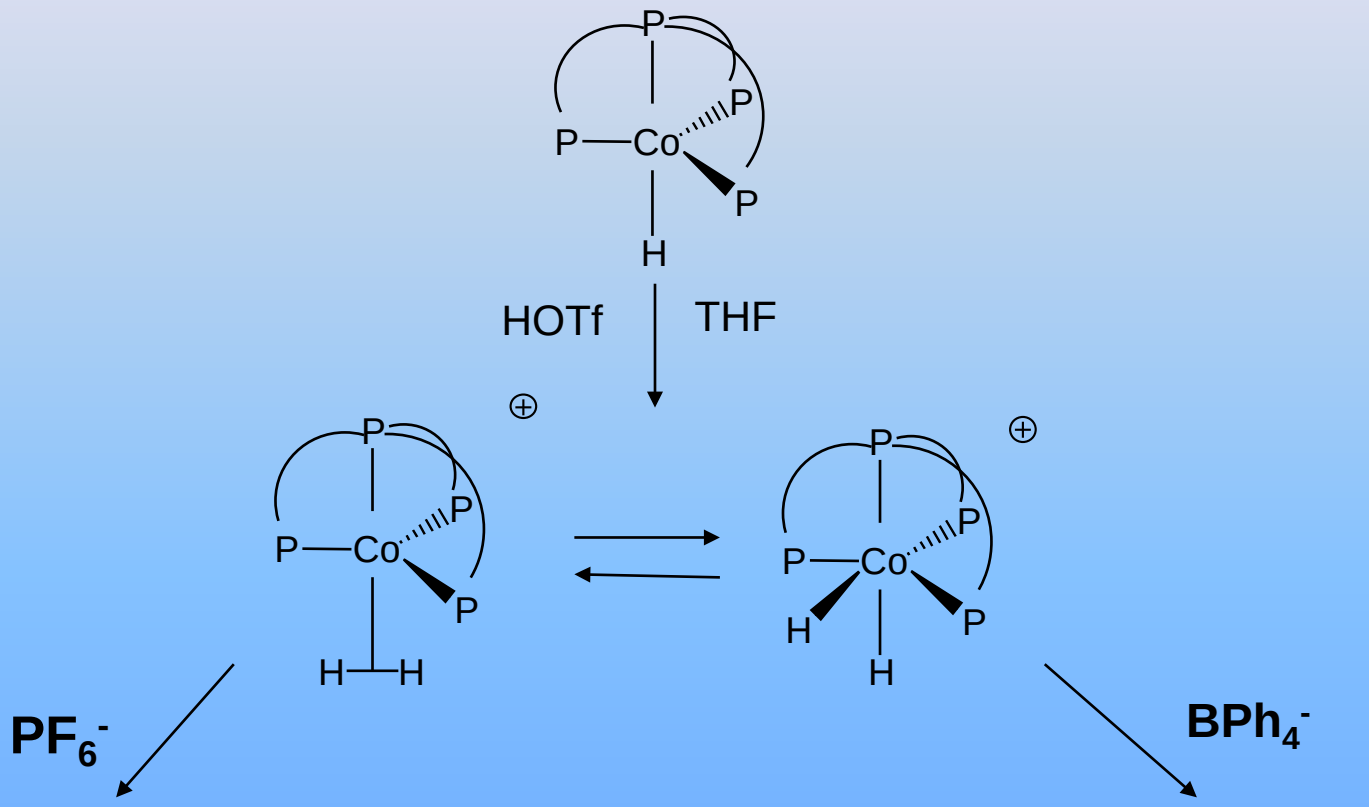

Red solid

White solid

White Form: $[PP_3Co(H)_2]BPh_4$

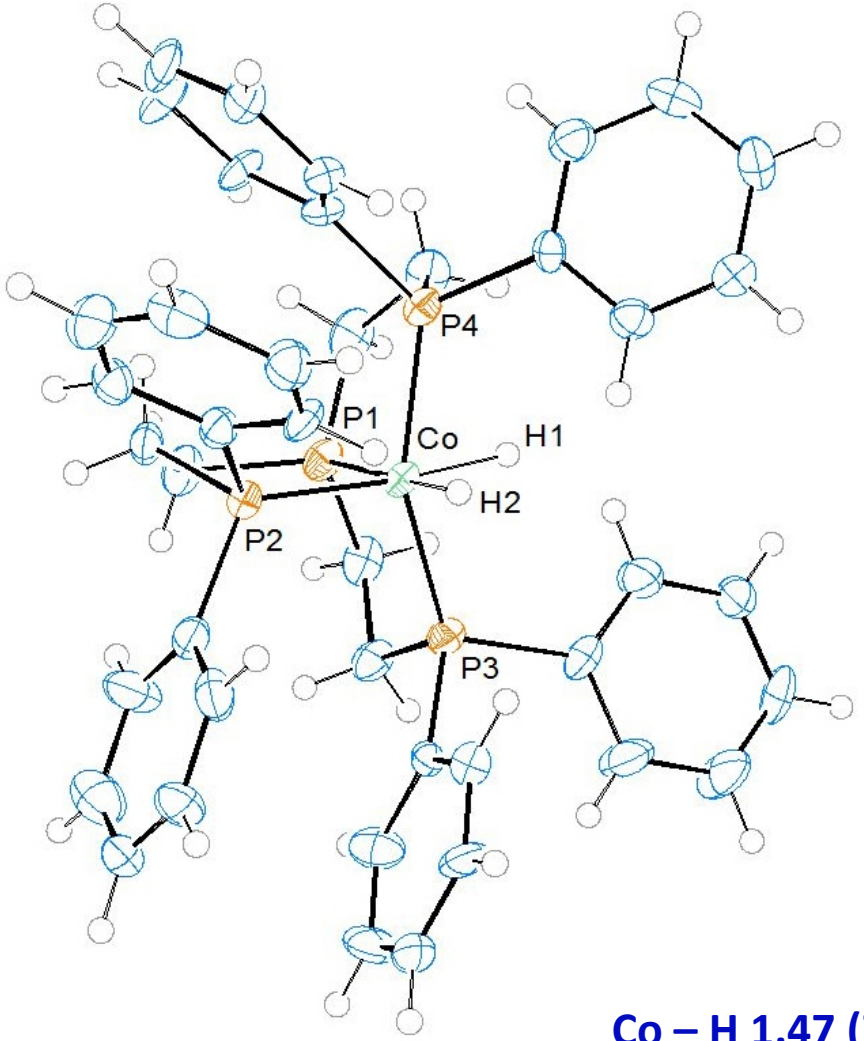

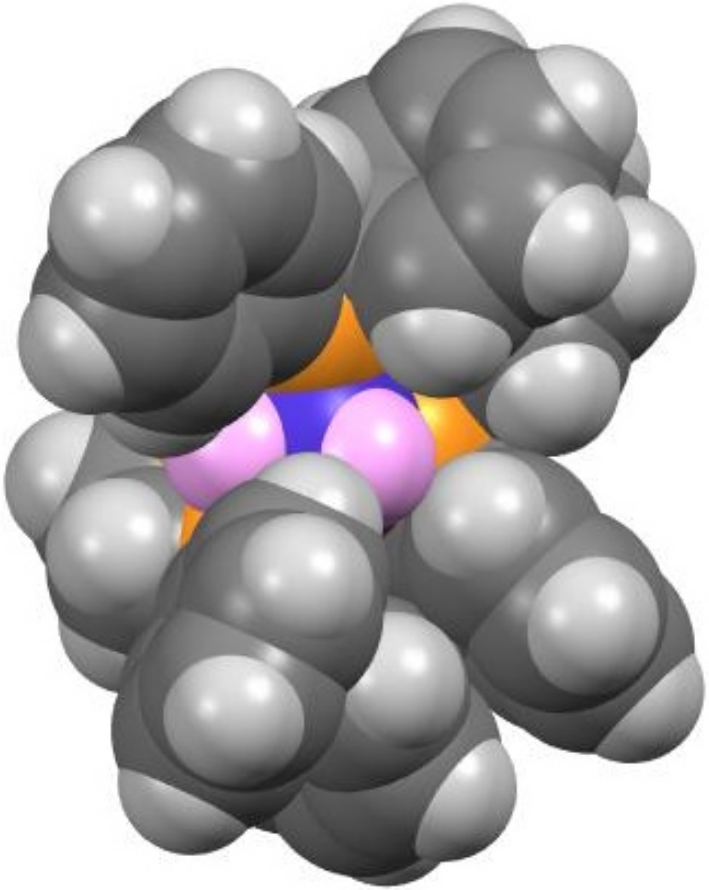

Co – H 1.47 (7) Å (av)

Red Form: $[PP_3Co(H)_2]PF_6$

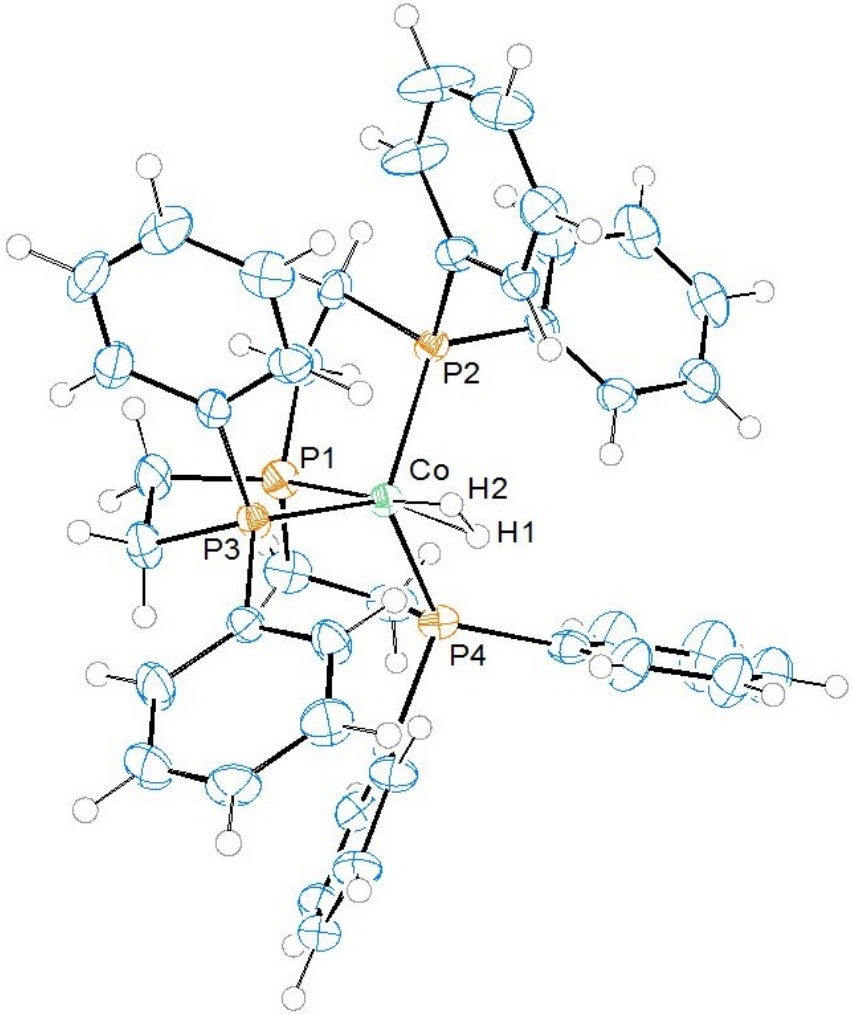

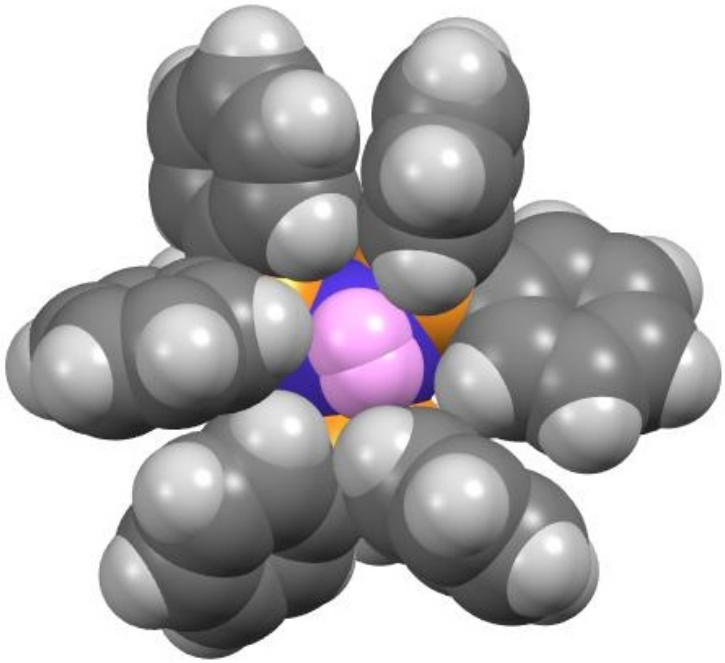

H – H 0.65(8) Å 0.807 Å (calc)

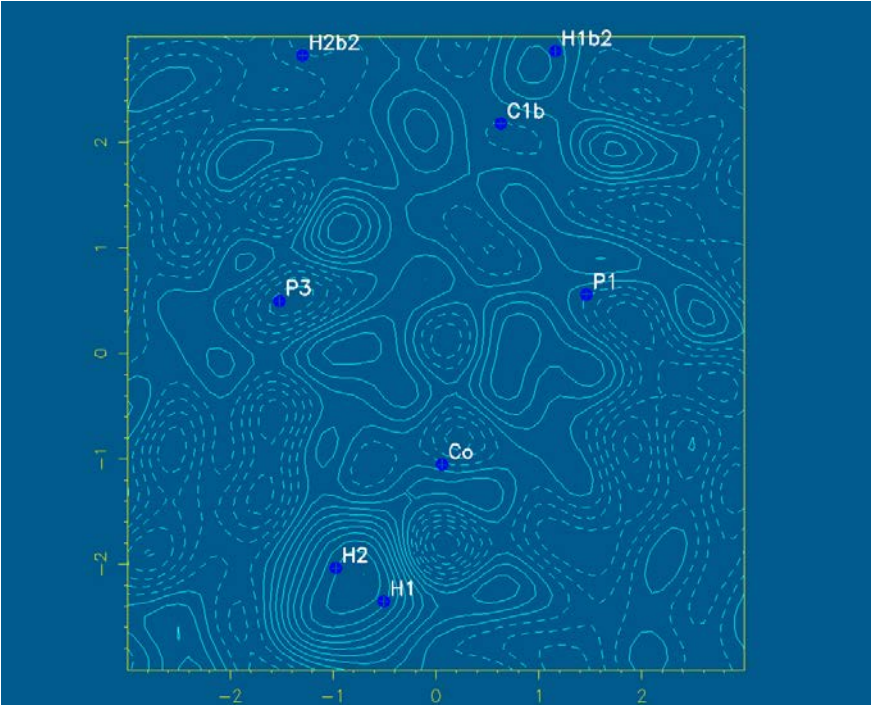
H2b2
H1b2
C1b
P3
P1
Co
H2
H1

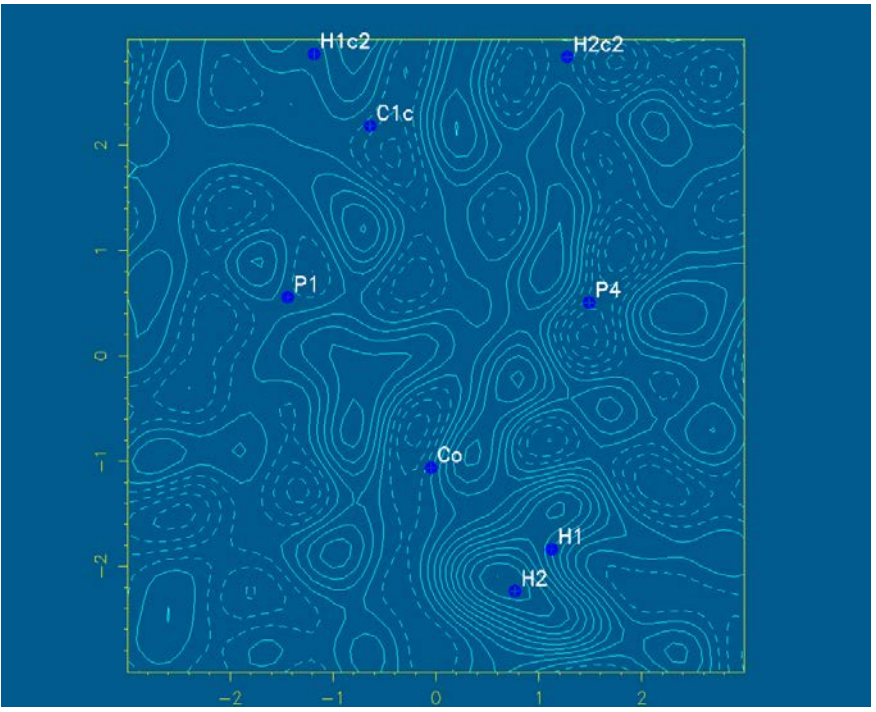
H1c2
H2c2
C1c
P1
P4
Co
H1
H2

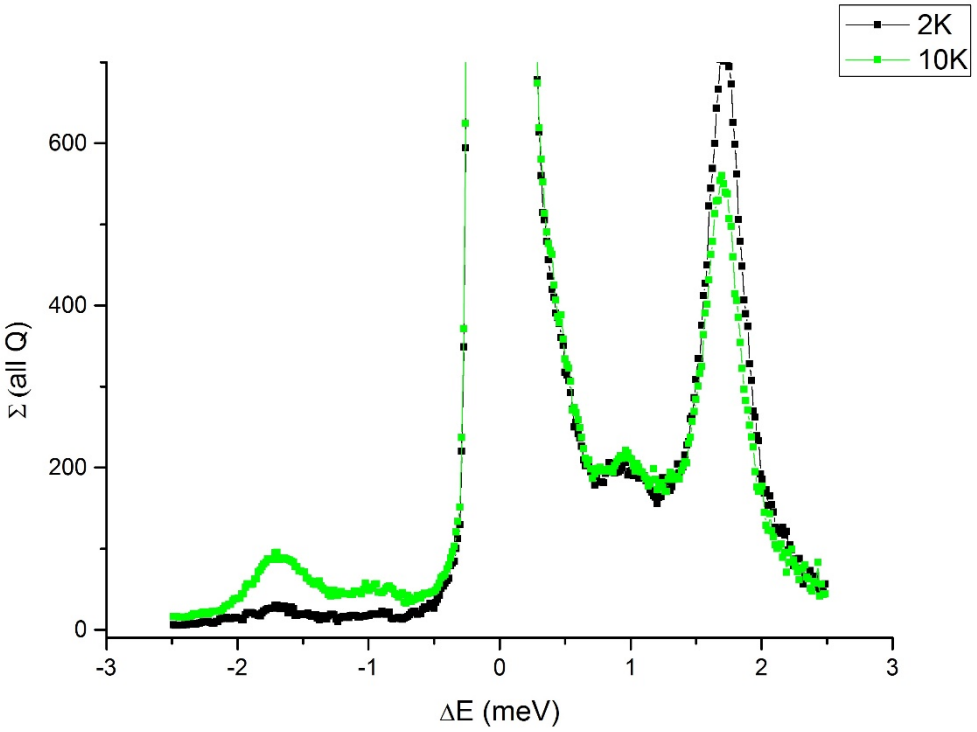
2K
10K
Σ (all Q)
ΔE (meV)
0
200
400
600
-3
-2
-1
0
1
2
3

White Form: $[PP_3Co(H)_2]BPh_4$

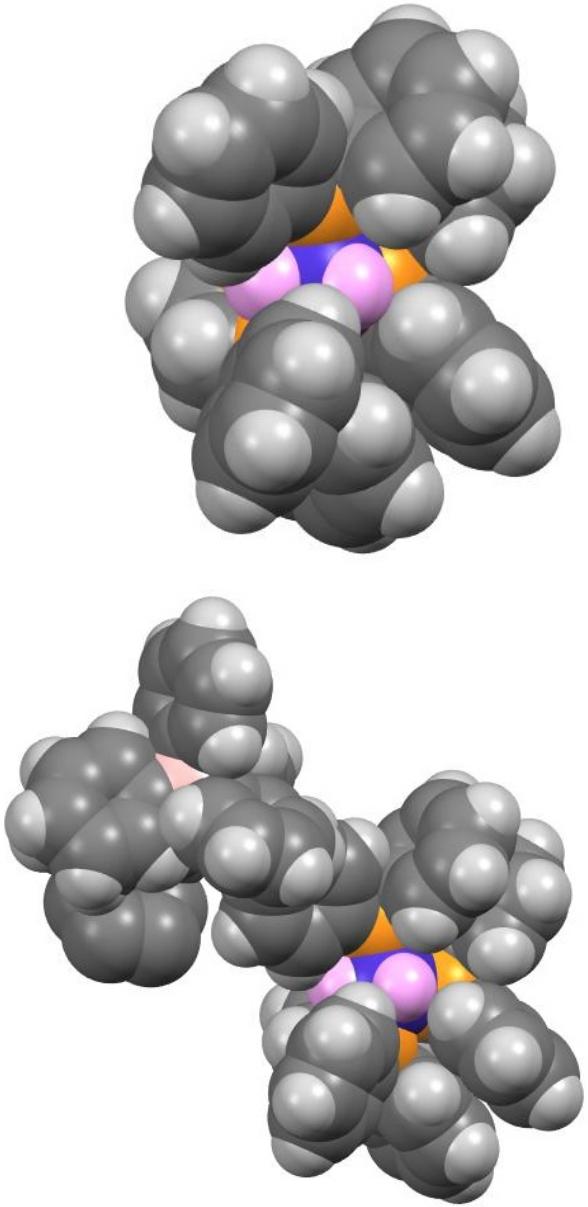

Red Form: $[PP_3Co(H)_2]PF_6$

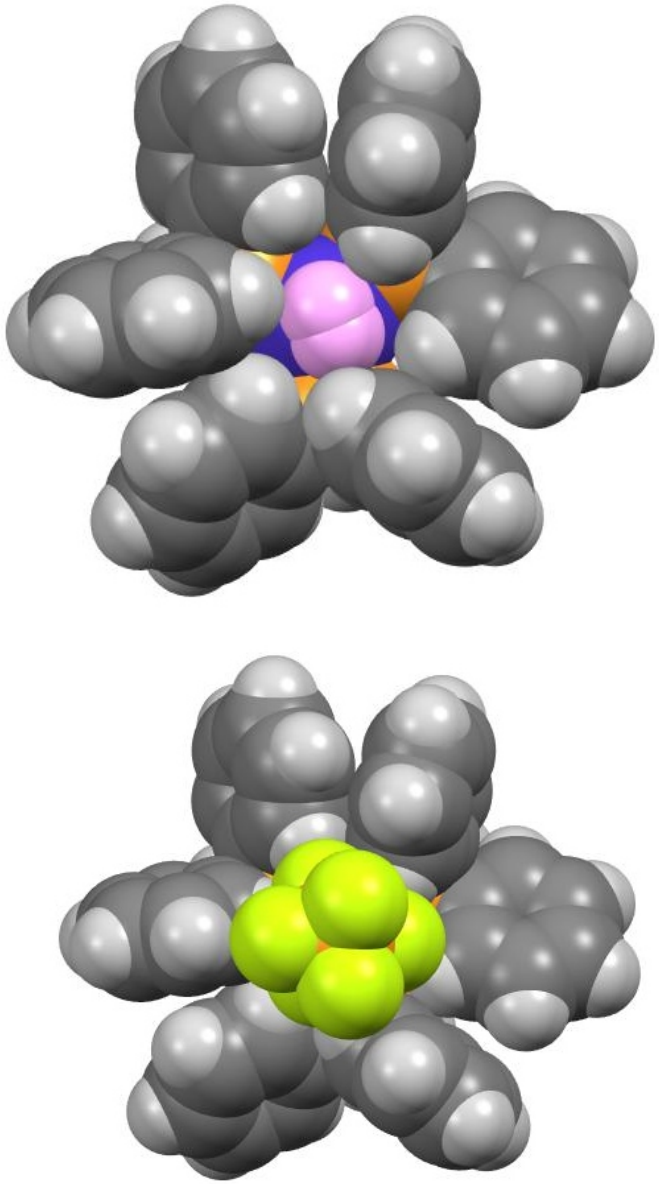

$[PP_3Co(H)_2]BPh_4$ – H.P. Raman Spectrum

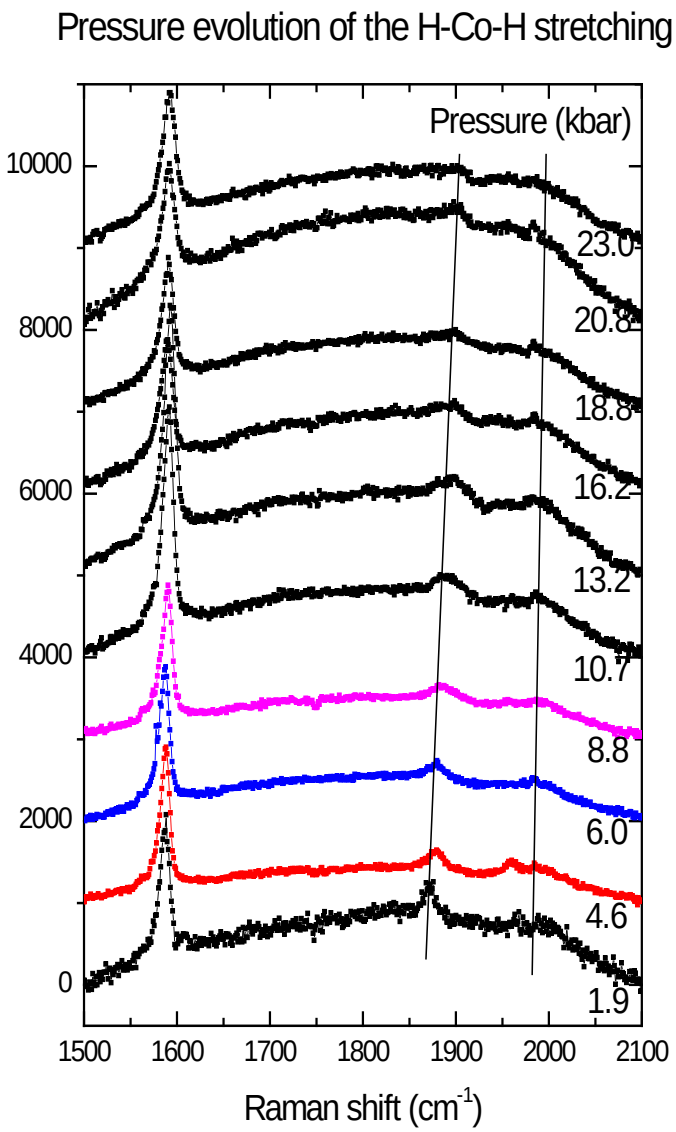

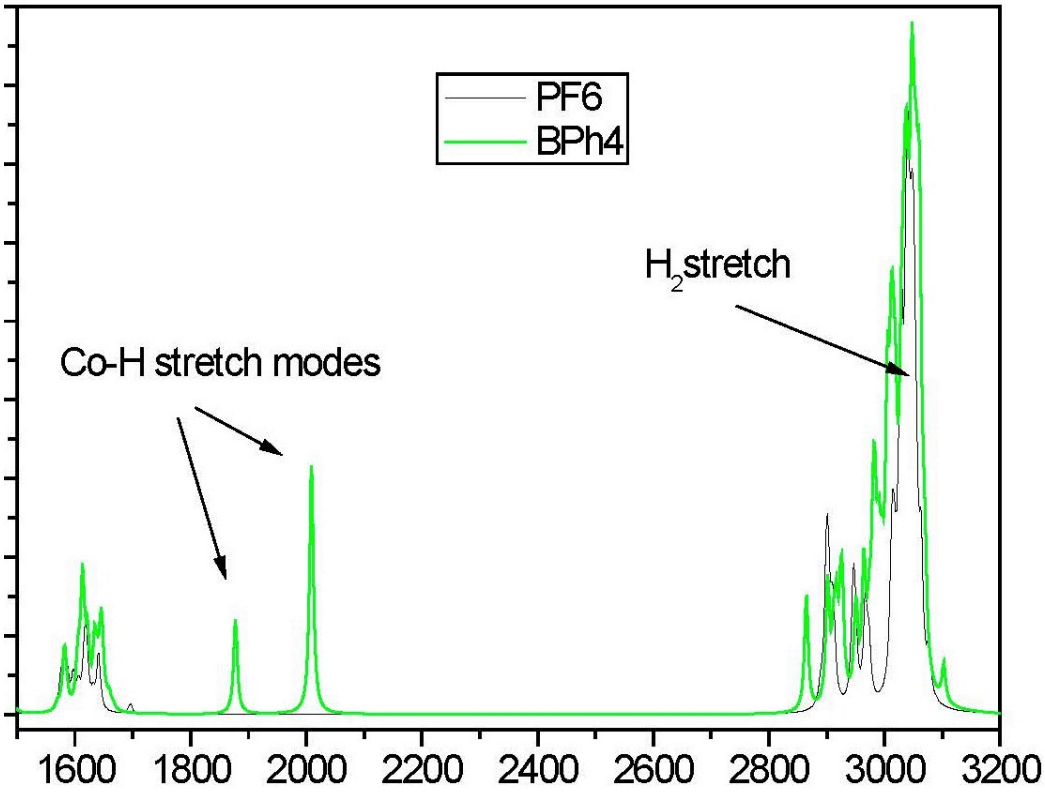

The Hydrogen Storage Problem

Hydrogen as an Energy Vector

- **Jules Verne** ***The Mysterious Island (1874).***

"… hydrogen and oxygen which constitute [water], used singly or together, will furnish an inexhaustible source of heat and light…"

- **Max Pemberton** ***The Iron Pirate (1893).***

hydrogen from coal "…fuels *the most powerful engines that have yet been placed on a battleship …"*

Hydrogen Production

Energy wise 3.8L gasoline ~ 1Kg of H_2

Burning 3.8L gasoline produces ~ 9Kg of CO_2

1 Kg of H_2 by electrolysis ≡ 32 Kg of CO_2

$$CH_4 + H_2O \leftrightarrows CO + 3H_2$$
$$CO + H_2O \leftrightarrows CO_2 + H_2$$
$$H_2/CO_2 = 2/1$$

- **Biomasses**
- **Photovoltaic**
- **Electrolysis + Nuclear Power (Solar Energy)**

J.J. Romm “The Hype about Hydrogen” (2004) Ch.4

Parameters Values and Methods

- Capacity >6% wt, 60kg H_2/m^3 at RT, P<100 bar.
  ~ 10% wt , at least, for the bare storage material itself.

- Thermodynamics and kinetics of the adsorption /desorption process. $-20<Q_{st}(\Delta H)<-40$ kJ/mol H_2; $D_{chem}>10^{-9}cm^2/s$.

- Structural stability upon cycling/activation; Resistance against poisoning agents H_2O, CO, CO_2, N_2, etc. Cost and Environment safety.

- Microscopically probe the interactions between H_2 and individual adsorption sites – INS and Model calculations .

U.S. Department of Energy
Energy Efficiency and Renewable Energy

Proposed H_2 Storage Concept

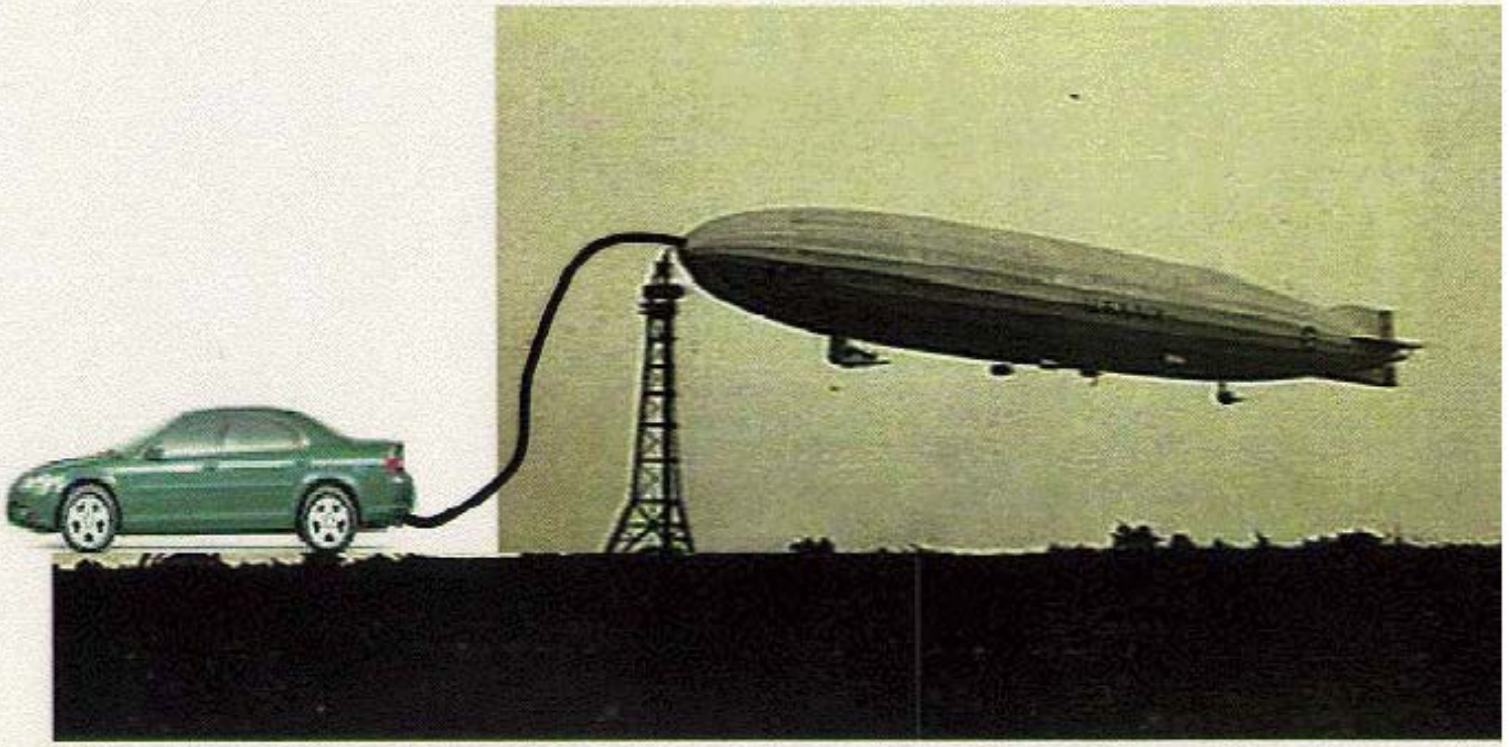

Proposed H_2 Storage Materials

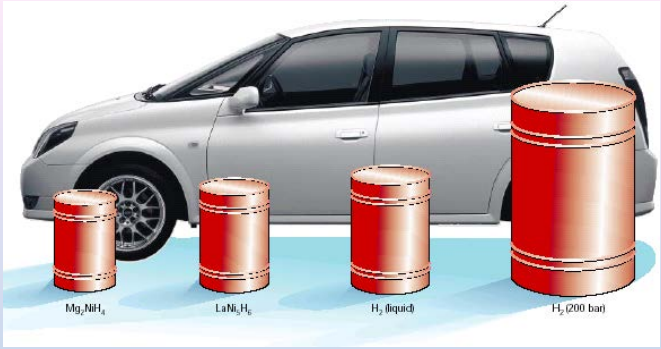

Mg_2NiH_4 $LaNi_5H_6$ $H_2(l)$ H_2 *(200 atm)*

4Kg Hydrogen

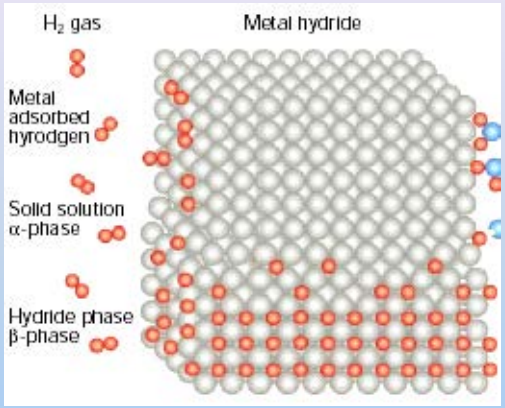

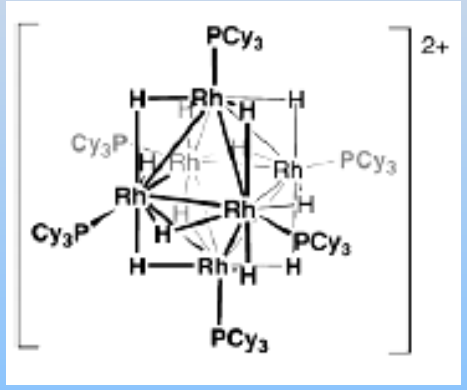

[Weller (2006)]

$$2NaAlH_4 \rightleftarrows 2NaH + 2Al + 3H_2\uparrow$$

[Chem. Rev. (2004, 2012)]

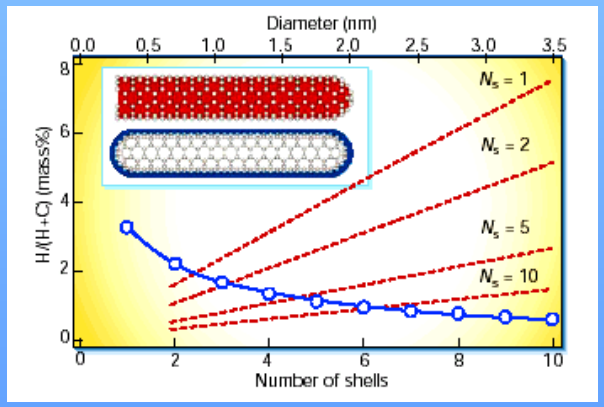

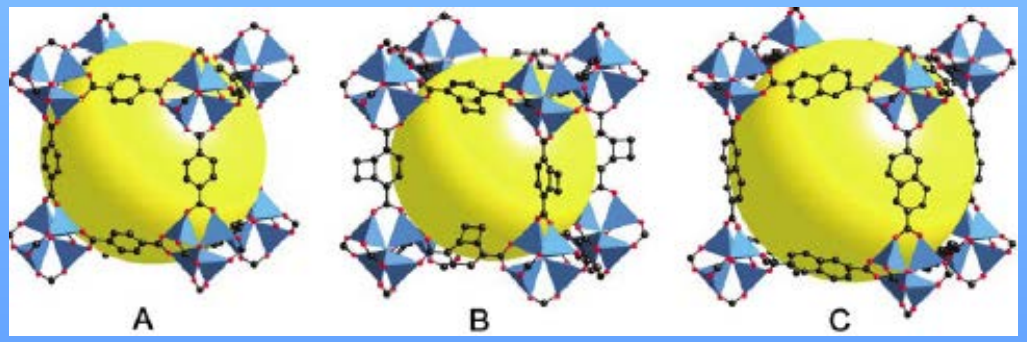

[Yaghi (2001)]

Expected Interactions and Associated Thermodynamics

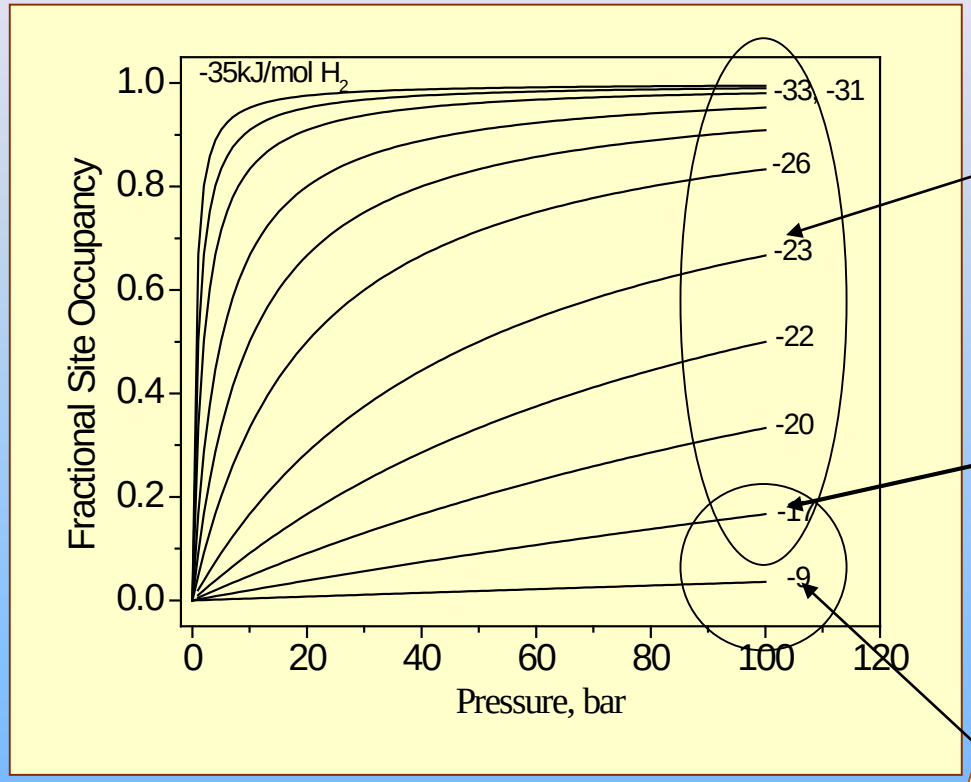

Interstitial hydrides-$LaNi_5$, Non-classical hydrides: M-(η^2-H_2) complexes of Transition Metals

Very likely a combination of electronic and dispersive interactions. Most challenging to model and characterize. It was hoped that MOF's would fall here.

Van der Waals–a few kJ, electrostatic

-<10 kJ/mol H_2

Graphite, activated carbons, Carbon Nanotubes, Na^+ , Li^+… -exchanged Zeolites

Rotational Energy Levels of the Hydrogen Molecule

Symmetry Properties

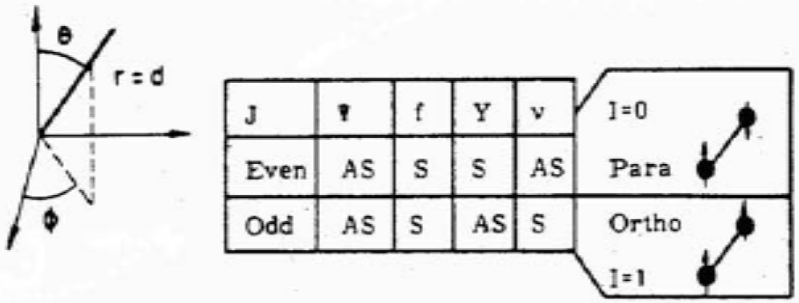

J	ψ	f	Y	v	I=0
Even	AS	S	S	AS	Para
Odd	AS	S	AS	S	Ortho I=1

$$\Psi = f(r)\ Y_{J,m_J}(\theta,\phi)\ v_I$$

Rotational Energy Levels

$$E = BJ(J+1)$$

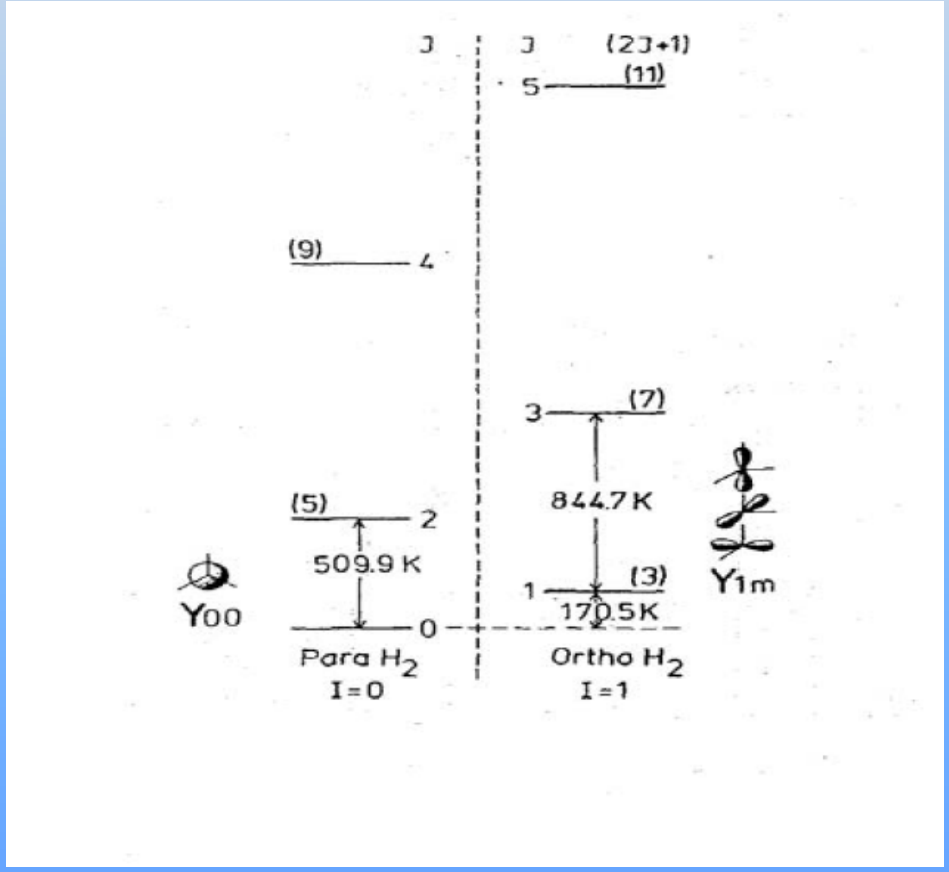

Introduction of a Barrier to Rotation of the H_2 Molecule

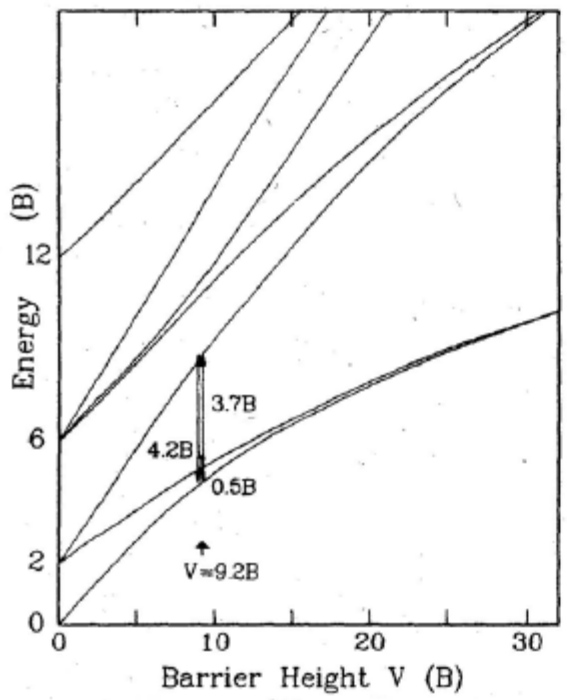

Some degeneracy in J levels is lifted

Note sensitivity to V of "0-1" transition
Levels depends on the form of the barrier

Transitions can be observed by neutron scattering - deduce barrier height V (as shown)

Barrier height can be compared with computational studies

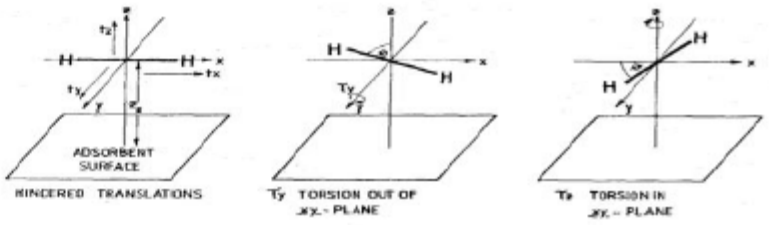

H_2 Absorption in Nanoporous Materials

SWCNT

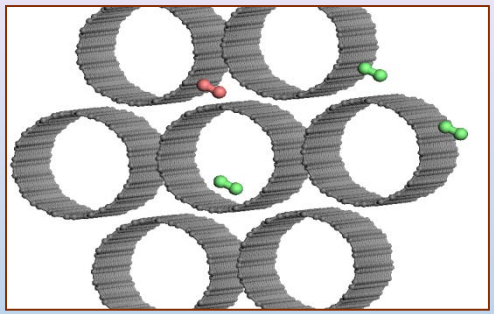

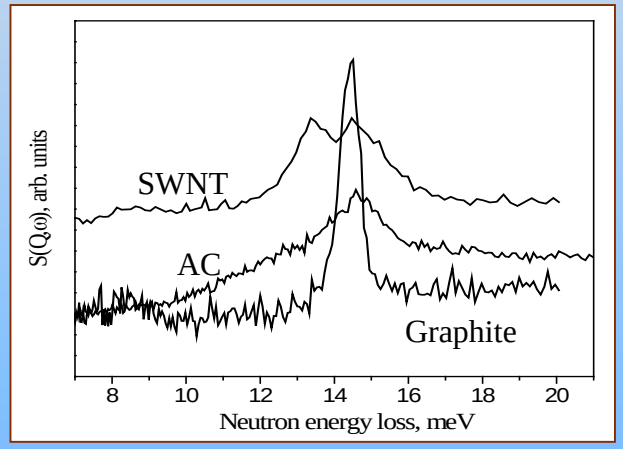

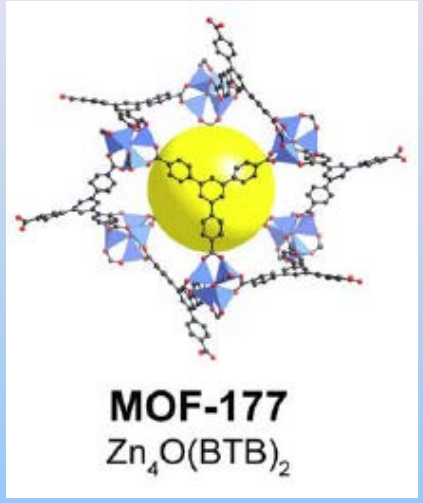

MOF-177

$Zn_4O(BTB)_2$

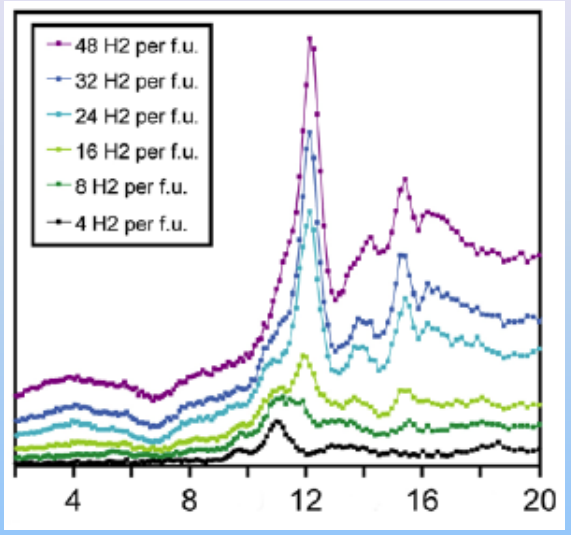

IRMOF-11

$Zn_4O(HPDC)_3$

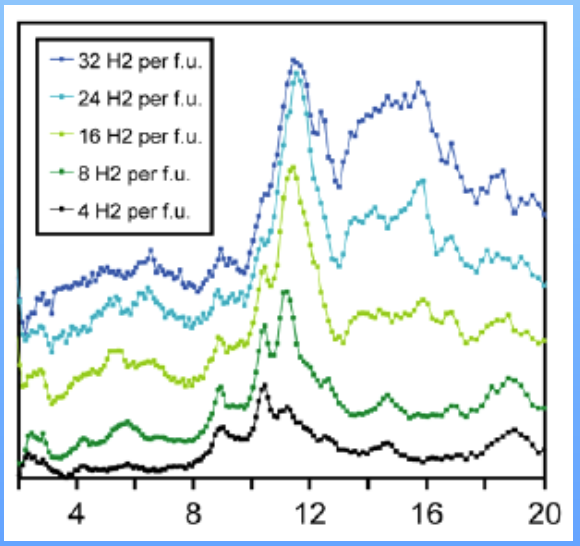

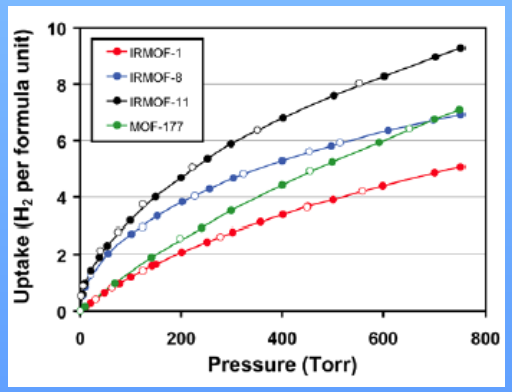

J. Eckert & al. JACS (2005)

Expected Interactions and Associated Thermodynamics

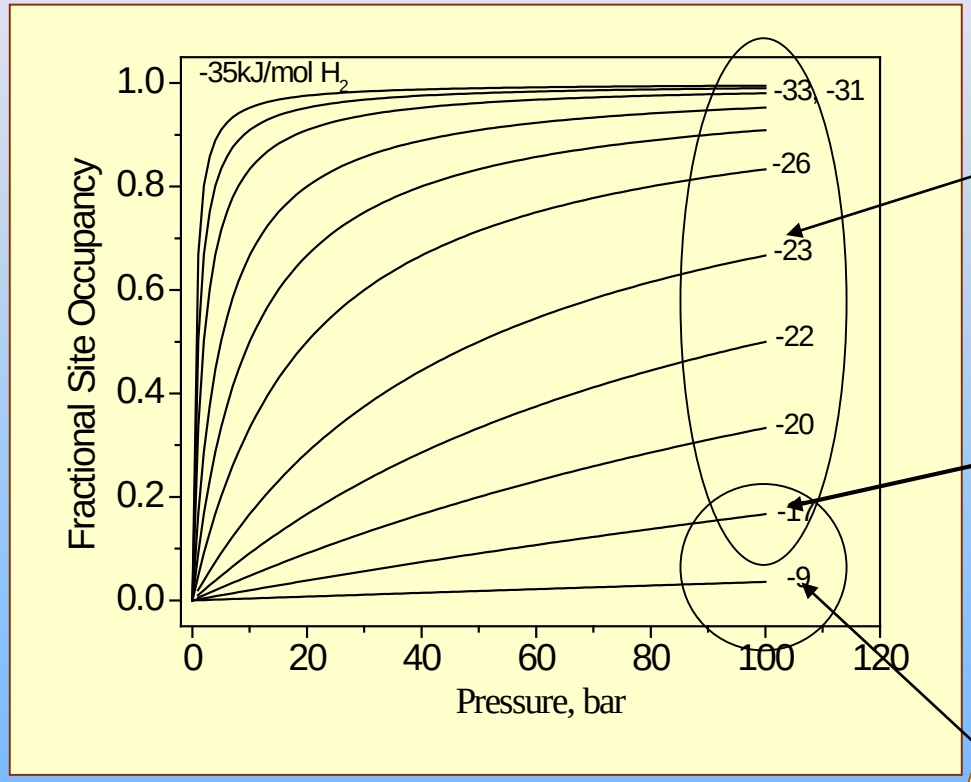

Interstitial hydrides-$LaNi_5$, Non-classical hydrides: M-(η^2-H_2) complexes of Transition Metals

Very likely a combination of electronic and dispersive interactions. Most challenging to model and characterize. It was hoped that MOF's would fall here.

Van der Waals–a few kJ, electrostatic

-<10 kJ/mol H_2

Graphite, activated carbons, Carbon Nanotubes, Na^+ , Li^+… -exchanged Zeolites

Chemisorption of H_2 in Fe -ZSM-5

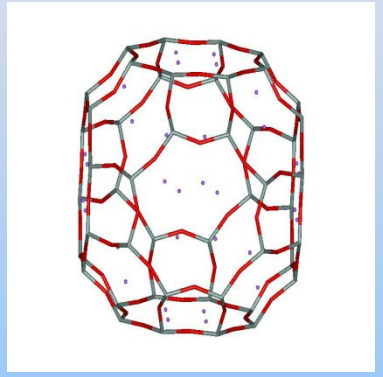

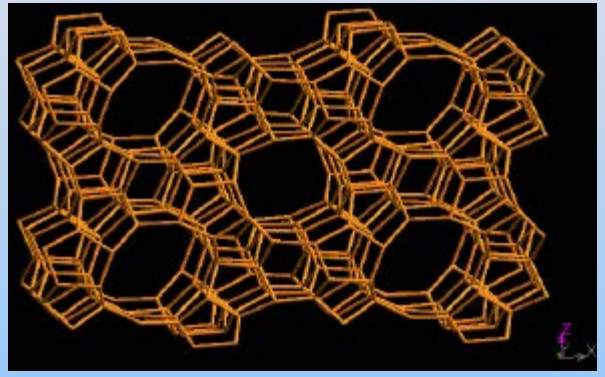

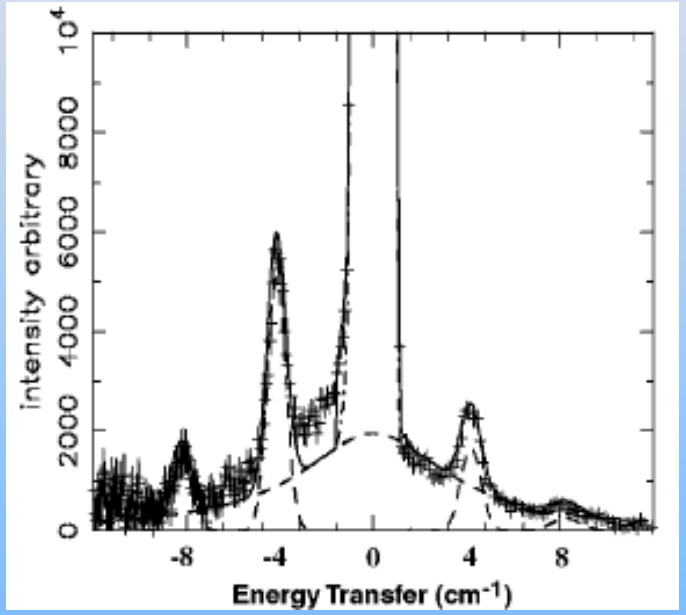

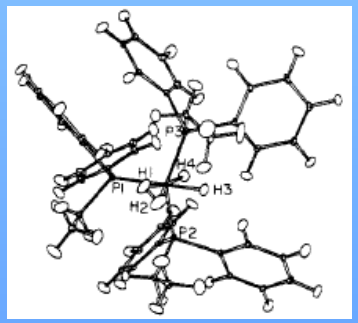

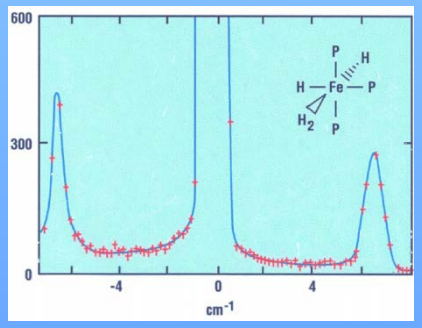

ω = 4.2(2) cm^{-1} 8.3(2) cm^{-1}

NEAT @5K - λ = 5.1Å

Van der Sluys & al. *JACS* **1990**, *112*, 4831

Chemisorption of Molecular Hydrogen in: Cu–ZSM5

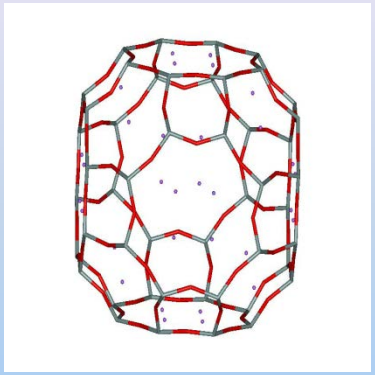

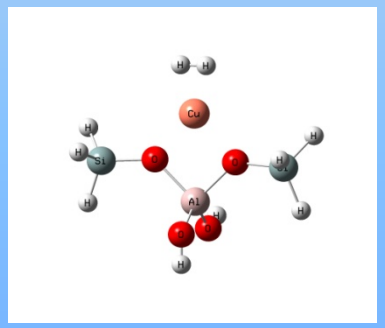

H_2/Cu
0.4

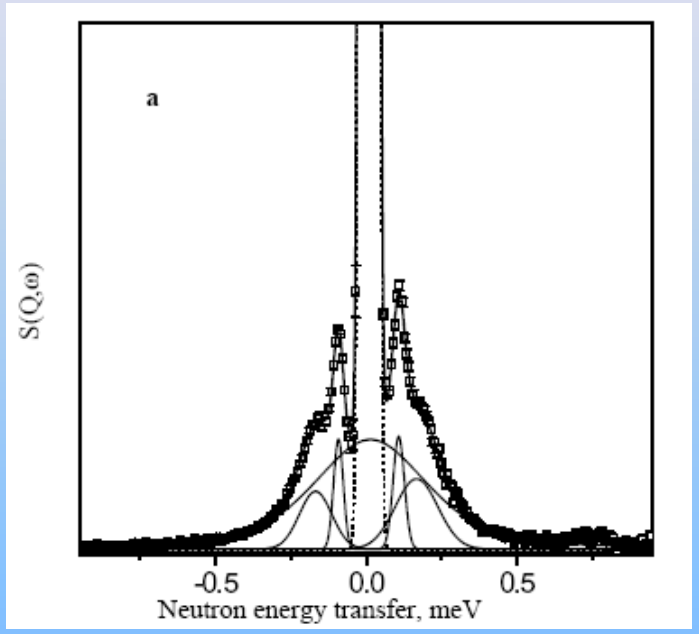

H_2/Cu
2.0

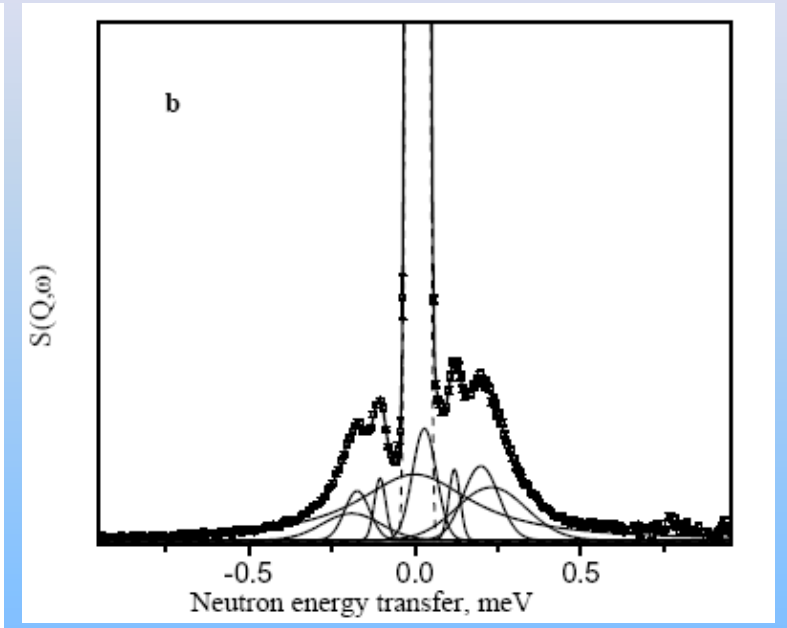

ω_τ ±0.80 cm^{-1} ±1.37 cm^{-1}

IN5 @4K - λ = 7.0Å

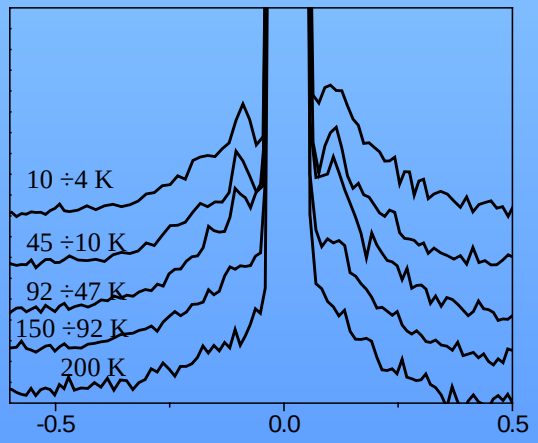

Dihydrogen Adsorption Isotherms - H_2 in Cu-ZSM5

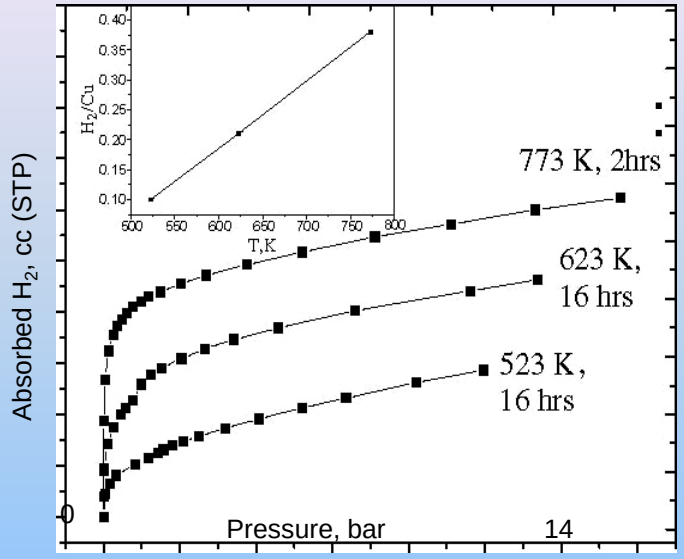

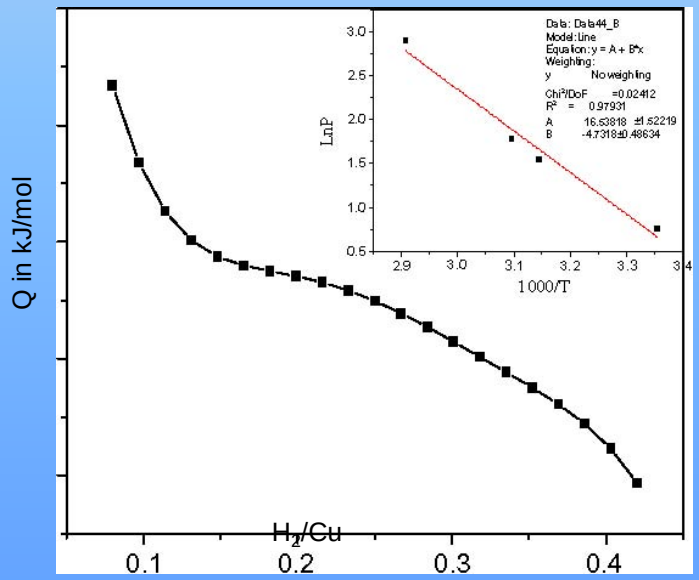

Isosteric Heat of adsorption

H_2 on Cu 39±4 - 73±4 kJ/mol

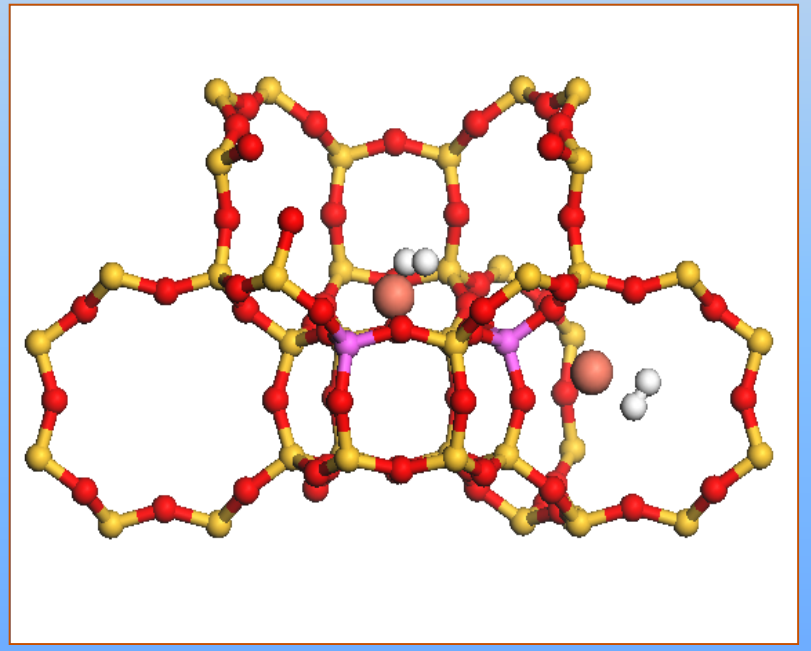

Chem Phys Lett **449**, 182 (2007)

Sorption Based Materials with Greater H_2 - Binding Energy

Molecular Chemisorption at Unsaturated Transition Metal Binding Sites

(can reach > 20 kJ/mol)

Density too high?

Not enough binding sites?

Bind Multiple DihydrogenLigands

Lighter Metals: alkali, alkaline earth hybrids

Framework modifications: anionic frameworks, different metals…

Combine two or more of these approaches in one material

H_2 Adsorption in Non-Catenated MOFs

Functionality has little impact on uptake

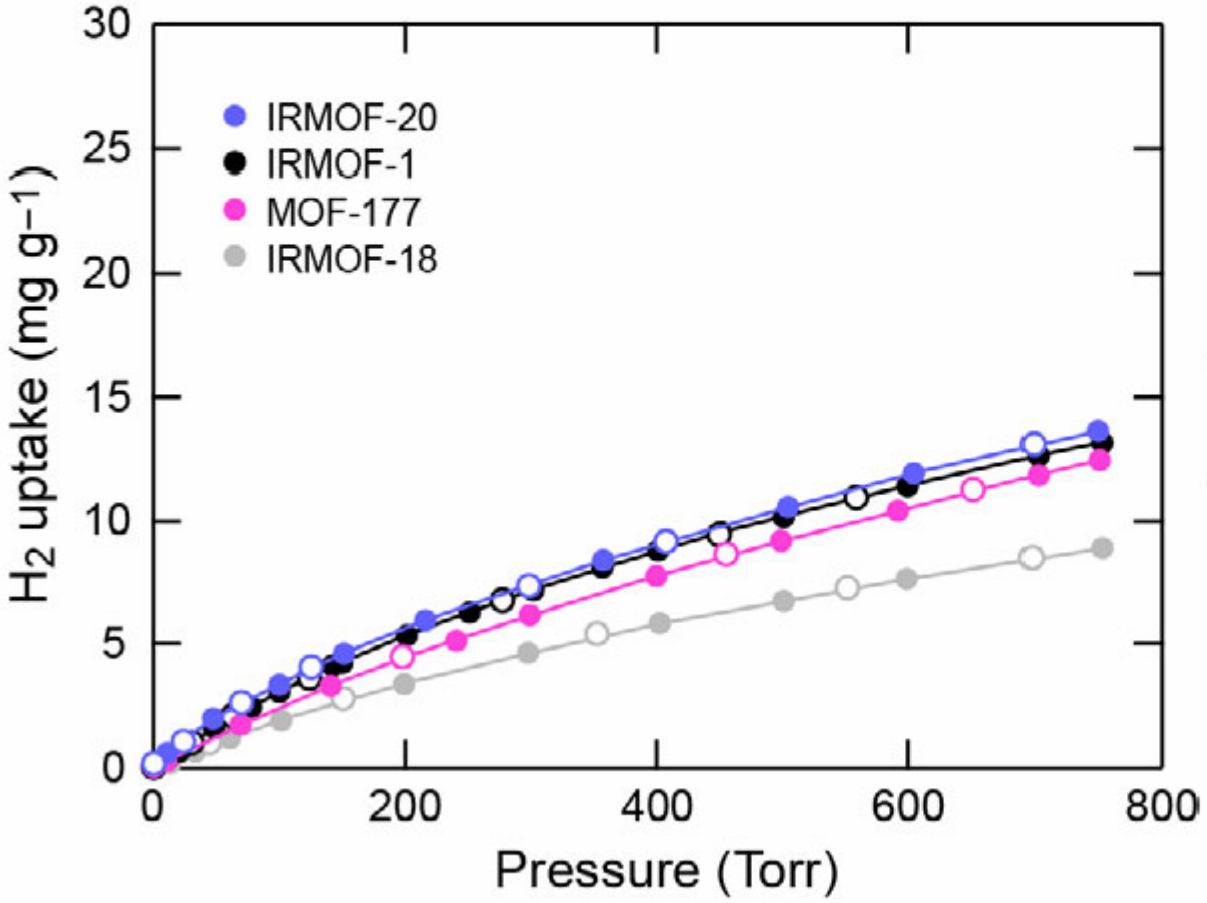

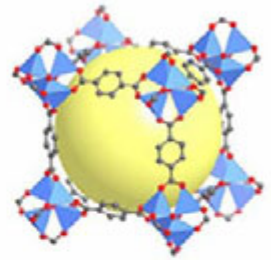

IRMOF-1

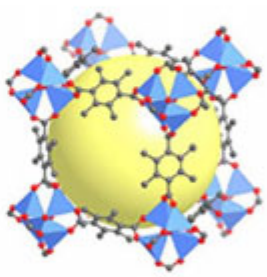

IRMOF-18

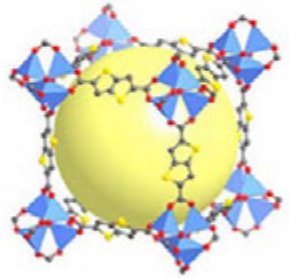

IRMOF-20

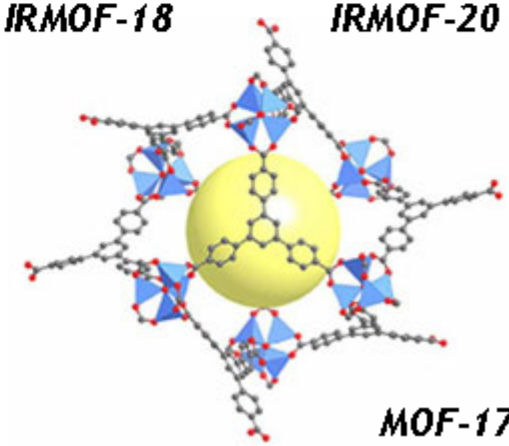

MOF-177

The Effect of Framework Catenation

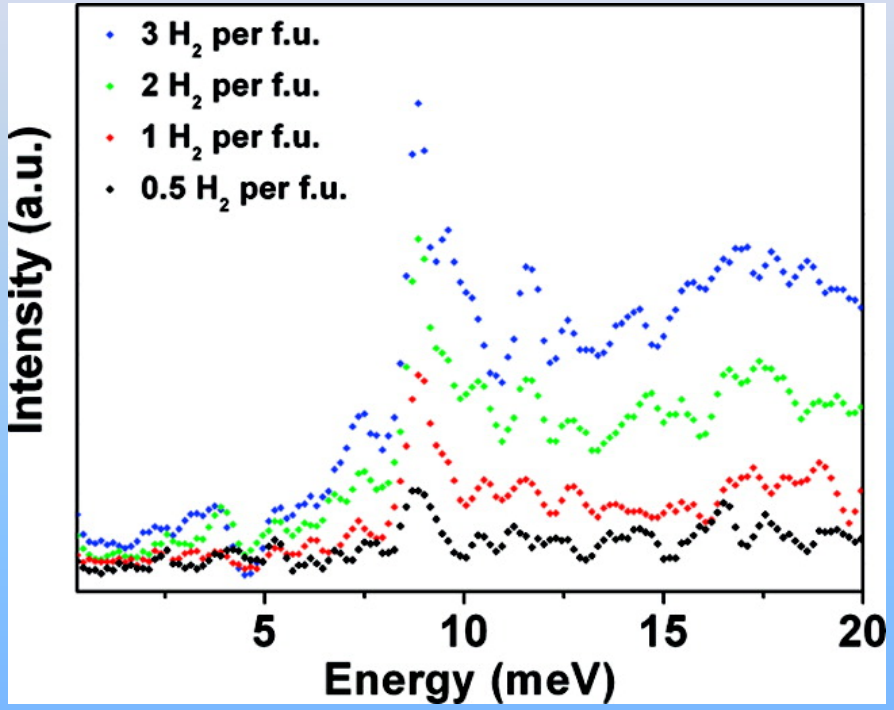

PCN-6 (15K)

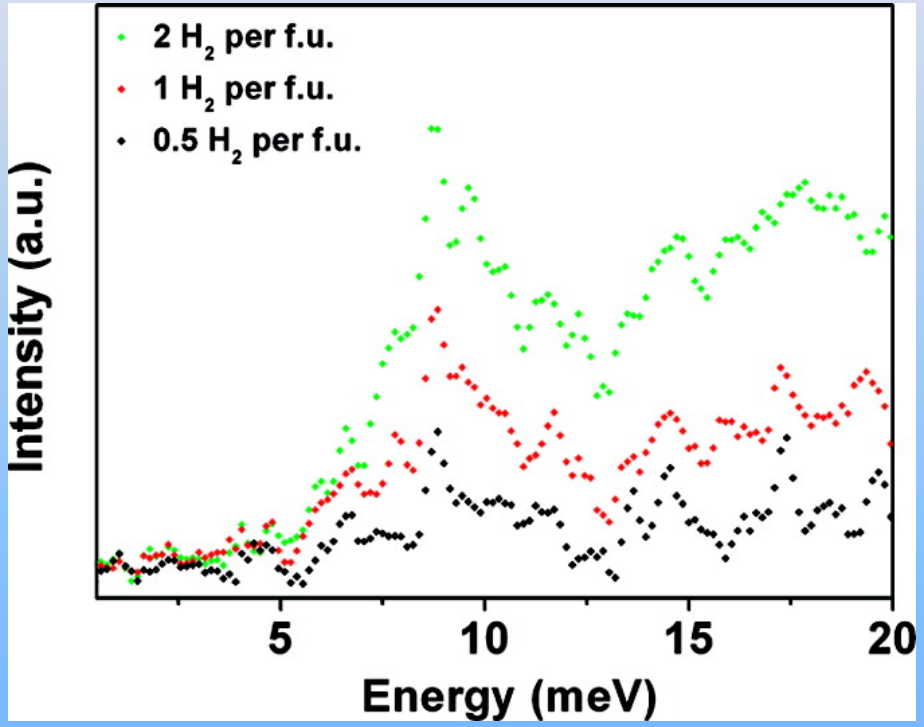

PCN-6' (15K)

JACS (2008)

H_2 Uptake by MOFs with Open-Metal Sites

Open metal sites increase uptake by 70%

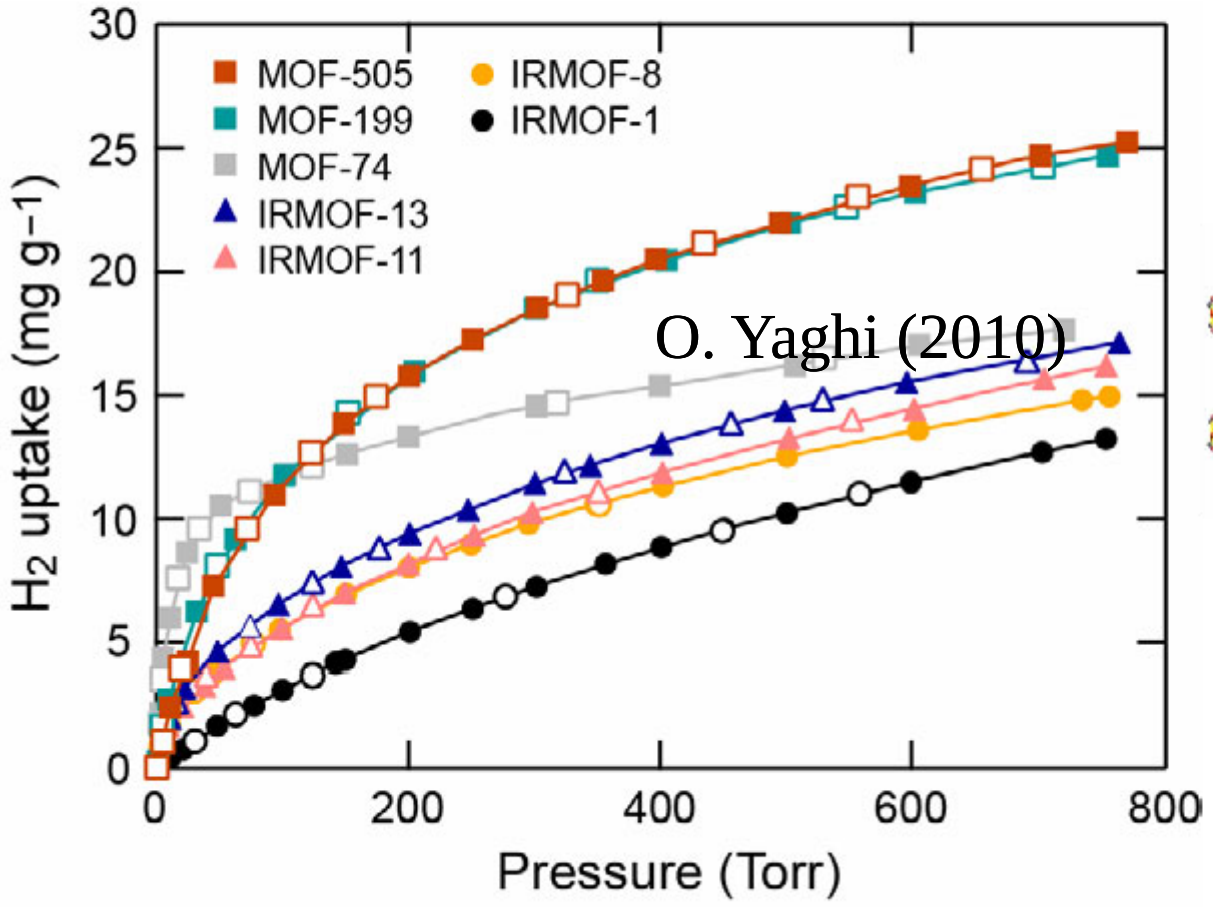

O. Yaghi (2010)

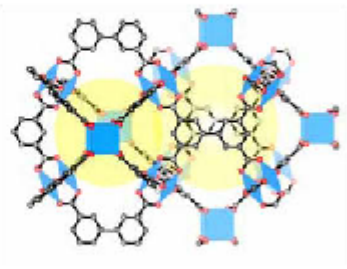

MOF-505

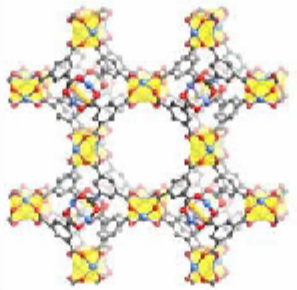

MOF-199

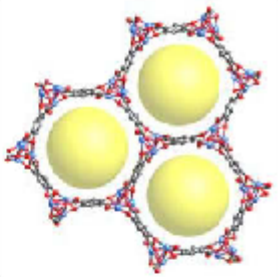

MOF-74

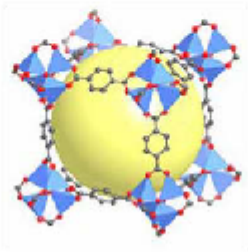

IRMOF-1

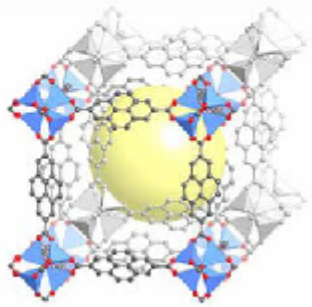

IRMOF-13

Weak-H_2 Chemisorption - HKUST-1

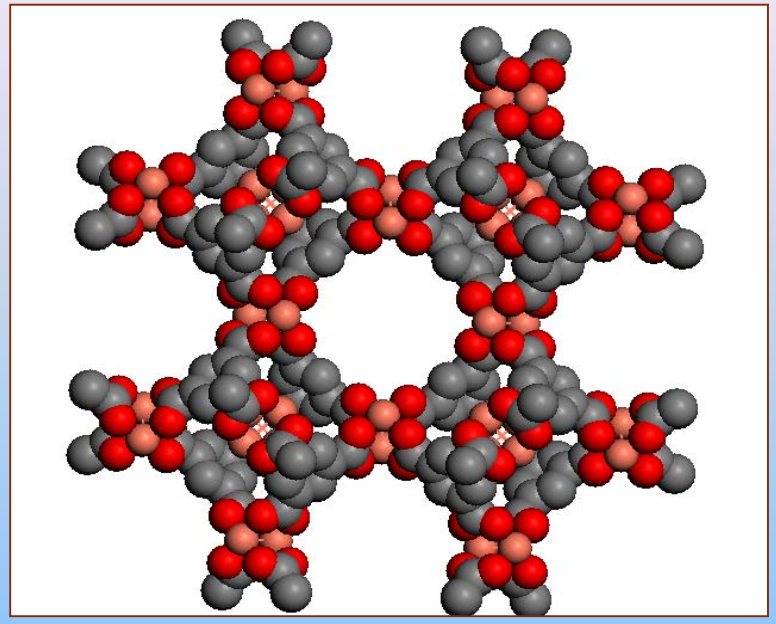

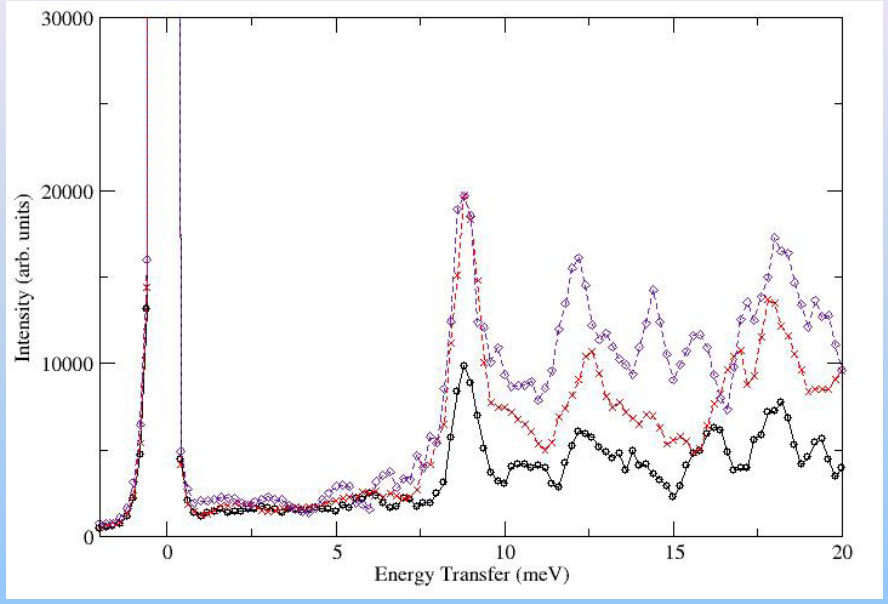

Peak at ~ 9.1 meV

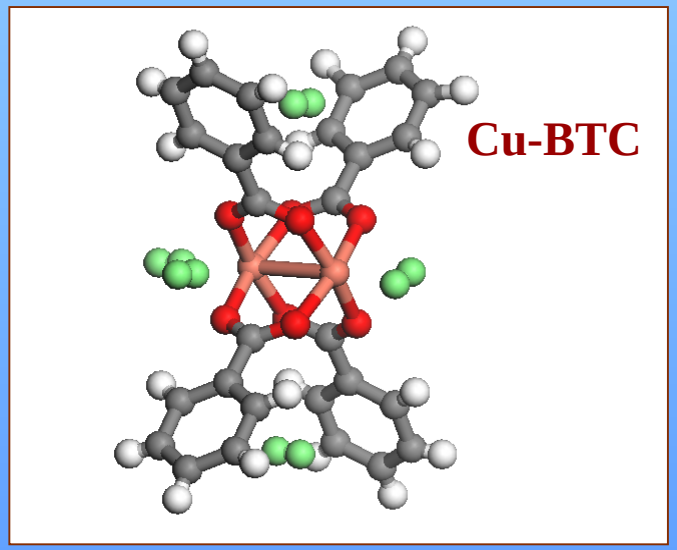

Aimed at achieving heats of adsorption of ~20 kJ/mol H_2

S.S.-Y. Chui et al. Science *283*, 1148 (1999)

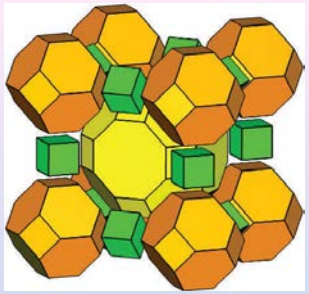

ZIF's: Zeolite Type Frameworks

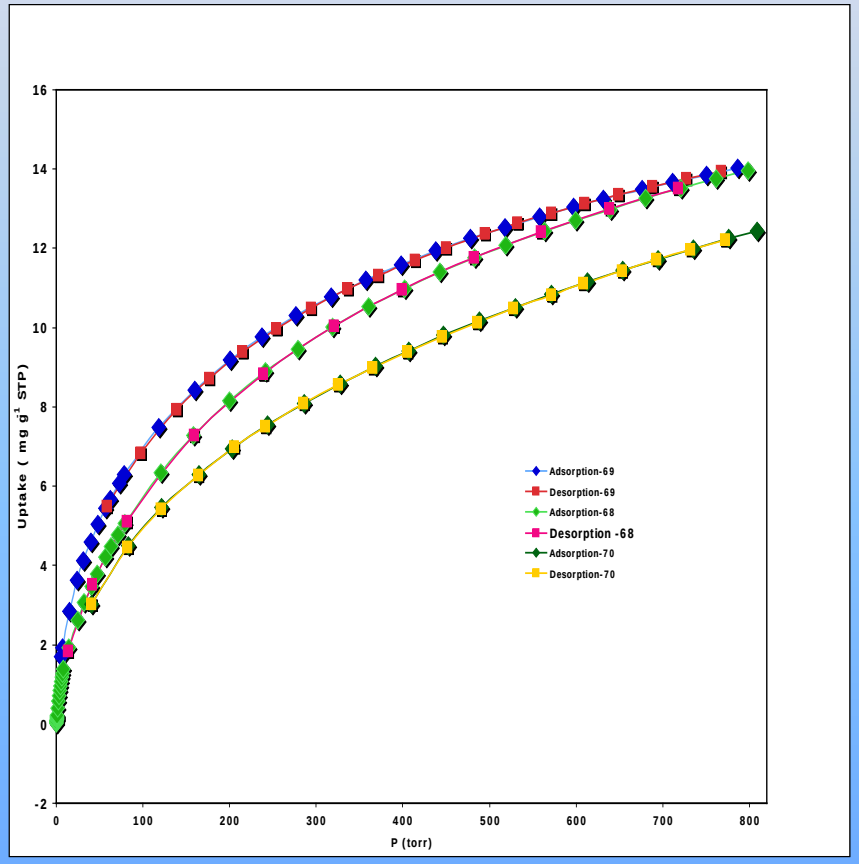

ZIF-68

ZIF-69

ZIF-70

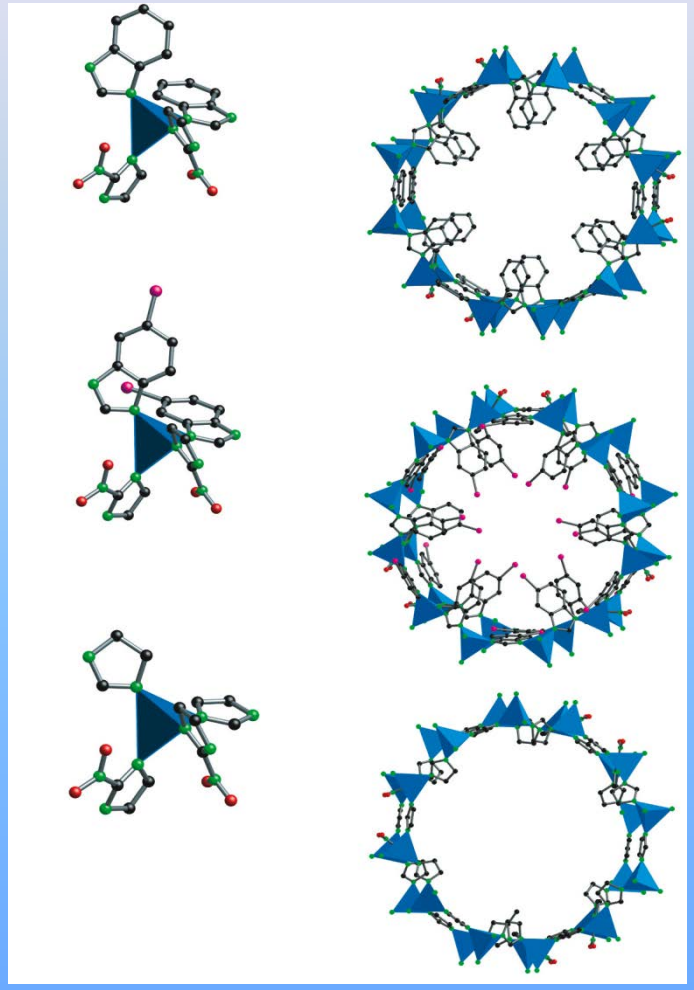

Cl substitution on benzene ring in ZIF-69

Banerjee & al. Science 319, 939, 2008.

INS of H_2 in ZIF-68, ZIF-69

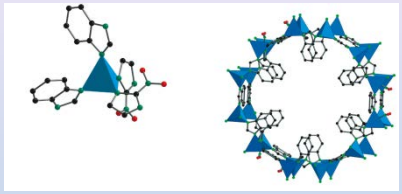

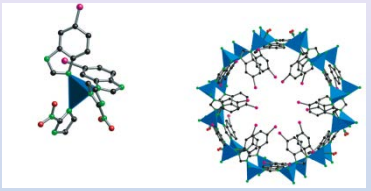

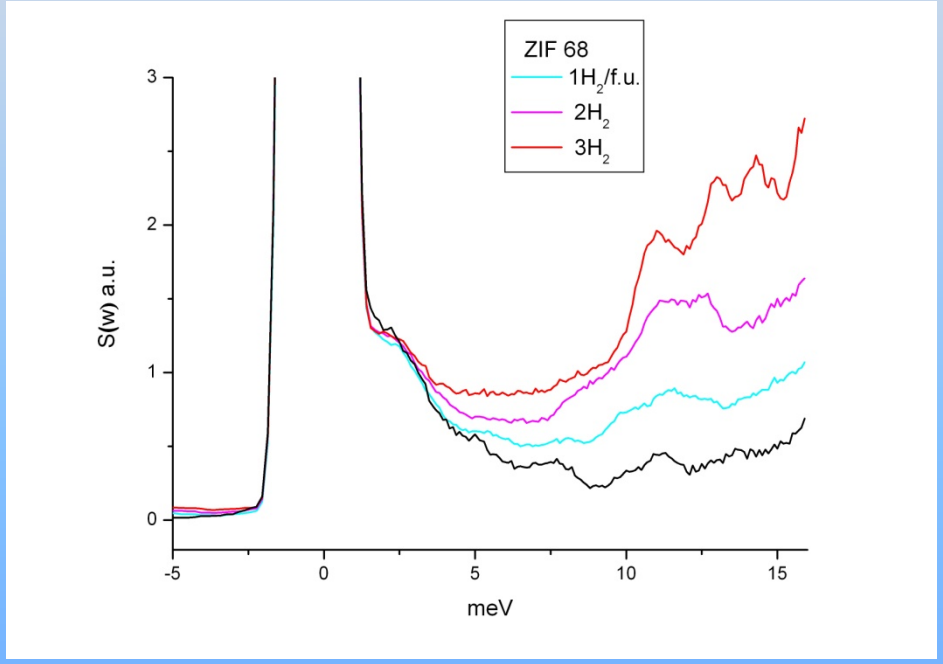

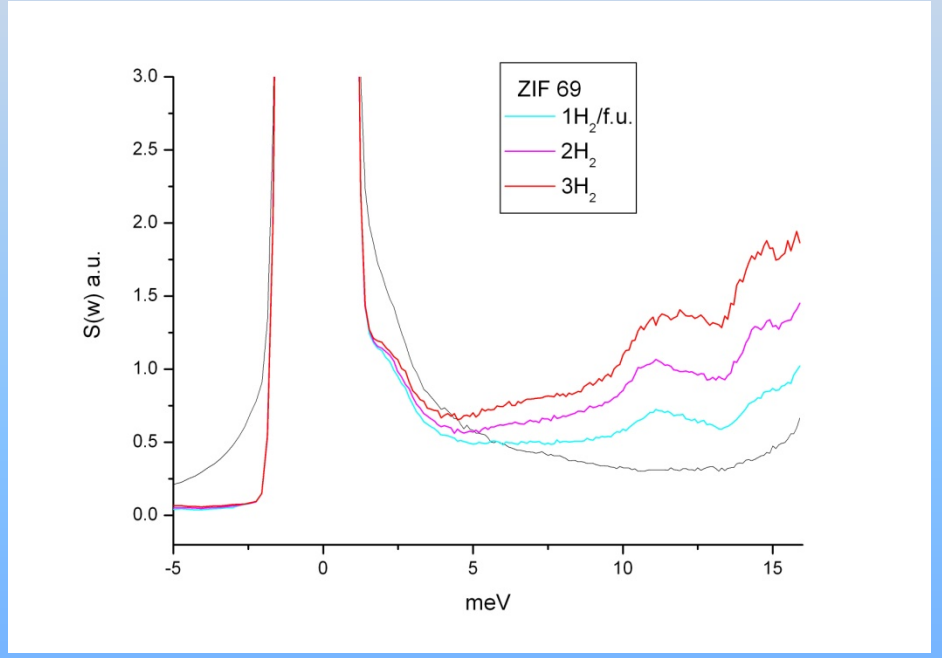

NEAT Spectrometer (BENSC) T = 5K

Possible binding sites:
ZnN_4 cluster, Im, $-NO_2$, organic, and -Cl (ZIF-69)

CPO-27-Co $[Co_2(dhtp)(H_2O)\bullet 8(H_2O)]$

(dhtp = 2,5- dihydroxyterephthalic acid)

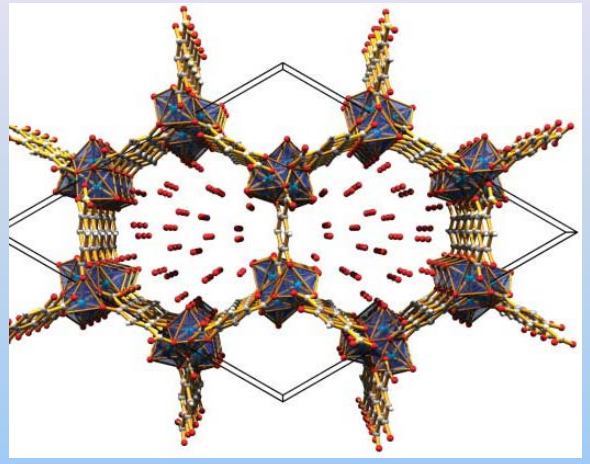

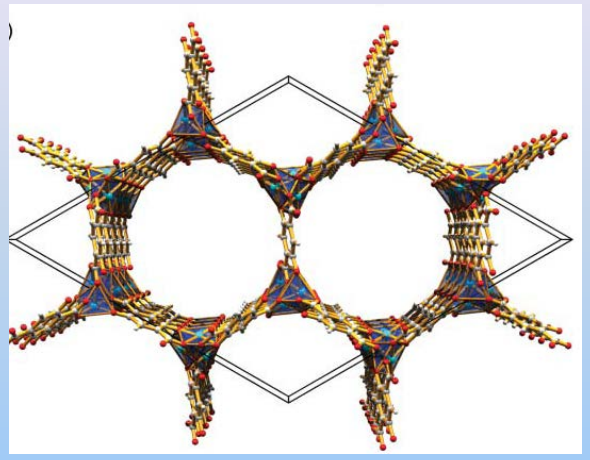

P.C. Dietzel & al. Chem. Comm.(2006)

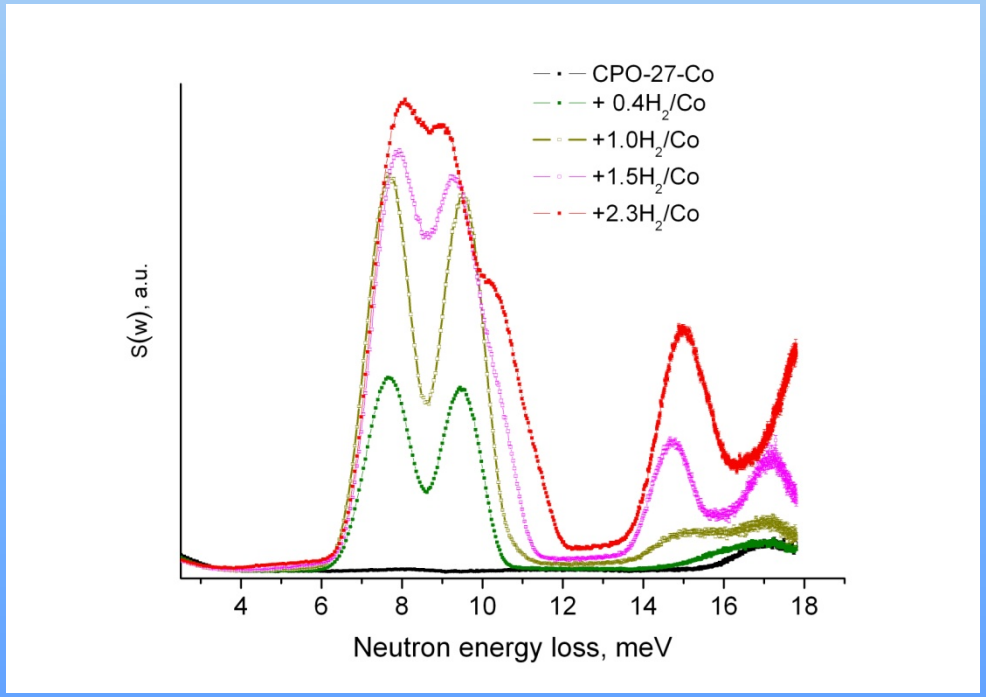

Georgiev, Albinati Eckert

CPO-27- M

$[M_2(dhtp)(H_2O)\bullet 8(H_2O)$, M = Mg, Ni, Co]

(dhtp = 2,5- dihydroxyterephthalic acid)

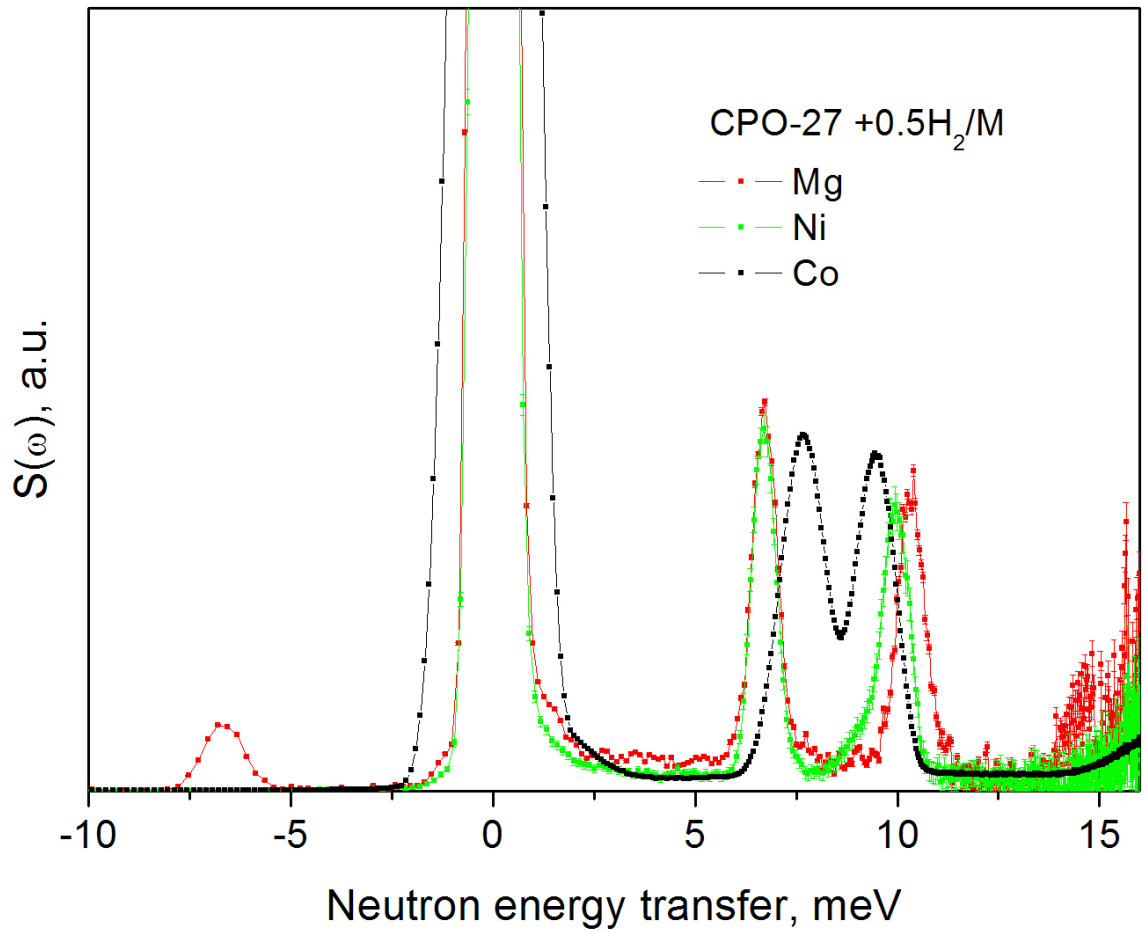

Georgiev, Albinati Eckert

Dr. S. Rizzato, *University of Milan*

Dr. P. A. Georgiev, *University of Milan*

Dr. T. F. Koetzle, *Argonne National Laboratory*

Dr. W. Klooster, *Amethyst Scientific Consulting LLP, Singapore*

Dr. S. Capelli, *Institut Laue – Langevin*

Dr. S. A. Mason, *Institut Laue – Langevin*

Dr. G. J. McIntyre, *Institut Laue – Langevin*

Dr. J. Ollivier, *Institut Laue – Langevin*

Dr. J. Eckert, *Los Alamos National Laboratory*

Prof. P. S. Pregosin. *ETH – Zürich*

Prof. H. Berke, *University of Zürich*

Dr. B. Chaudret, *CNRS Toulouse*

Dr. S. Sabo - Etienne, *CNRS Toulouse*

Dr. M. Grellier, *CNRS Toulouse*

Prof. B. L. Mojet, *University of Twente*

Prof. K. C. Caulton, *Indiana University*

Prof. M. B. Hall, *Texas A&M*

Prof. R. Morris, *University of Toronto*

Funded by:

C.N.R., M.U.R,

EU FP5-RTM, NATO